THE GEOLOGY AND GEOCHEMISTRY OF THE NORTH-WESTERN PORTION OF THE USUSHWANA COMPLEX, SOUTH-EASTERN TRANSVAAL

THESIS

Submitted in partial fulfilment of the
Requirements for the Degree of
Master in Economic Geology
in the Department of Geology,
Rhodes University.

by

ANGELA RIGANTI

December 1991

ABSTRACT

The 2.9 Ga old Usushwana Complex in the Piet Retief-Amsterdam area (south-eastern Transvaal) represents an exposed segment of a layered intrusion. It has the form of a dyke-like body elongated in a north-westerly direction, and extends to an estimated depth of 3000-5500 m. Lithologically, the Complex consists of a cumulate succession of mafic rocks capped by granitoids and has intruded along the contact between the basement and the supracrustal sequences of the Kaapvaal Craton.

Differentiation of an already contaminated gabbroic magma resulted in an ordered stratigraphic sequence comprising progressively more evolved lithotypes, with at least two imperfect cyclic units developed over a stratigraphic thickness of about 700 metres (Hlelo River Section). Meso- to orthocumulate textured gabbros and quartz gabbros grade upwards into magnetite- and apatite-bearing quartz gabbros, interlayered with discontinuous magnetitite horizons. The gabbros in turn grade into hornblende-rich, granophyric granodiorites. The differentiation process is regarded as having been considerably enhanced by the assimilation of acidic material, derived by partial melting of the felsic country rocks at the roof of the magma chamber. Recrystallisation of these rocks gave rise to the microgranites that locally overlie the granodiorites. Mineralogical, textural and geochemical features indicate a relatively advanced fractionation stage, suggesting that the exposed sequence of the Usushwana Complex in the study area represents the upper portion of the intrusion.

No significant mineralised occurrences were identified. However, on the basis of similarities between the Usushwana Complex and other mafic layered intrusions which host significant ore deposits, it is suggested that economic concentrations of base metal (Cu-Ni) sulphides, PGE and chromitites are likely to be developed at lower stratigraphic levels.

ACKNOWLEDGMENTS

I would like to express my sincere gratitude to those people and organisations that helped me in the fulfilment of my thesis. In particular I wish to thank:

* the C.S.I.R. for the Bursary that enabled me to study at Rhodes University;
* Anglo-American Prospecting Services Pty (Ltd), Transvaal Office, for the financial and logistic support;
* the F.R.D. for the contribution towards my microprobe analyses (through the Departmental funding).

I am indebted to my supervisor Dr. A.R. Butcher, for his helpful criticism and suggestions. After joining the Camborne School of Mines in October 1991, his cooperation continued by way of discussions and corrections. I also wish to thank him for all his efforts in improving my English in drafts and writing.

I also would like to thank Prof. F. Pirajno, Prof. J.M. Moore, Prof. R.E. Jacob and C.A. Mallinson, for their careful guidance and valuable advice throughout my studies at Rhodes University.

I would like to express my gratitude to Prof. A.H. Wilson (University of Natal, Pietermaritzburg) and to Prof. W.J. Wadsworth (University of Manchester), for their contibutions during my field work and for my microscope studies, respectively. My thanks extend to Prof. H.V. Eales (Rhodes University) for his help during the preparations of microprobe sections.

I wish to thank all technical staff of the Dept. of Geology (Rhodes University), specifically R.Skae for his assistance during my microprobe studies, and J.Hepple, B.Bongwana and W.Hashe for organising my samples and preparing thin and microprobe sections.

Many thanks are due to the farming and catholic communities of Piet Retief, for their hospitality and friendly welcome.

I wish to thank all my fellow students, (Johan, Bernd and Phoenix in particular) for their precious advise and help at various stages of my work. Cecilia's help for the proof-reading of my thesis is also gratefully acknowledged.

I also would like to thank for their nice companionship my friends Marilena, Milica, Monica, Gina and all the M.Sc. students who, in these two years, shared with me the difficulties of this course. In particular thanks are due to Fiona, for her friendship and help.

Finally, I would like to thank my parents for their constant encouragement and support, and my sister Luisa for her help.

DECLARATION

All work in this thesis is the original work of the author except where specific acknowledgment is made to the work of others.

No portion of this thesis, or the analytical data presented herein, may be reproduced or published without written permission of the author.

Date: 13/12/91.....

Signed: .....
A. Riganti

CONTENTS

Page

ABSTRACT i

ACKNOWLEDGMENTS ii

DECLARATION iii

LIST OF CONTENTS, FIGURES, TABLES AND PLATES iv

CHAPTER 1: INTRODUCTION 1

CHAPTER 2: LOCALITY AND GEOMORPHOLOGY OF THE STUDY AREA 2

CHAPTER 3: REGIONAL GEOLOGICAL FRAMEWORK

3.1 Geological and structural evolution of the Kaapvaal Craton 5
3.2 Regional stratigraphy of south-eastern Transvaal and western Swaziland 9
3.2.1 The Basement Complex 9
3.2.2 The Pongola Sequence 11
3.2.3 The Thole ultramafics 11
3.2.4 The Amsterdam Formation 12
3.2.5 The Usushwana Complex 13
3.2.6 The Pongola granite 14
3.2.7 The Karoo Sequence 14

CHAPTER 4: GEOLOGY OF THE USUSHWANA COMPLEX

4.1 Introduction 15
4.2 Historical Review 15
4.3 Extent, shape and thickness of the Complex 15
4.4 Structural setting of the Complex 19
4.5 Age of the Complex 20
4.6 Lithology and stratigraphy of the Complex 21
4.6.1 Hlelo River Section 23

4.6.2 Sterkwater Section 32
4.6.3 Morgestond Section 36
4.6.4 Derby Section 38
4.6.5 Blesbokspruit 515 IT 39
4.7 Intrusive relationships and mode of emplacement of the Usushwana Complex 40
4.8 Summary 43

CHAPTER 5: PETROLOGY OF THE USUSHWANA COMPLEX

5.1 Introduction 46
5.2 Petrology of the Hlelo River Section 46
5.2.1 1st cyclic unit 46
5.2.2 2nd cyclic unit 55
5.3 Petrology of the Sterkwater Section 58
5.4 Petrology of minor Usushwana Complex lithologies 63
5.5 Summary and discussion 65

CHAPTER 6: MINERALOGY OF THE USUSHWANA COMPLEX

6.1 Introduction 70
6.2 Plagioclase variation 70
6.3 Clinopyroxene variation 74
6.4 Summary and discussion..... 77

CHAPTER 7: WHOLE-ROCK GEOCHEMISTRY

7.1 Introduction 81
7.2 Chemical variations with stratigraphic height 81
7.2.1 Major elements 81
7.2.2 Trace elements 86
7.3 Interelement relationships 88
7.3.1 Major and trace elements vs MgO 88
7.3.2 Trace elements vs Zr 90
7.4 Comparison of the main rock-types 93
7.5 Summary and discussion 96

CHAPTER 8: PETROGENESIS OF THE USUSHWANA COMPLEX

8.1 Introduction 98
8.2 Nature of the parental magma and evidence for contamination 98
8.3 Origin of the granophyric rocks 101
8.4 Evidence for addition of new magma 104
8.5 Discussion 106

CHAPTER 9: ECONOMIC MINERAL POTENTIAL OF THE USUSHWANA COMPLEX

9.1 Introduction 109
9.2 Relevant features for the assessment of the economic mineral potential of the Usushwana Complex 109
9.3 Base metal (Cu-Ni) sulphide mineralisation 111
9.4 PGE mineralisation 114
9.5 Chromitites 116
9.6 Magnetitites 117
9.7 Skaergaard-type Au mineralisation 119
9.8 Discussion and suggestions for exploration 120

CHAPTER 10: SUMMARY AND CONCLUSIONS 123

REFERENCES 126

APPENDICES:

Appendix A: List of thin sections
Appendix B: Analytical details for the JEOL CXA-733 superprobe and the X-ray fluorescence
Appendix C: Microprobe data
Appendix D: Whole-rock data
Appendix E: Base and precious metal data

LIST OF FIGURES

Fig. 1 Simplified geological setting of the Usushwana Complex and locality of the study area 3

Fig. 2 Drainage pattern and cadastral details of the study area 4

Fig. 3 Tectonic provinces of southern Africa 5

Fig. 4 Geology of south-eastern Transvaal and western Swaziland, and chronostratigraphy of the Usushwana Complex, cover and country rocks 10

Fig. 5 Generalised geological map of the Piet Retief-Amsterdam area 16

Fig. 6 Depth interpretation of the Usushwana Complex and Pongola sequence in the study area (from gravity data) 18

Fig. 7 Geology and location of the Hlelo River section 24

Fig. 8 Schematic stratigraphic column of the Usushwana Complex at the Hlelo River Section 25

Fig. 9 Geology and location of the Sterkwater Section 33

Fig. 10 Geology and location of the Morgestond Section 37

Fig. 11 Schematic mode of emplacement of the Usushwana Complex 42

Fig. 12 Variations in the amount of intercumulus material 50

Fig. 13 Transition from gabbro to granodiorite 54

Fig. 14 Variations from granodiorite to granite 57

Fig. 15 Average compositions of plagioclase in the Hlelo River Section 71

Fig. 16 Cryptic variations of cumulus silicate phases through the Usushwana Complex (Hlelo River Section)..... 72
a) Plagioclase - Anorthite content;
b) Plagioclase - FeO content;
c) Clinopyroxene - Mg #.

Fig. 17 Total iron versus anorthite content of plagioclase cores 74

Fig. 18 Compositional range of clinopyroxene in the Hlelo River Section 75

Fig. 19 Crystallisation trends of pyroxenes in the Bushveld and Usushwana Complex 76

Fig. 20 Comparison of phase layering and cryptic layering patterns in the later fractionation stages of the Usushwana Complex and other mafic intrusions 79

Fig. 21 Chemical variations of major elements with stratigraphic height (Hlelo River Section) 82

Fig. 22 Fractionation trends of the Usushwana, Bushveld and Skaergaard complexes 85

Fig. 23 Chemical variations of trace elements with stratigraphic height (Hlelo River Section) 87

Fig. 24 Interelement relationships of selected major elements and Mgo 89

Fig. 25 Interelement relationships between selected trace elements and MgO 91

Fig. 26 Interelement relationships of a) Nb vs Zr; b) Y vs Zr; c) Rb vs Zr 92

Fig. 27 Ti/Zr vs Zr variation for the Pongola and Usushwana rocks 101

Fig. 28 Incompatible trace elements ratios against stratigraphy 105

Fig. 29 Fe-S-O system at 1200° 113

LIST OF TABLES

Table I Relative proportions of various lithologies of the Usushwana Complex 21

Table II Average chemical compositions of the main rock-types of the exposed part of the Usushwana Complex 94

Table III Composition of magnetitites 118

LIST OF PLATES

Plate 1 Contact between the basement gneisses and the Usushwana gabbro 27

Plate 2 Alignment of mafic minerals parallel to the contact of the intrusion 27

Plate 3 Irregular hornblende aggregates in the granodiorite .. 29

Plate 4 Grain-size variations in the granodiorite 29

Plate 5 Magnetitite layers at the Hlelo river Section 30

Plate 6 Centimetre scale layering in the magnetite-bearing gabbro 35

Plate 7 Channel-type structure in the layered gabbros 35

Plate 8 Orthocumulate basal gabbro 47

Plate 9 Uralitisation of clynopyroxene 48

Plate 10 Hornblende rims around augite grains 48

Plate 11 Titaniferous biotite rim around Fe-Ti oxides 51

Plate 12 Orthocumulate magnetite apatite quartz gabbro 52

Plate 13 Primary hornblende in the granophyric granodiorite ... 56

Plate 14 Granophyric granodiorite 59

Plate 15 Replacement of plagioclase by granophyric intergrowths 59

Plate 16 Granophyric texture in the granodiorite 60

Plate 17 Metamorphic hornblende 61

Plate 18 Websterite 64

CHAPTER 1: INTRODUCTION

The Usushwana Complex is an elongated layered intrusion situated along the Republic of South Africa-Swaziland border. In spite of the significant areal extent of the Complex (estimated at 600 km^2; Wilson, 1990), surprisingly little is known about this intrusion (Humphrey and Krige, 1931; Winter, 1965; Hunter, 1970a; Hammerbeck, 1977).

This thesis reports on the results of a detailed geological and geochemical study of the north-western portion of the Complex.

Information obtained from regional mapping, detailed sampling, microscope examination of thin sections and geochemical analyses (XRF and microprobe) has led to:

(a) establishment of the stratigraphy of the Complex;

(b) identification of differentiation trends;

(c) an assessment of the economic mineral potential of the Complex.

CHAPTER 2: LOCALITY AND GEOMORPHOLOGY OF THE STUDY AREA

The study area is situated in south-eastern Transvaal, between the towns of Piet Retief and Amsterdam (Fig. 1), close to the South African-Swaziland border, and is delineated by latitudes 26°30'S and 27°S and longitudes 30°30'E and 31°E. It is geographically covered by the South African Government topographic sheets 2630 DA (Amsterdam), 2630 DB (Nerston), 2630 DC (Iswepe) and 2630 DD (Kemp). A main road (R33) and numerous forestry roads allow easy access to most of the study area.

Geographically, the area is considered to be part of the Transvaal Highveld (average elevation of 1250 m above sea-level), and consists of gently undulating hills, with differences in height usually in the range of a few hundred metres.

The drainage pattern is defined by numerous perennial streams (average rainfall 920 mm in Piet Retief) and major rivers (e.g. Ngwempisi and Hlelo River), which flow eastwards and form tributaries of the Great Usutu River in Swaziland. Often, their courses are controlled by major joints and shears in the underlying rocks, and locally they have deeply dissected the rolling grassland which is typical of the region. Figure 2 depicts the drainage pattern of the area and also provides cadastral details.

Thick afforestation (pine and eucalyptus) within the last 40 years has partly modified the original physiography of the region. Tropical climatic conditions, with rainy-misty summers and dry-cool winters, favour the extensive weathering of the rocks outcropping in the area and locally the development of a deep soil profile.

Thus, the combination of topographic, climatic and anthropic factors has resulted in very poor exposures, the best outcrops being preserved along the main river courses.

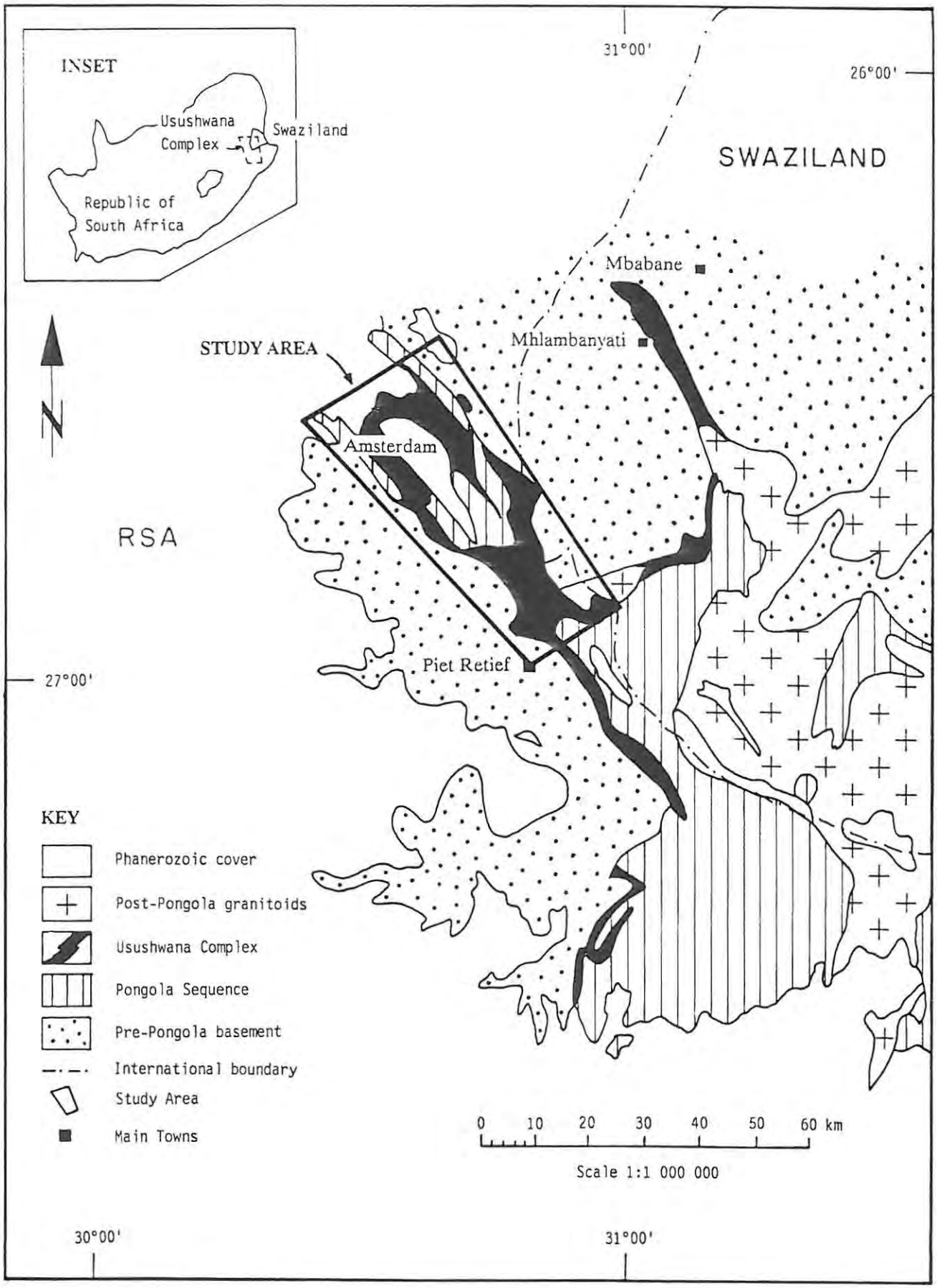

Fig. 1 - *Simplified geological setting of the Usushwana Complex and locality of the study area (modified after Tankard et al., 1982). Inset shows geographic position covered by figure.*

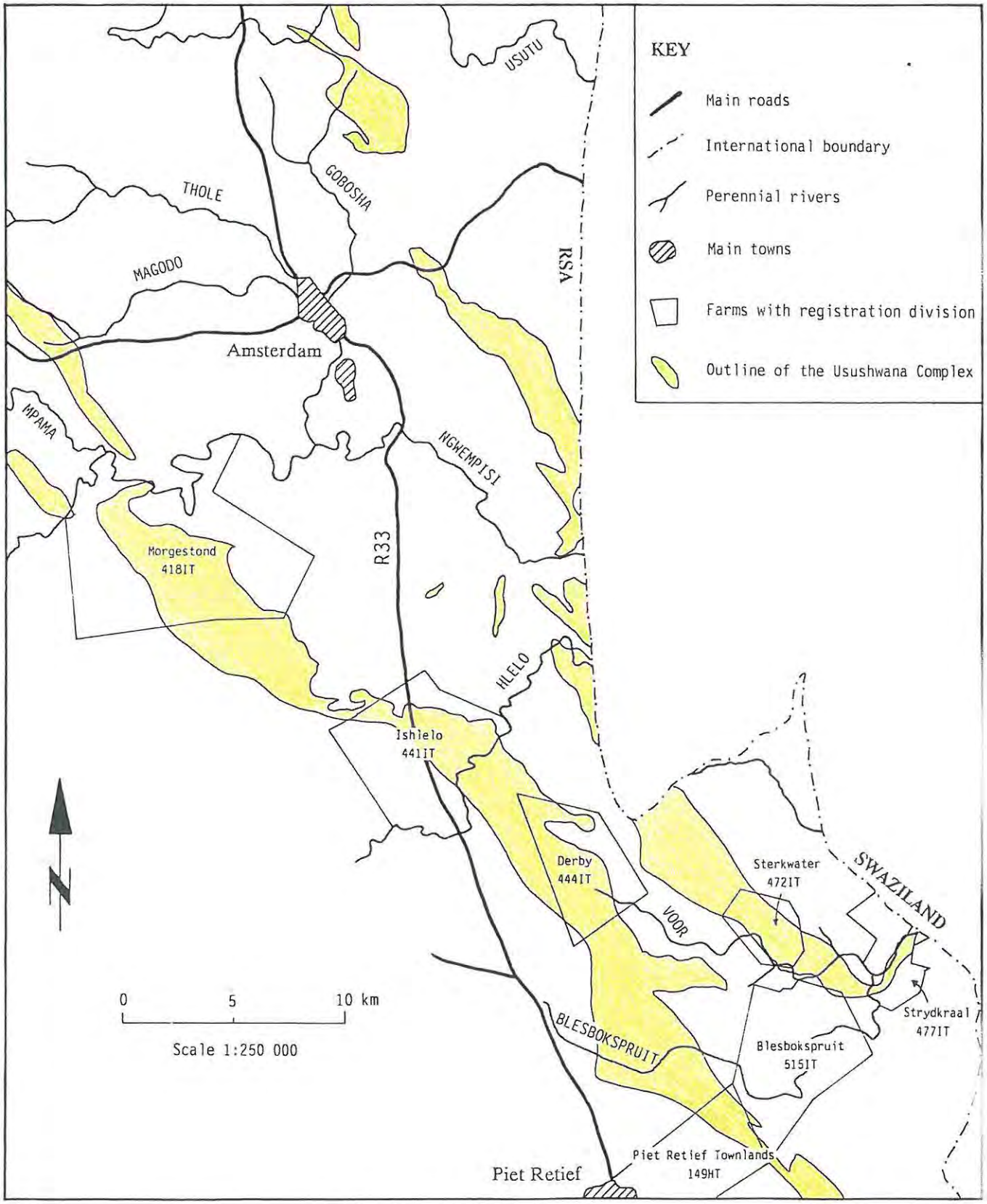

Fig. 2 - *Drainage pattern and cadastral details of the Piet Retief-Amsterdam area. Only farms where sampling traverses were carried out have been reported in the figure.*

CHAPTER 3: REGIONAL GEOLOGICAL FRAMEWORK

3.1 GEOLOGICAL EVOLUTION OF THE KAAPVAAL PROVINCE

The Kaapvaal Province represents one of the major geological elements of southern Africa (Fig. 3), and consists of an old stable cratonic block which occupies most of north-eastern and central South Africa. A brief account of the geology and the structure of the Kaapvaal Province is given below, with special reference to its south-eastern portion.

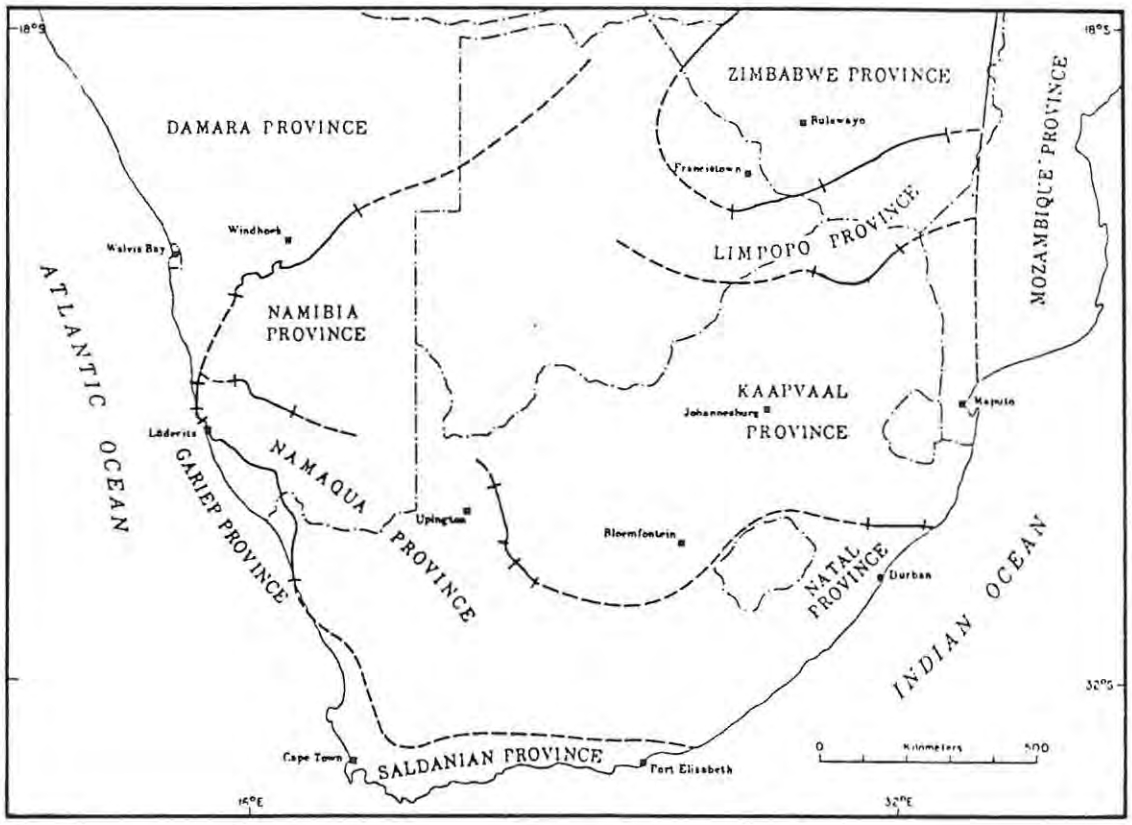

Fig. 3 - *Tectonic provinces of southern Africa (modified after Tankard et al., 1982). Boundaries obscured by cover are shown as dashed lines.*

The main geological and tectonic features of the Kaapvaal Province were developed during Archaean to early Proterozoic times. The nature and distribution of lithologies in the Kaapvaal Province clearly indicate a process of progressive crustal development and

cratonisation, followed by the deposition of supracrustal sequences. Subsequently, these were largely obscured by younger intracratonic cover rocks (Tankard et al., 1982).

The exposed Archaean basement of the Kaapvaal Province (3.0 Ga and older rocks) consists predominantly of massive and foliated granitoids with subordinate gneisses, within which are minor deformed greenstone relics of volcano-sedimentary origin. In the south-eastern portion of the Kaapvaal craton, the sialic crust is now represented by Na-rich tonalites and trondhjemites plus a complex series of bimodal gneisses and migmatites. These are collectively known as the Ancient Gneiss Complex (Hunter, 1970b) and are described as the products of a first magmatic cycle (Anhaeusser and Robb, 1981). The Swaziland Supergroup is among the most famous of the greenstone sequences, and comprises a lower ultramafic-mafic volcanic assemblage, a middle calc-alkaline volcanic group and an uppermost sedimentary, dominantly clastic succession (Anhaeusser, 1986).

Repeated high strain events and the intrusion of later potassic granites have inevitably obliterated the original relationships between the granitoids and the greenstone terrains. As a consequence, whether the gneiss-granitoid pair pre-dates the development of the greenstone belts (Windley, 1973; Hunter, 1974a; Kröner, 1985), or whether they are intrusive (later) (Glikson, 1972; Anhaeusser, 1973; Anhaeusser and Robb, 1981) is still debatable. Barton (1981) noted that the oldest age for the sialic rocks of the Ancient Gneiss Complex (3555 ± 111 Ma, Rb-Sr; Barton et al., 1980) suggests that they were, at best, coeval with the mafic crust, for which an age of 3540 ± 30 Ma is reported (Sm-Nd; Hamilton et al., 1979). However, the geochemistry of clasts from the greenstone metasediments indicates that a highly evolved continental crust represented the source terrain for the greenstone sequence (Reimer et al., 1985; Compston and Kröner, 1988). The hypothesis that these upper crustal granites were part of the Ancient Gneiss Complex of Swaziland is generally favoured (McLennan and Taylor, 1983; Tegtmeyer and Kröner, 1987; Kröner and Compston, 1988).

Whichever model is preferred, the emplacement of composite potash-rich batholithic bodies (e.g. Granodiorite Suite, Nelspruit and Lochiel granites) represents the main event which contributed to the crustal stabilisation of the protocratonic nuclei, after which tectonic stability prevailed. Anhaeusser and Robb (1981) regard this period of magmatic activity as part of a second cycle, which commenced at 3.2 Ga and appears to have terminated approximately 3.0 Ga ago. At this stage the eastern Transvaal and Swaziland areas are considered to have attained a crustal thickness of ± 25 km (Hunter, 1974b).

The process of cratonic stabilisation led to the deposition of ensialic supracrustal successions. Five major cratonic sequences can be recognised within the Kaapvaal Province. In stratigraphic order these are: the Pongola, the Witwatersrand, the Ventersdorp, the Transvaal and the Waterberg Supergroups. These volcano-sedimentary successions accumulated in epicontinental basins between 3.0 and 1.8 Ga ago, and rest unconformably on erosional surfaces which cut the deformed schist belts and associated granitoid rocks. As the Archaean-Proterozoic boundary is now defined geochronologically at 2.5 Ga (Plumb and James, 1986), it follows that in the Kaapvaal Province cratonisation and evolution of the cover sequences were diachronous processes (Cheney et al., 1990).

A broad similar cyclic pattern of basin development is displayed by these sequences (Tankard et al., 1982). The onset of sedimentation generally followed an initial phase of volcanism, during which lavas ranging in composition from basalt to rhyolite were erupted. Sedimentary units consisted of varying proportions of marine quartz arenites and shales, intercalated with fluvial conglomerates and arkoses. A decrease in energy levels with time is reflected by the greater volume of finer clastics in successively younger basins, with non-terrigenous sediments restricted to the Transvaal-Griqualand Supergroup. The evolution of the basin was frequently terminated by a second phase of volcanic activity. The source material for the sedimentary basins was homogeneous, porphyritic, K-rich granites (Anhaeusser and Robb, 1981), whose loci of emplacement progressively migrated from south-east to north-west. As a result, the depositional

axes of the sedimentary basins moved across the craton in the same direction. This feature is reflected by the present distribution of the five supergroups and by their northward younging ages (Anhaeusser, 1973).

The oldest basin, in which the Pongola Sequence accumulated between 3.1 and 2.9 Ga, is confined to the south-eastern corner of the Kaapvaal Province. The Pongola Sequence comprises a lower, dominantly volcanic, Nsuze Group, and an upper sedimentary Mozaan Group. Low pressure, crystal fractionation from evolved basaltic parents and extensive crustal contamination are suggested by the geochemistry of the subaerial volcanic rocks (Hegner et al., 1984). A stable, non-orogenic environment with some degree of crustal extension is indicated as the tectonic setting of the Nsuze volcanism, though an exact analogue in modern environments cannot be envisaged (Armstrong et al., 1986). The waning of volcanic activity was followed by the onset of sedimentation (Mozaan Group) on braided alluvial plains, interacting with a wave-dominated shallow marine shelf (Watchorn, 1980; Beukes and Cairncross, 1991).

The granitic plutons intruding the supracrustal sequences of the Kaapvaal Province represent the products of a third magmatic cycle (Anhaeusser and Robb, 1981). Two peaks of activity have been recognised, with "older" plutons (2.9 - 2.7 Ga) geochemically distinguished from "younger" plutons (2.6 - 2.4 Ga) (Condie and Hunter, 1976). Smaller plutons were successively emplaced at 2.3 and 2.0 Ga; they are frequently associated with felsic volcanism or are connected with the emplacement of mafic bodies. The magmatic activity of this third cycle coincided with the termination of cratonisation, representing the ultimate cycle in the formation of the granitic basement.

Intrusions of mafic complexes into the cratonic sedimentary cover occurred at various times during the Proterozoic evolution of the Kaapvaal Province, generally in a north-westerly direction (Hunter, 1974b). In particular, epicontinental sedimentation and volcanism in the Pongola basin were terminated at 2.8 Ga by the intrusion of the

Usushwana Complex, whereas the 2.0 Ga old Bushveld Complex post-dates sedimentation of the Transvaal Supergroup.

During middle to late Proterozoic and Phanerozoic times the Kaapvaal Province acted as a stable cratonic block. Deformation was restricted to marginal areas during the Proterozoic orogenic activity which led to the formation of the Namaqua-Natal metamorphic terrane and its fusion to the Kaapvaal craton. The latter represented the foreland onto which a series of nappe sheets were obducted from the south (Matthews, 1981). Either a tectonised or a gradational contact zone marks the transition to the eastern Namaqua Province (Joubert, 1981). Following the break-up of the Gondwanaland supercontinent, the Late Palaeozoic to Mid Mesozoic development of the intracratonic Karoo basin led to the accumulation of an extensive sedimentary and volcanic cover, which obscured approximately 70% of the Precambrian cratonic terranes (Anhaeusser and Wilson, 1981).

3.2 REGIONAL STRATIGRAPHY OF SOUTH-EASTERN TRANSVAAL AND WESTERN SWAZILAND

The stratigraphy and distribution of rock-types in south-eastern Transvaal and western Swaziland are shown in figure 4. The main features of the various rock units are briefly described below.

3.2.1 THE PRE-PONGOLA BASEMENT

In the area under discussion, the pre-Pongola basement comprises two main varieties of granitic rocks. Tonalitic gneisses are prominent south of Piet Retief and in Swaziland, while granites predominate to the north. The granites are considered to represent a later intrusive event (Hunter, 1973) as they contain abundant xenoliths of tonalite gneisses. Gneissic varieties and pegmatitic phases are also characteristic of the granite. An age of 3555 ± 111 Ma (Rb-Sr) has been indicated for the basement gneisses (Barton et al., 1980).

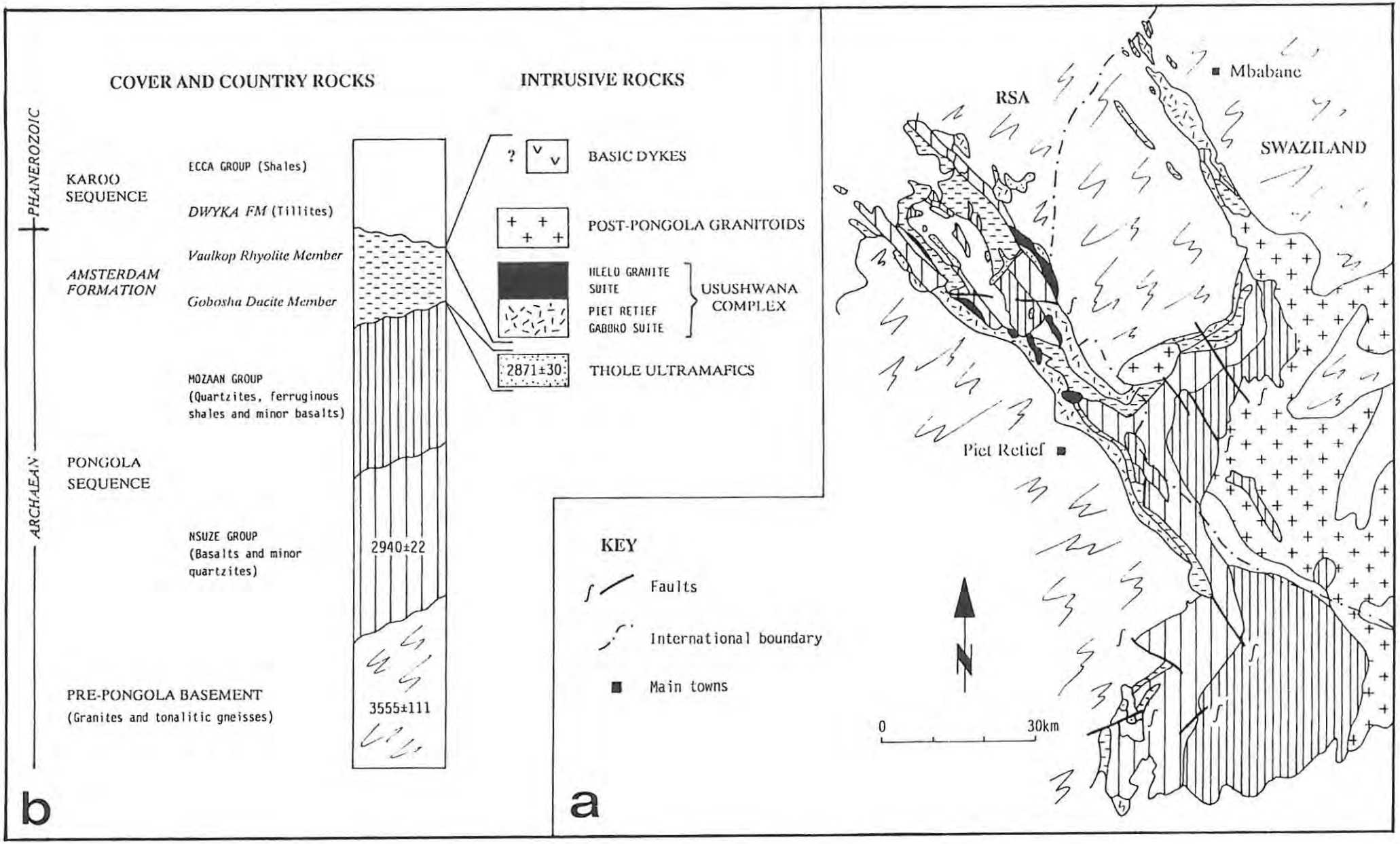

Fig. 4 - *a) Geology of south-eastern Transvaal and western Swaziland;*
b) chronostratigraphy (not to scale) of the Usushwana Complex, cover, country rocks, and other intrusives.
Basic dykes not shown on the map; terminology after SACS, 1980.

3.2.2 THE PONGOLA SEQUENCE

Formations of the volcano-sedimentary Pongola Sequence are preserved in the Amsterdam area and progressively thicken southwards towards Piet Retief, attaining a maximum thickness of 10,650 m (SACS, 1980). A lower volcanic Nsuze Group and an upper sedimentary Mozaan Group can be distinguished. The Nsuze Group rests with a marked unconformity on gneissic and granitoid rocks of the basement and has been dated at 2940 ± 22 Ma (Sm-Nd; Hegner et al., 1984). It consists of a thick pile of basaltic and subordinate andesitic lavas, overlying a package of quartzites with sporadic iron formations near the base. A regional unconformity generally marks the contact between the Nsuze and the Mozaan Group. The lower part of the Mozaan Group mainly consists of quartzites in two different units separated by a persistent ferruginous shale horizon. A succession of quartzite, ferruginous shale and iron formation follows, with bands of basaltic lava occurring near the top of the sequence.

An erosional hiatus followed the accumulation of the Pongola Sequence, preceding the onset of magmatic events, both intrusive and extrusive in character. Structural deformation occurred at this stage, and resulted in extensive shearing and folding along NW-trending axes (e.g. formation of the Amsterdam syncline).

3.2.3 THE THOLE ULTRAMAFICS

Slightly transgressive to concordant, ultramafic to mafic sills were emplaced at various levels into the Mozaan Group of the Pongola Sequence, during or shortly after its deformation. The Thole ultramafics have their greatest development west of Amsterdam, but similar rocks are also observed outside this basin. The bodies attain a maximum thickness of 70 m (Van Vuuren, 1965) and are usually differentiated with a gradual transition from harzburgite at the base, to pyroxenite in the central and upper portions; locally, gabbro or norite may occur at the top. The emplacement of the Thole ultramafics has been regarded by Hammerbeck (1982) as the first manifestation of

the magmatic cycle that culminated with the intrusion of the Usushwana Complex.

3.2.4 THE AMSTERDAM FORMATION

The Amsterdam Formation consists of a succession of intermediate to acidic volcanics which transgressively overlie the sedimentary rocks of the Pongola Group (SACS, 1980). The lower Gobosha Dacite Member outcrops in two continuous belts on both limbs of the Amsterdam syncline. This Member is characterised by an abrupt southerly termination and is only sporadically developed outside the Amsterdam area. It consists of dark, massive, fine-grained ash-flow tuffs of dacitic composition, in places grading into a pyroclastic breccia. The Vaalkop Rhyolite Member unconformably overlies the dacitic pile. It occurs as a 60 km long, NW-trending, continuous belt on the Transvaal side of the South Africa-Swaziland border. A second limb branches off north-east of Piet Retief, and extends in a more easterly direction into Swaziland. The rhyolite is massive, without signs of bedding, banding or flow structures, and displays a typical red colour on weathered surfaces.

The relationships of the volcanics to older formations suggest that the deposition of the Amsterdam volcanics occurred on an uneven floor. The latter was represented by a palaeo-landscape with considerable relief and marked topographic depressions.

The distribution of the Amsterdam Formation closely follows the outcrop pattern of the Usushwana plutonics, but it is not strictly confined to the latter. In particular, the present outcrops of the Vaalkop Rhyolite possibly represent the erosional relics of an originally larger blanket.

3.2.5 THE USUSHWANA COMPLEX

The magmatic activity that was initiated with the emplacement of the Thole ultramafics and the extrusion of the Amsterdam volcanics culminated with the intrusion of the Usushwana Complex. A detailed description of the latter is presented in chapter 4, and only a brief account is given below.

The Complex is an elongated, layered, dominantly gabbroic intrusion, comprising two bodies, trending NW-SE, which were intruded along the contact between the pre-Pongola Basement and either the Pongola or younger sequences. The western body extends for about 100 km from the White River to south of Lothair. Near Piet Retief, it bifurcates and forms a north-easterly extension, which in turn joins the eastern body south of Mhlambanyati (western Swaziland). The eastern segment is only 40 km long and outcrops approximately 45 km east of Amsterdam. A significant areal extent of about 600 km^2 has been estimated for the Usushwana Complex as a whole (Wilson, 1990).

Lithologically, the Complex has been subdivided into a mafic and an acid portion, named the Piet Retief Gabbro Suite and the Hlelo Granite Suite respectively (Hammerbeck, 1977). The former is mainly composed of quartz gabbro, with minor ferrogabbro containing discontinuous magnetitite layers. Gabbro and hypersthene gabbro are sporadically developed in the South African portion of the Complex, and their relationships to the other rock-types are uncertain. Ultramafic rocks (pyroxenite and locally serpentinite) outcrop more extensively in Swaziland, where the Complex is considered to attain a total thickness of at least 2170 m (Hunter, 1970a). The acid suite overlies the mafic portion and comprises hornblende-rich granodiorite and microgranite. Both lithologies can be either dominantly granophyric in texture or contain only minor amounts of quartz-feldspar intergrowths. A combination of two major processes (differentiation from a mafic magma and partial melting of country rocks) is considered to account for the formation of the acid suite. Layering characteristics within the Complex are generally not well developed, the best examples being preserved in Swaziland. Sub-economic, sulphide-hosted Cu-Ni

mineralisation is reported from several localities in Swaziland, where disseminated pyrrhotite and chalcopyrite occur in close association with ultramafic rocks and the more mafic varieties of gabbro.

Basic dykes of unknown age are found mainly east of Amsterdam, and although they display pre-Karoo intrusive relationships, it cannot be established whether they pre- or post-date the Usushwana intrusion.

3.2.6 THE POST-PONGOLA GRANITE

A medium- to coarse-grained granite (so-called Sicunusa granite) intrudes the basement and the Usushwana Complex, outcropping in a small area close to the Swaziland border and in the Amsterdam area. A number of dykes have been found associated with this granite, which represents one of the Younger Plutons described by Hunter (1973).

3.2.7 THE KAROO SEQUENCE

After a long hiatus, the accumulation of the Phanerozoic Karoo Sequence extensively blanketed the older rocks in the south-eastern part of the Kaapvaal Province. The Karoo cover consists of Dwyka tillites and fine-grained fluvio-glacial sediments, deposited after a long period of glaciation. Shales of the Ecca Group accumulated later and, together with older formations, were subsequently intruded by dolerite sheets and dykes. The latter are typically characterised by the presence of conspicuous euhedral plagioclase phenocrysts.

CHAPTER 4: GEOLOGY OF THE USUSHWANA COMPLEX

4.1 INTRODUCTION

In this chapter, an account is given of the geological setting of the Usushwana Complex, based on geological information gained from published papers and unpublished theses, together with data collected in the field by the present author during the period October-December 1990. Field work involved regional reconnaissance mapping, followed by systematic sampling along transverse sections of the Complex.

The geology of the Complex in the study area is shown in figure 5 and on Map 1 (back pocket), which are based on the geological maps of Hammerbeck (1977).

4.2 HISTORICAL REVIEW

The name Usushwana originates from the Usushwana River in Swaziland (meaning "Little Usutu"), and was first used by Hunter (1951) to identify a suite of plutonic rocks ranging in composition from gabbro to micro-granodiorite, which is best developed in that area of Swaziland. The first comprehensive account of the Complex in Swaziland was published by Winter (1965) and later by Hunter (1970a). Extensions of the Complex into South Africa (south of latitude 27°S) were mapped by Humphrey and Krige (1931) and recently reinvestigated by Smith (1983). The area north of latitude 27°S was studied by Van Vuuren (1965) and by Hammerbeck (1977).

4.3 EXTENT, SHAPE AND THICKNESS OF THE COMPLEX

Within the study area, the Usushwana Complex is represented by two parallel belts of intrusive rocks of variable width, separated from one another by sediments and volcanics of the Pongola Sequence and the Amsterdam Formation, and bordered by granitic rocks of the pre-Pongola

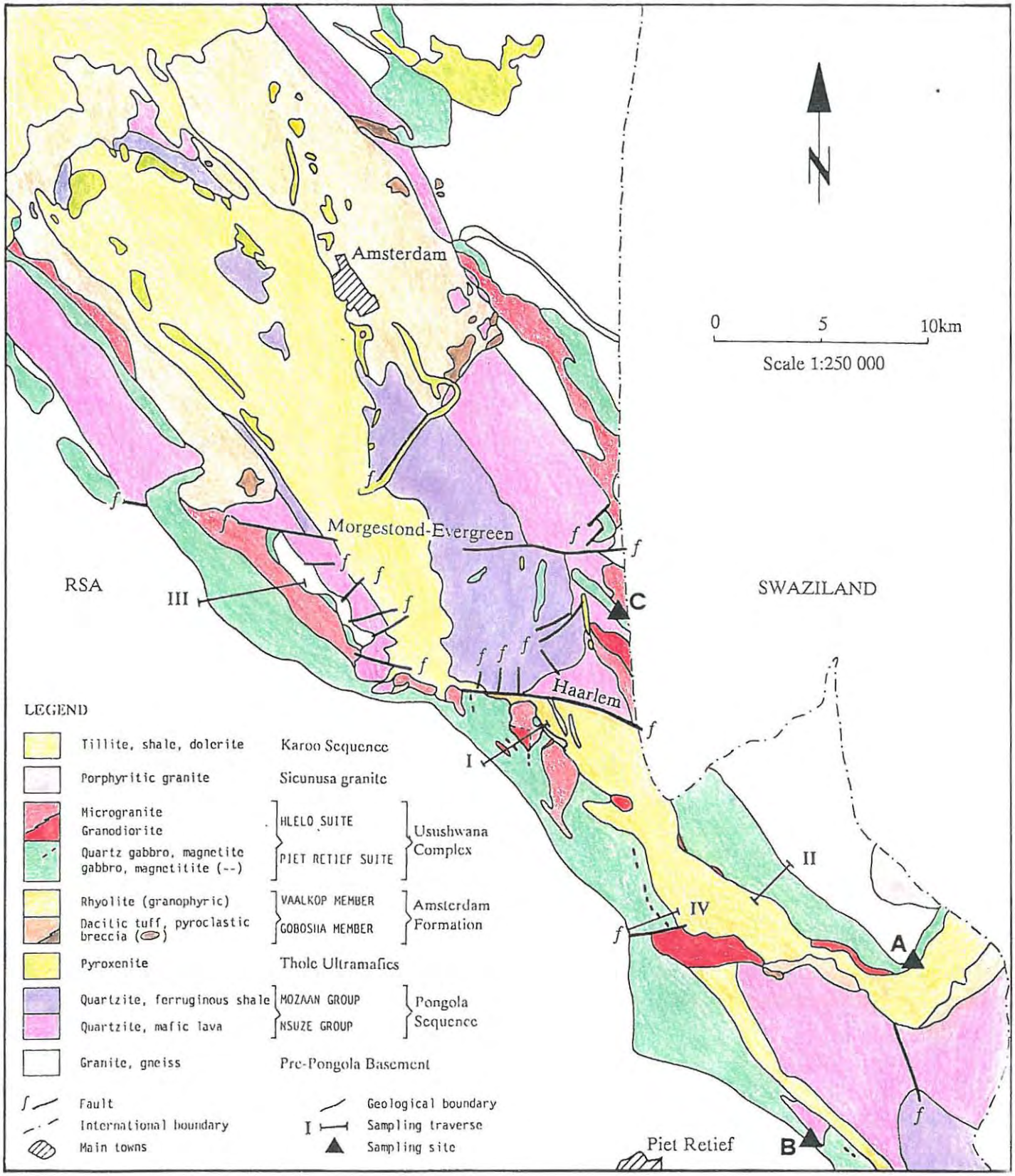

Fig. 5 - *Generalised geological map of the Piet Retief-Amsterdam area, south-eastern Transvaal (modified after Hammerbeck, 1982).*

basement. In the present study, these two belts are informally referred to as the Western and Eastern limbs.

The true extension of the Usushwana Complex at surface, together with its geometry at depth, can be estimated from available geophysical data. Aeromagnetic and gravity surveys undertaken by the Geological Survey of South Africa in the late sixties and early seventies (Hammerbeck, 1977) indicate that, at their north-western extensions, both segments of the Complex can be traced for a further 20 km beneath the younger Karoo cover. The northernmost part of the Complex terminates abruptly against a NE-trending feature of uncertain status.

Detailed reconnaissance surveys have shown that there are gravity highs over the mafic rocks of the Usushwana Complex, with much reduced gravity relief over the surrounding granitic and sedimentary rocks (maximum Δg in the order of +40 mgal). The preferred interpretation of the gravity data is that the geometry of the intrusion at depth changes from north to south. In the Amsterdam area (Fig. 6, traverse I and II), the structure (as defined by the Usushwana Complex and the overlying Pongola sediments) is that of a nearly flat-bottomed basin; contacts of the intrusion appear to dip inwards at about 45°. A connection between the two limbs of the Complex in the central part of the structure is supported by aeromagnetic data. Maximum inferred depths are in the order of 4200 to 5500 m. North-east of Piet Retief (Fig. 6, traverse III), a longitudinal, funnel-shaped cross-section best fits the observed residual gravity anomaly, and may represent a feeder zone. The geometry of the Usushwana Complex, as interpreted from Traverse III, resembles that of the Great Dyke (Zimbabwe), in particular the southern part of the Wedza Subchamber (Podmore, 1970). A break in the continuity of the two mafic limbs at depth is suggested from the interpretation of Traverse IV (Fig. 6), which also indicates that the intrusive contacts of the Complex become steeper southwards (up to 65° dip). Inferred depths of the Complex in the Piet Retief area vary between 3000 and 4500 m.

A precise evaluation of the thickness of the Usushwana Complex in the study area is difficult, due to the combination of limited exposure,

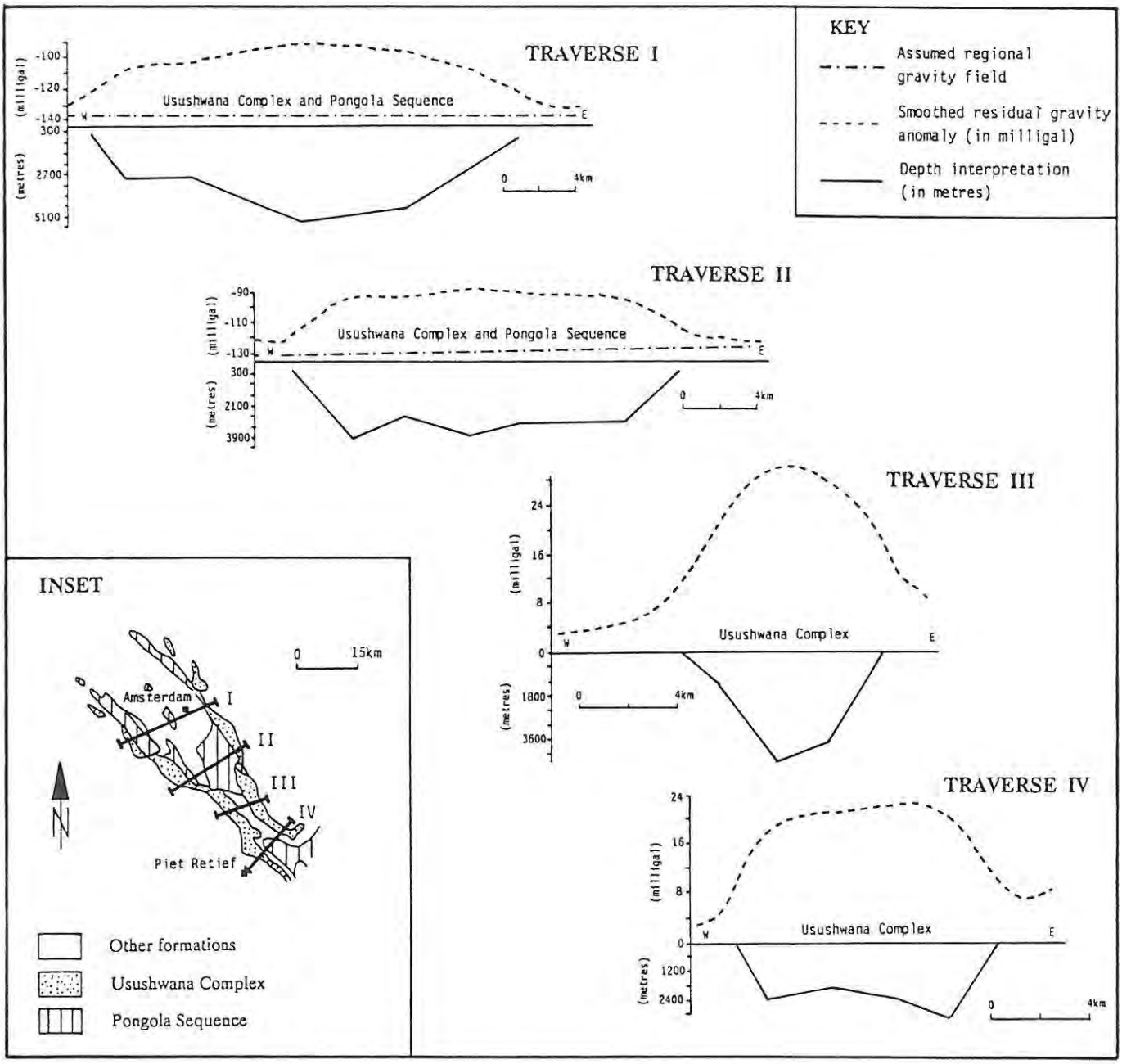

Fig. 6 - *Depth interpretation of the Usushwana Complex and Pongola Sequence from gravity data (modified from Hammerbeck, 1977).*
Inset shows approximate position of the gravimetric traverses.

gentle topography and a general lack of structures such as layering. Thus, the stratigraphic thickness of the Usushwana Complex can only be estimated. Attempts to assess the thickness on the farm Sterkwater 472 IT proved unsuccessful on two accounts: firstly, layered gabbros

(strike 090°, vertical) were found to be only a local feature, restricted to a few outcrops; secondly, their present attitude has been influenced by tectonic movements subsequent to their formation. On the farm Ishlelo 441 IT, the exposed section of the Usushwana Complex is considered to attain a minimum thickness of ≈750 metres. This calculation is based on information gained from the attitude of the magnetitite layers (060°, 20°), as determined from aerial photographs. Significant differences in dip were observed between the magnetitite layers and the basement gneisses at this locality, (dipping at 20° to the E-NE and at 80° to the W-SW, respectively). The inclination of the magnetitites also differs from that of the walls of the intrusion (≈65°), as suggested by the gravity survey carried out immediately south of Ishlelo 441 IT (Fig. 6, traverse III). From the above, it can be concluded that the stratigraphic thickness of the Usushwana Complex is much greater than that indicated by its present-day outcrop.

4.4 STRUCTURAL SETTING OF THE COMPLEX

The most important structural feature in the study area is represented by the Pongola-Usushwana fold axis, to which an age of approximately 3000 Ma has been assigned (Van Eeden, 1972). This NW-trending structure was formed after the deposition of the Pongola Sequence and constituted a zone of weakness along which the Usushwana Complex was thought to have intruded. The Pongola-Usushwana fold structure comprises several major synforms, the most distinctive of which is the 20 km wide Amsterdam Syncline (Fig. 5). It extends north-eastwards for at least 40 km, passing under the Karoo cover in the north, and is terminated by the Haarlem fault in the south. After its formation, the Amsterdam Syncline (and similar synforms, east and south-east of Piet Retief) was disrupted by normal transverse and longitudinal faulting. Most of these tectonic lineaments are pre-Karoo in age and are presumably related to the emplacement of the Usushwana Complex. They define a structural pattern with a strike direction of 130°-170° (Hammerbeck, 1977). Additional important lineaments have a strike orientation of 90° to 110° and 0° to 20°. The latter direction in

particular is characteristic of lineaments traceable for more than 5 km. This is tentatively taken as evidence for interference folding along a NS axis, which could have been responsible for the sharp flexure of the Complex north-east of Piet Retief (Hammerbeck, 1982).

4.5 AGE OF THE COMPLEX

The Usushwana Complex has intruded along the contact between the pre-Pongola basement and the Pongola Sequence. These lithologies have been dated at 3070 ± 60 Ma (Homogeneous granite, Swaziland, Rb-Sr; Allsopp et al., 1962) and 2940 ± 22 Ma (U-Pb on zircons from felsic volcanic rocks; Hegner et al., 1984) respectively, the latter indicating a maximum age for the Usushwana Complex. Rb-Sr measurements on the granites that intruded the Usushwana suite in Swaziland are of little help in establishing a minimum age for the Complex, as they record ages between 2200 ± 50 and 2880 ± 340 Ma (Allsopp et al., 1962).

Direct measurements on the mafic rocks of the Complex were first attempted by Davies et al. (1970), but due to the very low Rb/Sr ratios, meaningful isochrons could not be constructed. Granophyric rocks yielded an age of 2874 ± 30 Ma (Davies et al., 1970), but the isochron is strongly dependent on a sample of aplogranite whose genetic association with the main body of acid rocks is apparently uncertain. More recently, Hegner et al. (1984) dated ultramafic rocks from the Amsterdam area at 2871 ± 30 Ma (Sm-Nd). These authors appear to have made measurements on samples from the Thole ultramafics, which are not strictly considered as a part of the Usushwana Complex, though they have been ascribed to the same magmatic cycle (see section 3.2.3). Therefore, considering the greater reliability of the Sm-Nd over the Rb-Sr methods (Hegner et al., 1984), and that the emplacement of the Thole ultramafics was followed by a hiatus prior to deposition of the Amsterdam Formation and the emplacement of the Complex, an age younger of 2871 ± 30 Ma may be considered reliable for the Usushwana intrusion.

4.6 LITHOLOGY AND STRATIGRAPHY OF THE COMPLEX

The Usushwana Complex comprises an assemblage of mafic, ultramafic and granitoid rocks, which have been traditionally grouped into mafic, dominantly gabbroic, and acid suites, the latter consisting mainly of granophyric granodiorite and microgranite. Broad estimates of the relative proportions of the various lithologies are reported in Table I. Disconnected lensoid bodies and layers of titaniferous magnetitite are commonly associated with the gabbroic rocks at a number of localities. In the study area, the mafic and acid suites appear to be symmetrically disposed along the two limbs of the Complex (Fig. 5, attached geological map). The former is generally observed to be in contact with the basement rocks which border the intrusion; the latter usually passes to the Vaalkop rhyolites, the Amsterdam lavas or the formations of the Pongola Sequence in the central part of the structure.

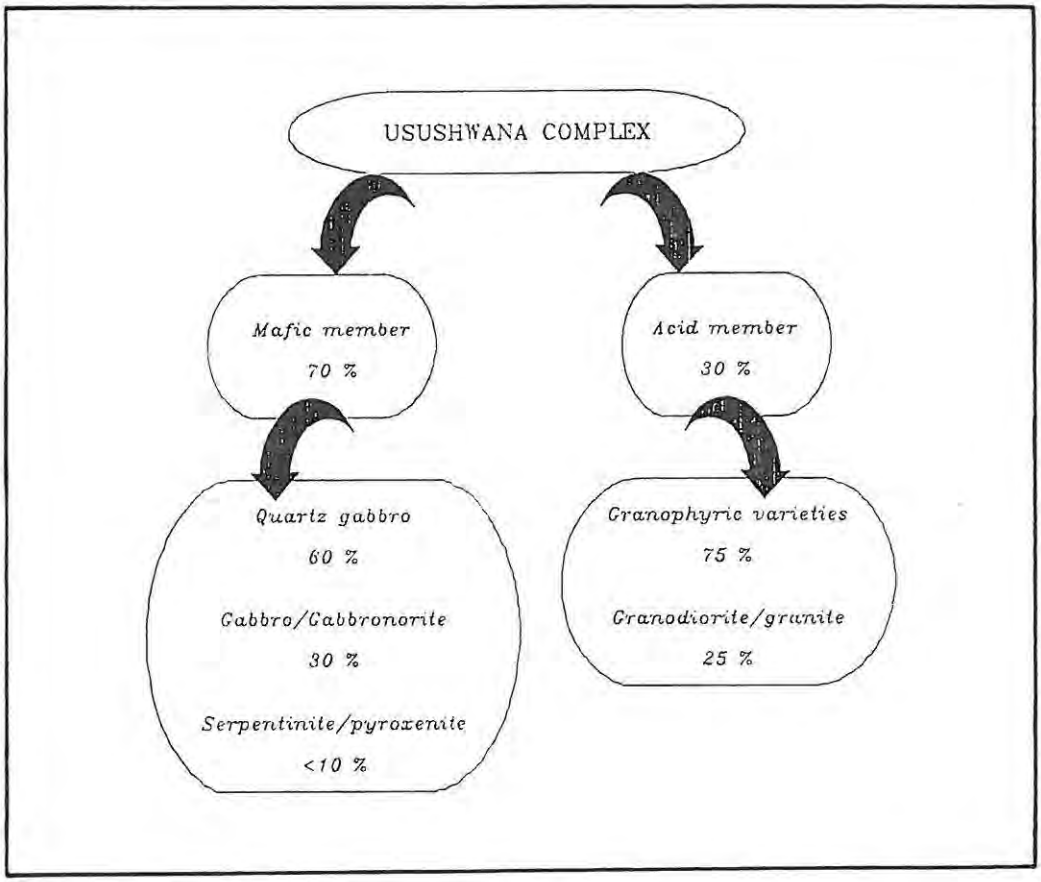

TABLE I - *Relative proportions of various lithologies of the Usushwana Complex (modified after Wilson, 1990).*

Interpretations put forward for the origin of the acid suite proposed that it formed either as a late independent phase of the intrusion (Haughton, 1969), or as the differentiation product of a late batch of mafic magma (Winter, 1965), with intervening remelting of the country rocks and extensive contamination (Hunter, 1970a; Hammerbeck, 1977).

A major objective of the present study was to determine the extent to which rocks of the Complex (including the mafic suite) have undergone igneous differentiation, and to establish the degree (if any) of contamination. A reconnaissance survey was first conducted by the writer in the study area, mainly aimed at acquiring familiarity with the rock-types of the Complex. The maps prepared by Hammerbeck (1977) formed the basis of the survey, and subsequently 4 sites were selected where detailed sampling could be carried out along transverse sections. The location of the sampling traverses is shown in figure 5, and the list of the localities is reported below:

- HLELO RIVER SECTION, Ishlelo 441 IT
- STERKWATER SECTION, Sterkwater 472 IT
- MORGENSTOND SECTION, Morgestond 418 IT
- DERBY SECTION, Derby 444 IT.

With the exception of the Sterkwater Section, all the traverses were selected from the Western limb of the Complex.

Working on the assumption that differentiation occurs from the base to the top of mafic intrusions, a decision was made to carry out sampling of traverses across the mafic member and up into the overlying acid member, that is from the basement-mafic contacts towards the inner part of the limbs. Due to the discontinuous exposure, some of the traverses had to be shifted laterally several times, thus introducing possible gaps or partial repetitions of the sequence. The description of the lithologies observed, their mode of occurrence and their vertical variation is given below for each traverse. Further descriptions of the rock-types of the Complex have been given from regional sampling sites of particular interest (for example where there are different lithologies present or where there is evidence of mineralisation). These localities are also shown in figure 5.

4.6.1 HLELO RIVER SECTION - Ishlelo 441 IT

The section of the Usushwana Complex outcropping on Ishlelo 441 IT (here referred to as the Hlelo River Section) is undoubtedly the most continuous and best exposed (Fig. 5, traverse I). It contains the greatest variety of rock-types, and preserves features which have important implications for the evolution of the Complex.

A total of 351 samples were collected at this locality, the sampling being carried out along the Hlelo River for about 4.5 km. Samples were taken from either the river bed or banks, at sampling intervals of 10 m. A schematic representation of the traverse indicating the position of each sample is reported in figure 7. Additional samples were collected in the surrounding area in order to fill in any gaps.

The stratigraphy of the Usushwana Complex as derived from the Hlelo River Section is depicted in the stratigraphic column of fig. 8, which combines both field and microscopic observations. A lithological cyclicity characterises the Section, for which a total stratigraphic thickness of at least 750 m has been calculated (see section 4.3). Two major cycles can be distinguished: the base of the first cyclic unit (samples U1 to U218) is taken at the contact with the basement gneisses. The unit then extends for a stratigraphic thickness of about 360 m. The second cyclic unit (samples U345, U219 to U262, U399 to U483) exhibits a sharp basal contact with the underlying unit and is at least 400 m thick (its total stratigraphic thickness cannot be indicated with certainty, as a major gap marks the transition to the Vaalkop rhyolites, which here are believed to represent the roof of the intrusion).

1st CYCLIC UNIT

The first cyclic unit consists mainly of quartz and magnetite-bearing gabbros, which grade upwards into granodiorites (Fig. 8).

The basal portion of the unit is characterised by medium-grained

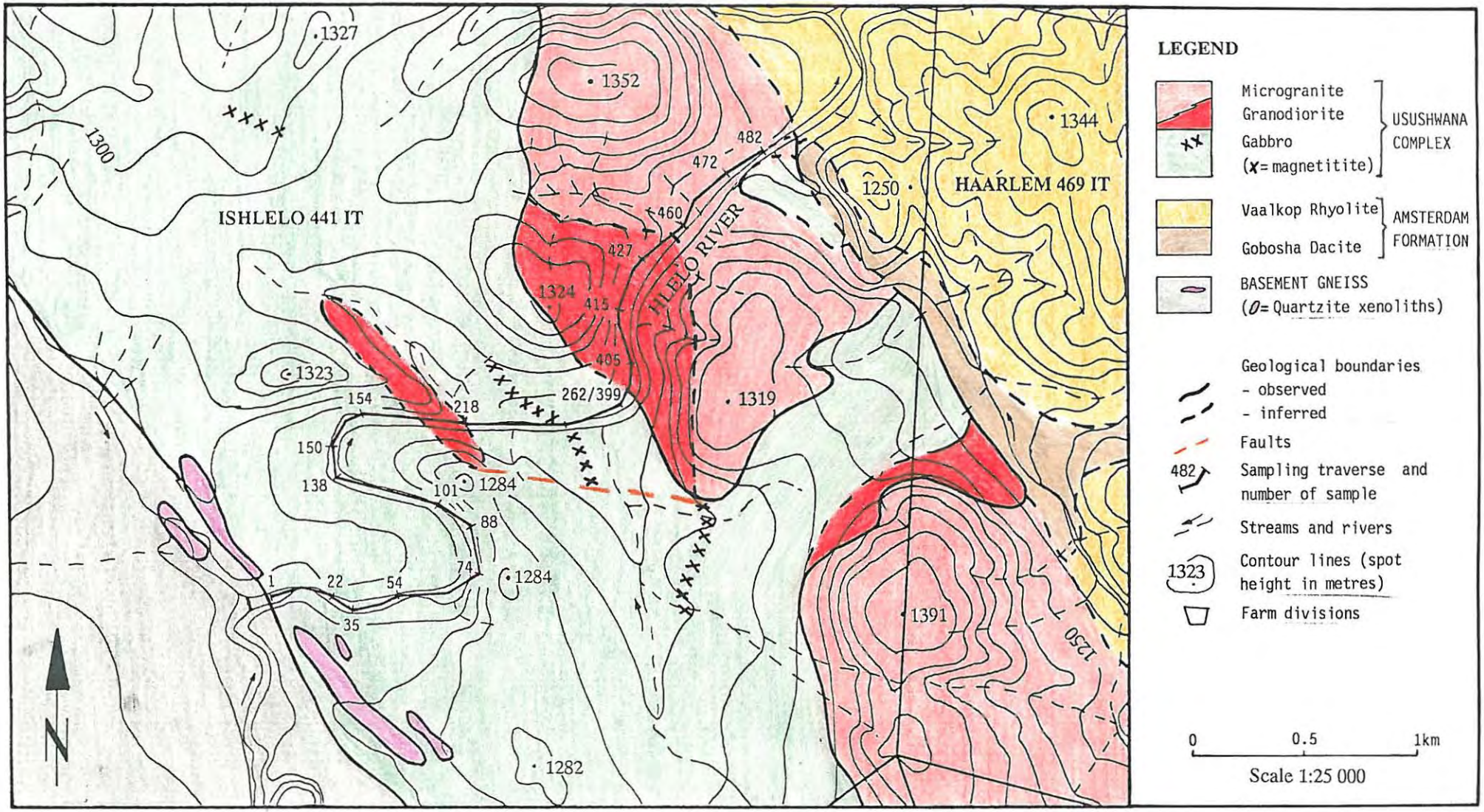

Fig. 7 - *Geology and location of the Hlelo River Section (for location of farm Ishlelo 441 IT, refer to figure 2).*

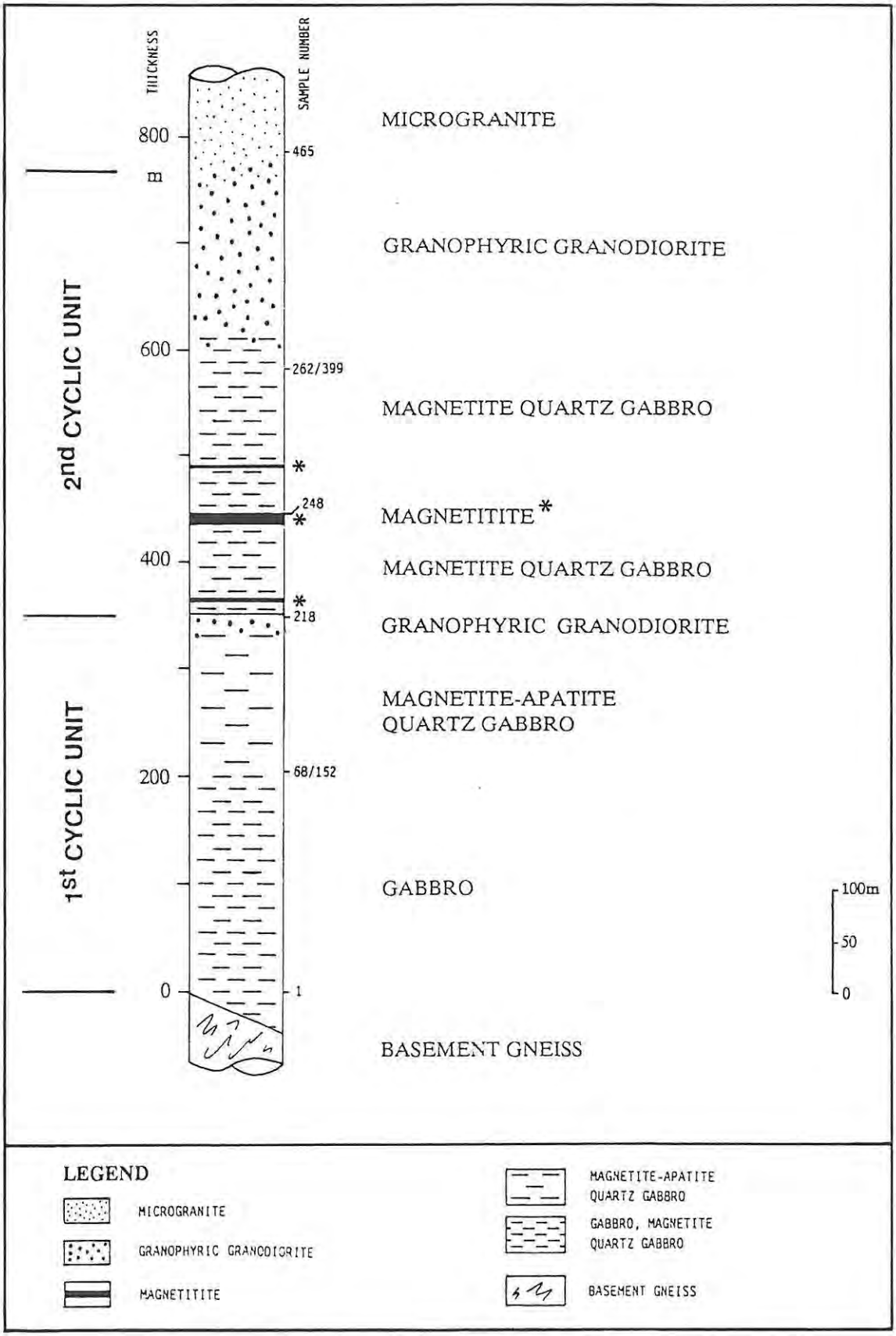

Fig. 8 - *Schematic stratigraphic column of the Usushwana Complex (Hlelo River Section, Ishlelo 441 IT).*

gabbros in sharp contact with the basement, which here is represented by a medium-grained gneissic variety of the Homogeneous Hood granite (Plate 1). No significant differences in strike were observed between the gneiss schistosity (attitude 250°, 80°) and the intrusive contact (striking at about 160°), but the Complex appears to dip to the E-NE at about 20° (see section 4.3). Neither reduction in the gabbro grain-size, nor increase in the amount of pegmatoidal material were observed close to the contact. A structural control on the emplacement of the Complex is indicated by the mafic minerals, which in the gabbro are aligned parallel to the contact of the intrusion (Plate 2). This feature provides evidence for shearing and deformation at high temperatures (at least in the order of 500° C; A.H. Wilson, pers. comm., 1990).

The basal gabbros generally consist of mesocratic, medium- to coarse-grained, equigranular, quartz-rich varieties. In places, the gabbros grade into plagioclase-bearing pyroxenites, due to local enrichment in pyroxene. Both plagioclase and pyroxene have been affected by alteration and weathering: the plagioclase is characterised by a greenish colouration due to saussuritisation, while pyroxenes are extensively uralitised and chloritised.

Upwards, a gradational change is observed into finer grained and more melanocratic varieties, the latter feature being possibly related to a more extensive alteration. The transition is marked by the presence of abundant, coarse- to medium-grained pegmatoidal material, consisting of euhedral crystals of plagioclase with minor clinopyroxene, and is indicative of a high concentration of fluids at this stage of evolution. Further up, quartz and magnetite become concomitantly more abundant in the succession, giving rise to a well-defined package of quartz and magnetite-bearing gabbros (*). Magnetitite layers are not

(*) The term magnetite-bearing gabbro is preferred to the term "ferrogabbro" used by Hammerbeck to describe gabbroic rocks which contain magnetite. In fact, the composition of pyroxene in these rocks (Enstatite 45%) is not of the extreme Fe-rich variety (Enstatite <0.30) which is typical of ferrogabbro in other layered intrusions (Wilson, 1990).

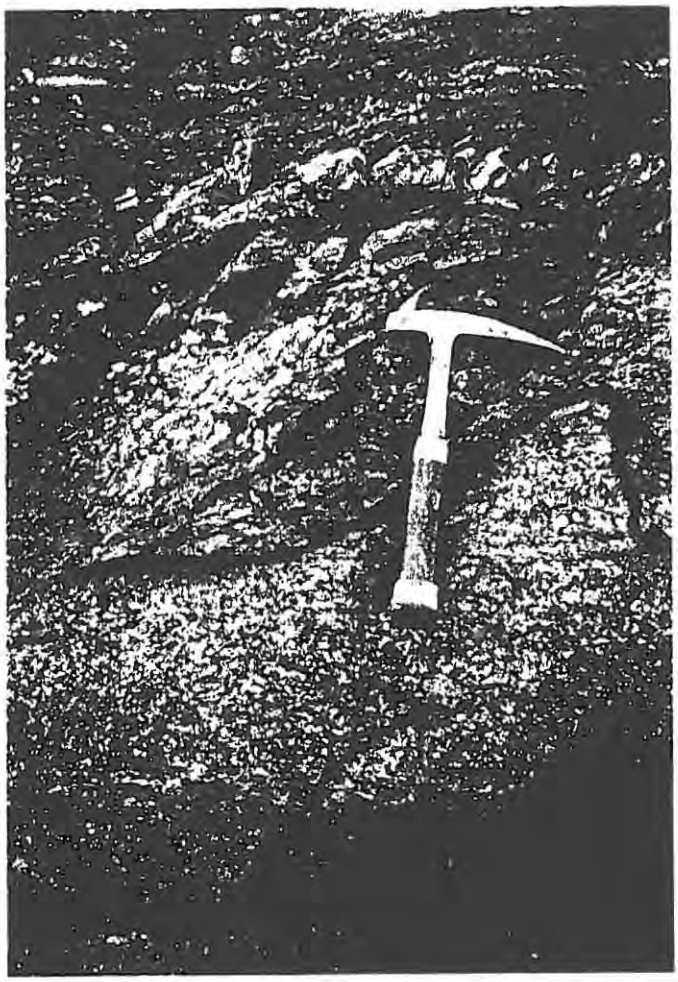

Plate 1 - *Contact between the basement gneisses (top) and the Usushwana gabbro (bottom) (Ishlelo 441 II).*

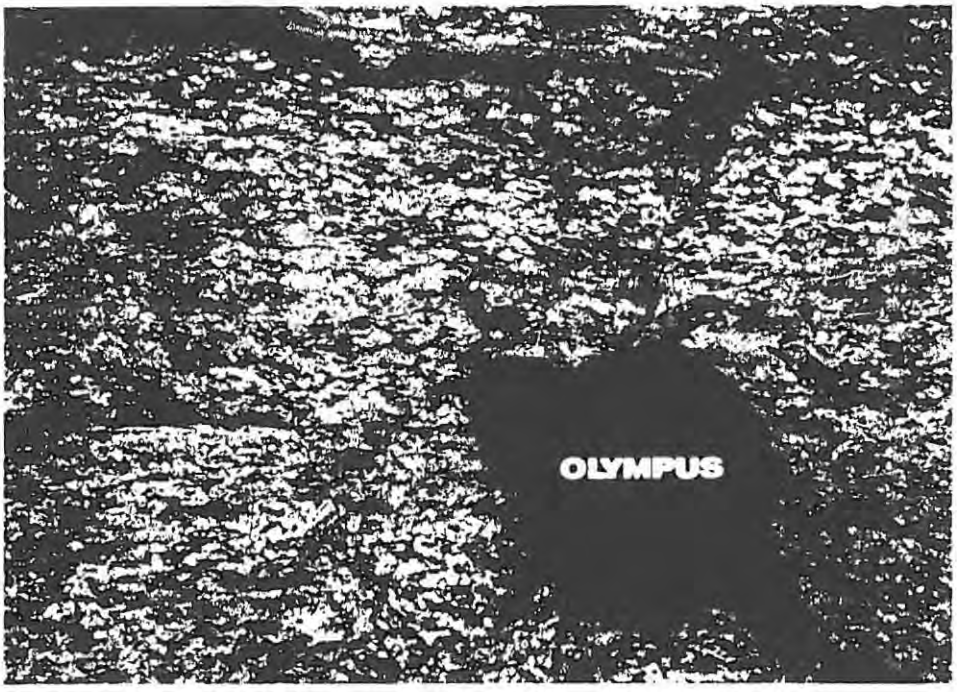

Plate 2 - *Alignment of mafic minerals (pyroxenes) in the gabbros, parallel to the contact of the intrusion (Ishlelo 441 II).*

developed in the first cyclic unit; the only significant occurrence is that of a small, fine-grained magnetite-rich lens, 1 m long and 30 cm thick. The lens appears to be discordant with the general attitude of the Complex, striking at 125°.

The top of the first cyclic unit is marked by a gradual transition to rusty coloured rocks of granodioritic composition, which outcrop in the study area as resistant ridges or hills. The most distinctive macroscopic feature of these rocks is the presence of amphiboles in the form of irregular aggregates and long needles (up to 15 cm in length; Plate 3). The modal proportion of amphibole present in the rock is highly variable, and is largely responsible for the changes in grain-size (Plate 4) and the observed gradation from mesocratic to more leucocratic varieties. No xenoliths of gabbro were observed in the granodiorite.

2nd CYCLIC UNIT

In the second cyclic unit, magnetite-rich gabbros with interlayered magnetitite layers at the base are overlain by granodiorites, which in turn grade into microgranites (Fig. 8).

The basal portion of the second unit is not well exposed, but quartz-rich, magnetite-bearing gabbros are in sharp contact with the granodiorite of the first unit. The magnetite-bearing gabbros are texturally similar to the mafic rocks of the first unit, and display a similar trend to more quartz-rich varieties.

Two layers of massive magnetitite are interlayered with the gabbros. The layers dip at 15° to 25° to the E-NE. An average inclination of 20° has been used to estimate the whole thickness of the outcropping portion of the Complex (see section 4.3). The lowest magnetitite is about 0.5 m thick and can be followed for a few tens of metres along strike. The second layer forms a prominent scarp and can be traced over a distance of 4.5 km north and south of the Hlelo River (Plate 5). It occurs as irregular lenses of extremely variable thickness (up

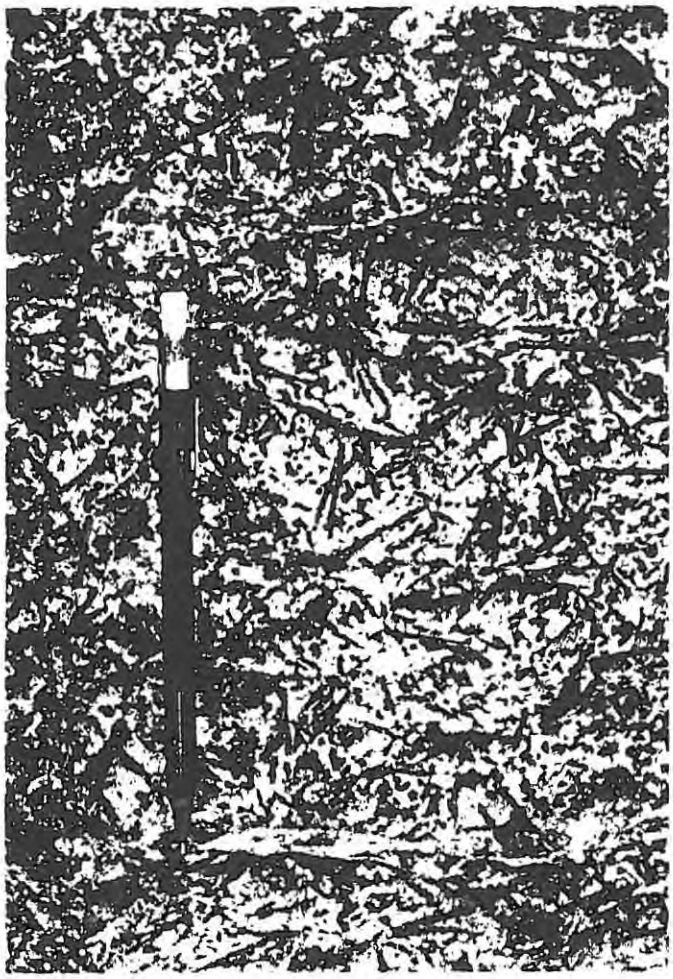

Plate 3 - *Irregular hornblende aggregates in the granodiorites (1st cyclic unit, Hlelo River Section, Ishlelo 441 11).*

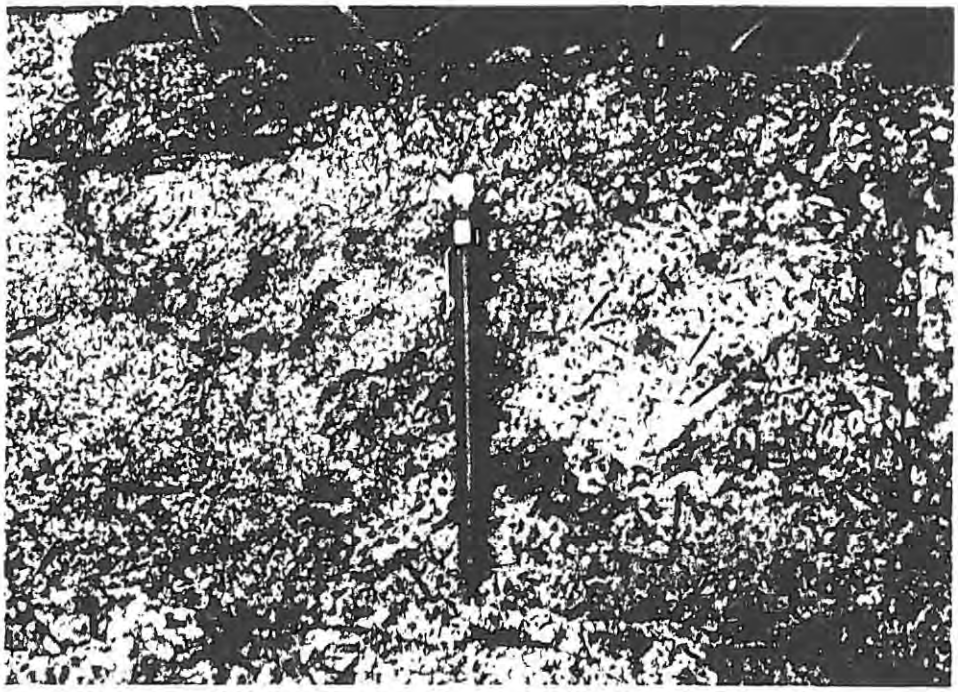

Plate 4 - *Grain-size variations in the granodiorites (2nd cyclic unit, Hlelo River Section, Ishlelo 441 11).*

Plate 5 - *Discontinuous magnetitite layers at the Hlelo River Section (Ishlelo 441 IT).*

to 10 metres), and is disrupted by minor faulting. The occurrence of a third layer, stratigraphically higher, is suggested by the presence of magnetite rubble parallel to the strike of and up slope from the other two layers. Contacts between magnetitites and contiguous rocks are not exposed, but a progressive increase in the amount of silicate material downwards into the underlying magnetite-bearing gabbros is discernible; the upper contacts appear to be abrupt, as suggested by the development of ore pavements. The magnetitite layers are essentially monomineralic rocks, consisting of fine-grained, equigranular aggregates of polygonal magnetite grains. These are up to 2-3 mm in diameter and reddish brown to purple in colour. Minor silicate impurities, now altered to a soft reddish clay and chloritic material, fill the interstices between the magnetite grains. The magnetitites are extensively weathered in outcrop and show advanced oxidation and hydration to haematite and goethite. Two perpendicular sets of joints are generally present and, as a consequence, the magnetitite breaks into small rectangular blocks. Goethite is particularly abundant along joint planes. Apart from evidence of minor

folding, the magnetitites are devoid of other internal structures.

Overlying the magnetite-rich layers, the magnetite-bearing gabbros grade upwards into granodiorites similar in character to those of the first unit. The modal content of amphibole, though highly variable, generally decreases upwards, and the granodiorites progressively give way to a fine- to medium-grained equigranular rock of granitic composition. The latter displays a distinct red colour on a fresh surface, and has been referred to as microgranite. Slender needles of amphibole (up to 1 cm long) may be present, best observed on weathered surfaces.

A characteristic feature of the Complex is the abundance of xenoliths, many of which show evidence of corrosion. On Ishlelo 441 IT, several elongated xenoliths of fine-grained, grey quartzite (probably remnants of the Nsuze Group quartzites) were observed along and near the contact with the pre-Pongola basement. Smaller, irregular to rounded quartzite xenoliths (some tens of cm to several m in extent) commonly occur within mafic rocks throughout the intrusion. Some of the quartzite xenoliths have been completely recrystallised, and now appear as equigranular aggregates of quartz (1-2 mm in diameter) with associated minor mafic minerals which impart a spotted appearance to the rock. Xenoliths of basement granites were not observed on Ishlelo 441 IT, but are reported from other parts of the Complex (Smith, 1983, in Wilson, 1990). A melanocratic rock of gabbroic composition, which contains small amounts of sulphide, was found within the granodiorites of the second cyclic unit, and is likely to represent a xenolith from the lower parts in the intrusion.

Sulphides have been observed throughout the entire stratigraphic sequence. Pyrite and chalcopyrite are the most common phases present; they are most abundant in the basal portion of the first cyclic unit, and tend to be concentrated along small fractures.

Mafic dykes of varying extent and thickness (up to a few tens of cm) are a common feature of the Hlelo River Section. Quartz-veins crosscut the gabbros; they vary in thickness from a few cm to more than 1 m.

4.6.2 STERKWATER SECTION - Sterkwater 472 IT

The Sterkwater Section represents the Eastern limb of the Usushwana Complex (Fig. 5, traverse II). Sixty specimens (U352-U398, U621-U633) were collected at a sampling interval of ≈10 m, from the contact with the basement, across the intrusion, and in to the Vaalkop rhyolites (Fig. 9). The contacts of the intrusion with the country rocks are not exposed at this locality.

A trend similar to that observed in the units of the Hlelo River Section was identified on Sterkwater 472 IT, though only one cycle can be recognised at this locality. The basal portion of the section consists of mesocratic, medium-grained, homogeneous quartz gabbros. A green and a brown pyroxene can be distinguished on the weathered surface. Weathering has also resulted in the oxidisation of the occasional sulphides (pyrrhotite?) observed in the quartz gabbros. Iron stainings (together with serpentine) are a common feature along fractures. In the vicinity of the basement, the quartz gabbros are crosscut by abundant quartz veins (060°, 65°) and in places an alignment of the pyroxenes parallel to the contact of the intrusion is observed.

In the central part of the section, the quartz gabbros become more melanocratic and progressively grade into medium-grained magnetite-bearing gabbros. The magnetic response of the latter is generally weak, due to weathering. However, the iron enrichment is well documented by the presence of magnetite in the residual material. Magnetitite layers have not been observed in the Sterkwater Section. In places, leucocratic pegmatoidal material occurs associated with the magnetite-bearing gabbro.

A remarkable outcrop of magnetite-bearing gabbro displays primary igneous layering (Plate 6), and represents the only occurrence of this kind observed in the study area. The layered gabbro strikes at 090° in a nearly vertical disposition, which is likely to have been disturbed by tectonic movements. The layering is developed on a centimetre scale and is defined by alternating layers, respectively enriched in

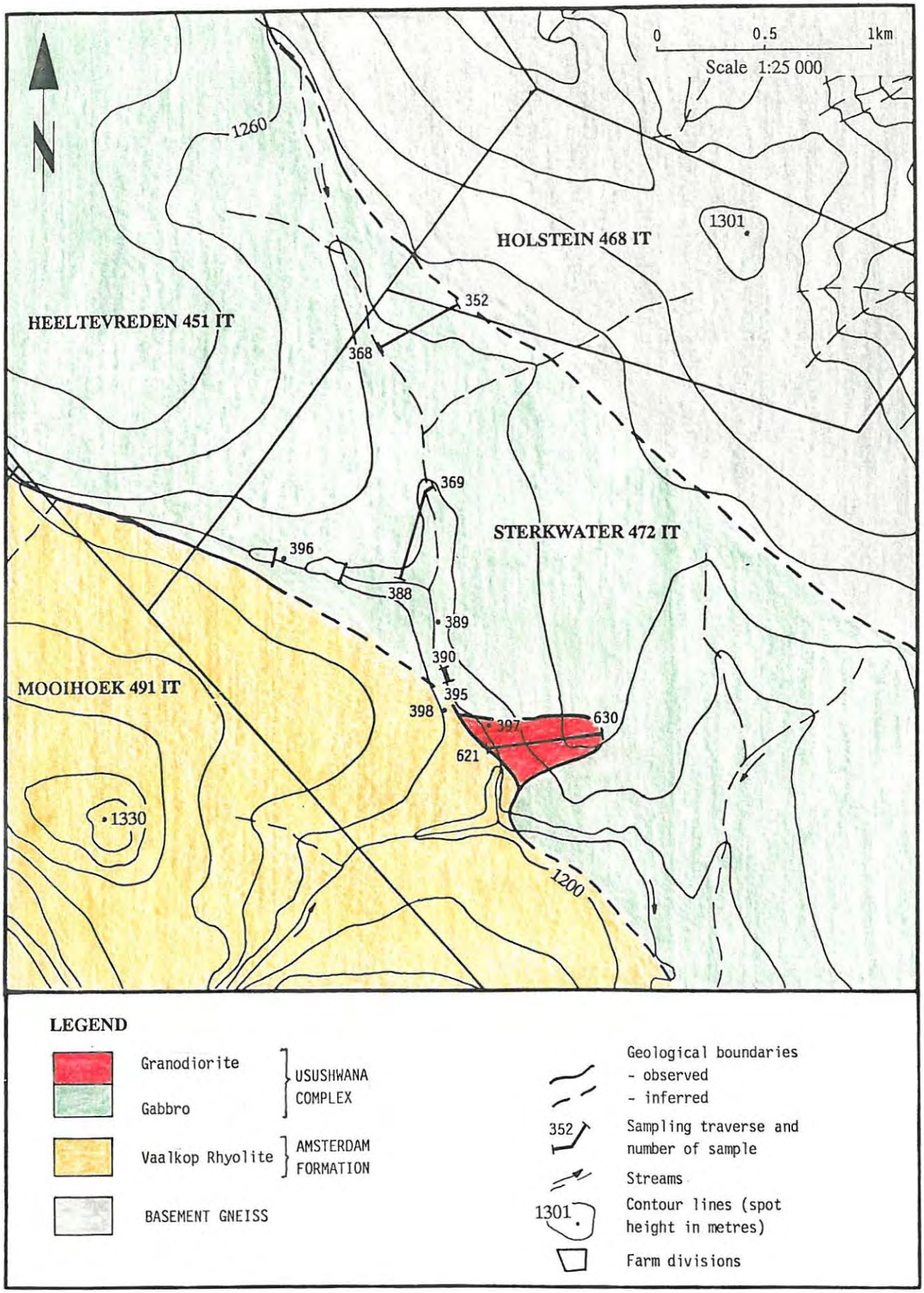

Fig. 9 - *Geology and location of the Sterkwater Section (for location of farm Sterkwater 472 IT, refer to figure 2).*

plagioclase and pyroxene. Inclusions of leucocratic gabbroic lenses occur subparallel to the layering. Erosional, "channel-type" structures are also common (Plate 7), and can be up to 1 m long and 25 cm in height. The polarity of these structures confirmed that the quartz and magnetite-bearing gabbro represent the lowest part of the intrusion, while the granodiorite stratigraphically overlies the mafic rocks.

A progressive increase in the amount of K-feldspar and amphibole (with a corresponding decrease in plagioclase and pyroxene) marks the transition from the magnetite-bearing gabbros to a medium-grained melanocratic granodiorite, which strikingly resembles the granodiorite found in the Hlelo River Section. No microgranite was observed along the Sterkwater Section, though the Vaalkop rhyolites (which here represent the roof of the intrusion) display similar macroscopic features. A pronounced break in the chemical trends was found by Hammerbeck (1977) to mark the transition between these two rock-types.

Though magnetitites do not occur in the Sterkwater Section, a magnetitite layer was observed 7.5 km to the south-east of this locality (on Strydkraal 477 IT; Fig. 5, point A), representing the only occurrence of magnetitite in the Eastern limb of the Complex. Scattered outcrops of massive, inequigranular magnetitite can be followed for at least 50 m in a north-easterly direction. No clear stratigraphic relationships of the magnetitite to the footwall and hanging-wall lithologies could be ascertained, due to poor exposure and intense tectonic deformation. However, the magnetitite is enclosed by more mafic rocks than elsewhere. These are represented by a package of medium-grained, melanocratic gabbros, in places grading into a plagioclase-bearing pyroxenite. Although no magnetic response was obtained from this gabbro, a high magnetite content is suggested by the widespread development of ferricrete in the surrounding area.

Plate 6 - *Centimetre scale layering in the magnetite-bearing gabbros, in an almost vertical disposition (Sterkwater 472 IT).*

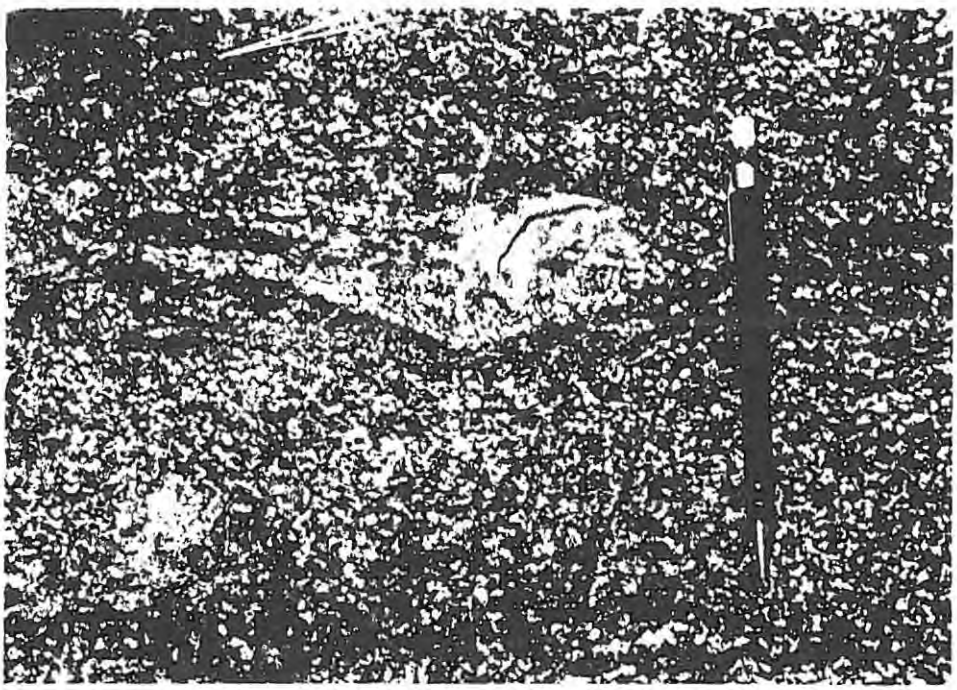

Plate 7 - *Channel-type structure in the layered magnetite-bearing gabbro (Sterkwater 472 IT).*

4.6.3 MORGESTOND SECTION - Morgestond 418 IT

The Morgestond Section is the northernmost of those considered on the Western limb of the Usushwana Complex (Fig. 5, traverse III). The section is relatively well exposed, but lacks the variety of rock-types and the lithological cyclicity of the Hlelo River Section. Therefore, the sampling was carried out at an average interval of 20 m, and a total of 88 samples were collected (U528-U615) (Fig. 10).

On Morgestond 418 IT, the Usushwana Complex is bordered by leucocratic, equigranular basement granites, characterised by abundant quartz veins. The mafic member of the Complex largely consists of mesocratic, quartz-rich gabbros with a typical knobbly surface (due to differential weathering of plagioclase and pyroxene). The grain-size of the quartz gabbro is highly variable, changing from fine- to coarse-grained varieties on a very small scale. Pyroxene enrichment occurs in places. Locally, biotite and very small amounts of sulphide (pyrite and chalcopyrite) represent additional phases. Irregular veins of finely crystalline quartz, up to 50 cm in thickness, are a common feature. Sulphide-bearing mafic dykes and sills are also frequently observed.

A sharp increase in the iron content characterises the upper part of the mafic member, and has led to the development of a medium- to coarse-grained magnetite-bearing gabbro. The real extent of the latter could not be established due to poor exposure in this part of the Section. A narrow band of a highly weathered, amphibole-rich rock is irregularly developed on top of the magnetite-bearing gabbro, and is considered to be the equivalent of the granodiorites observed in other traverses. A general decrease in the grain-size of the gabbro and granodiorite can be observed as the irregular contact with the microgranite is approached. Veins of grey, medium- to fine-grained granitic aplite are widespread in the magnetite-bearing gabbro, and could represent a downward injection from partially remelted acid country rocks. Xenoliths of granites were also observed.

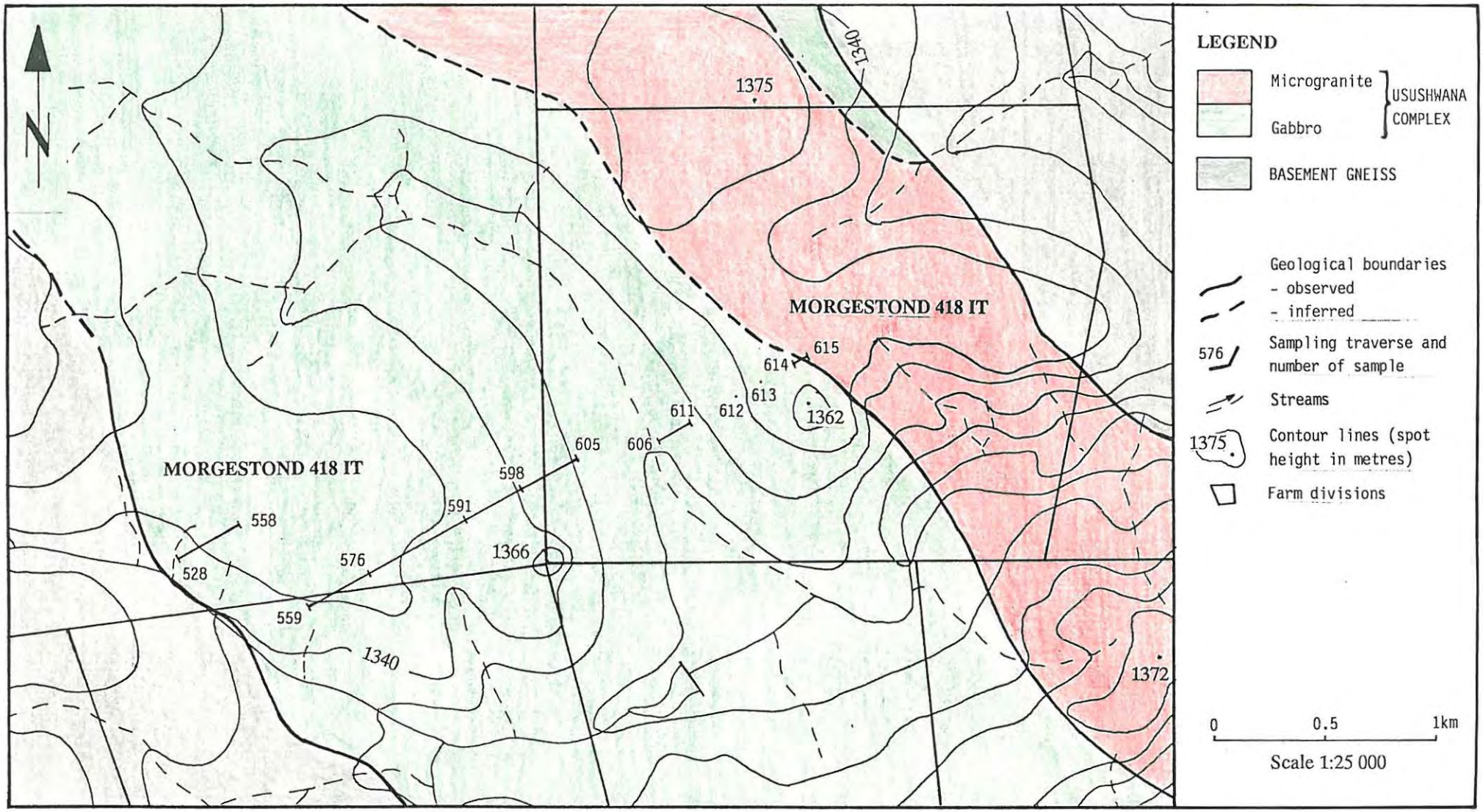

Fig. 10 - *Geology and location of the Morgestond Section (for location of farm Morgestond 418 IT, refer to figure 2).*

4.6.4 DERBY SECTION - Derby 444 IT

On Derby 444 IT, the Usushwana Complex is poorly exposed, but the area is of particular interest due to the presence of well-developed magnetitite layers (Fig. 5, traverse IV). The latter produce a fairly well-defined zone of magnetic anomalies in the order of 7000 nT (Hammerbeck, 1982).

The same stratigraphic trend observed elsewhere was established at this locality. Leucocratic basement granites are in sharp contact with medium-grained, mesocratic quartz gabbro, which displays evidence of shearing in the form of mafic minerals aligned parallel to the contact of the intrusion (striking at 085°).

A magnetite-bearing gabbro occurs higher up in the succession. It has been weathered extensively to produce a thick (50 cm at least), dark brown ferricrete. Lateritic material of this kind represents the footwall and hanging-wall of the two magnetitite layers outcropping on Derby 444 IT. These magnetitites display common features to those of the Hlelo River Section. The layers are only a few metres apart and can be followed for at least 4 km in a north-westerly direction. The magnetitites dip to the east at 30° to 60° and are extremely variable in thickness, thinning rapidly along strike. The magnetitite is massive, and in the less pure portions is highly weathered to a soft, clay-rich material. Because of the similarities displayed by the magnetitite layers at Derby and Ishlelo (see section 4.6.1), and their occurrence at approximately the same stratigraphic position, a tentative correlation between the two localities can be invoked.

Although granodioritic rocks of the acid member of the Usushwana Complex does not seem to be developed here, the transition from magnetite-bearing gabbro to the Vaalkop rhyolites is marked by the presence of highly weathered, hornblende-rich rocks. These form a narrow band only a few metres thick, and can be traced along the length of the magnetitite outcrops.

4.6.5 BLESBOKSPRUIT 515 IT

Only one well-mineralised sulphide occurrence was identified in the study area, that is on the farm Blesbokspruit 515 IT (Fig. 5, point B). Abundant pyrrhotite and chalcopyrite occur disseminated within a medium- to coarse-grained gabbro, which has weathered to form boulders. This rock-type has been described as "hyperite" by Hammerbeck (1977), but microscopic studies indicate that plagioclase and orthopyroxene are cumulus phases (see section 5.4), and therefore this rock is better classified as a noritic gabbro. Local variations to websterite were also observed.

Unfortunately, despite careful searching, no in-situ sulphide-bearing gabbro was found in the vicinity, thus precluding any evaluation of the extent of the mineralisation. For the same reason, difficulties arose when attempting to place this lithotype within the general stratigraphy of the Complex (as established from other localities). However, the proximity of the basement granites and the presence of basement xenoliths within the noritic gabbro/websterite indicate that the observed lithologies probably occur in the basal portion of the intrusion.

In places, the sulphide mineralisation is associated with leucocratic, coarse-grained pegmatoidal material, consisting of feldspar, pyroxenes and minor biotite. Quartz is observed to encrust the walls of small cavities.

A rock of similar composition outcrops along the Swaziland border (on the farm Evergreen 425 IT), but no occurrences of sulphides were observed in this area (Fig. 5, point C).

4.7 INTRUSIVE RELATIONSHIPS AND MODE OF EMPLACEMENT OF THE USUSHWANA COMPLEX

The Usushwana Complex has been emplaced along the contact between the basement lithologies and the Amsterdam Formation or the Pongola rocks. It is also intrusive into the Pongola Sequence itself, where major faults have apparently facilitated the emplacement (e.g. the Evergreen-Haarlem fault, Fig. 5; Hammerbeck, 1977). In the south-western portion, the Complex is bordered on either side by basement granites. Xenoliths of the latter, as well as of the Pongola quartzites and of volcanic rocks, are abundant in both the gabbroic and granitoid rocks of the Complex.

Complicated and somewhat contrasting relationships are observed between the mafic and acid suites of the Complex. As pointed out initially by Hunter (1970a), the volumetric proportion of the acid rocks to the gabbros exceeds that which would be expected if the former is a differentiated phase of the latter. The granodiorite can be traced along the contact between gabbroic and roof rocks, although its thickness can be considerably reduced to only few metres. On the other hand, microgranite does not always form the acidic counterpart of the mafic member, though it has never been found to outcrop in a different position. Hammerbeck (1977) reported an occurrence on Tweepoort 404 IT, where gabbro is chilled against the microgranite. Acidic magmatism post-dating the gabbroic rocks is indicated by aplite veins in the gabbro (e.g. on Morgestond 418 IT and Strydkraal 477 IT).

On the basis of the above-mentioned features and geochemical evidence presented later (see section 7.5 and chapter 8), the granodiorite is considered to be a differentiation product of a mafic parental magma; the microgranite is thought to have formed by partial remelting of acidic roof rocks, in particular the Vaalkop rhyolite.

Any interpretation of the mode of emplacement of the Complex must take into account the following:

- the occurrence of different lithotypes in different areas;
- the differentiation trend from mafic (or ultramafic) to acidic

rock-types;
- the evidence of the gravity data which generally suggest a steep-sided dyke-like body;
- the difference in dip between the layers of the Complex and the basement contact;
- the structural control of major NW-trending faults and synformal structures.

A schematic model for the emplacement of the Usushwana Complex is shown in figure 11. The Complex is thought to have intruded along graben structures in which the Pongola Sequence was preserved as major synforms (Fig. 11a, 11b). A common magmatic source, but separate feeders or different intrusive events, have been postulated by Hunter (1970a) and Hammerbeck (1977) to account for the composite lithological nature of the Complex. The greater abundance of ultramafic rocks in the Usushwana Complex as exposed in Swaziland is ascribed to a lower level of erosion (Wilson, 1990). The feeders are considered to have been distributed along two parallel lines of magma chambers, respectively extending through Piet Retief and through Mhlambanyati (in Swaziland). Differentiation of the mafic parental magma, together with extensive contamination and remobilisation of the country rocks, played an important role during the evolution of the Complex, and led to the formation of the acid suite. Intrusion of the Complex along zones of weakness caused the sagging of the grabens (Fig. 11c).

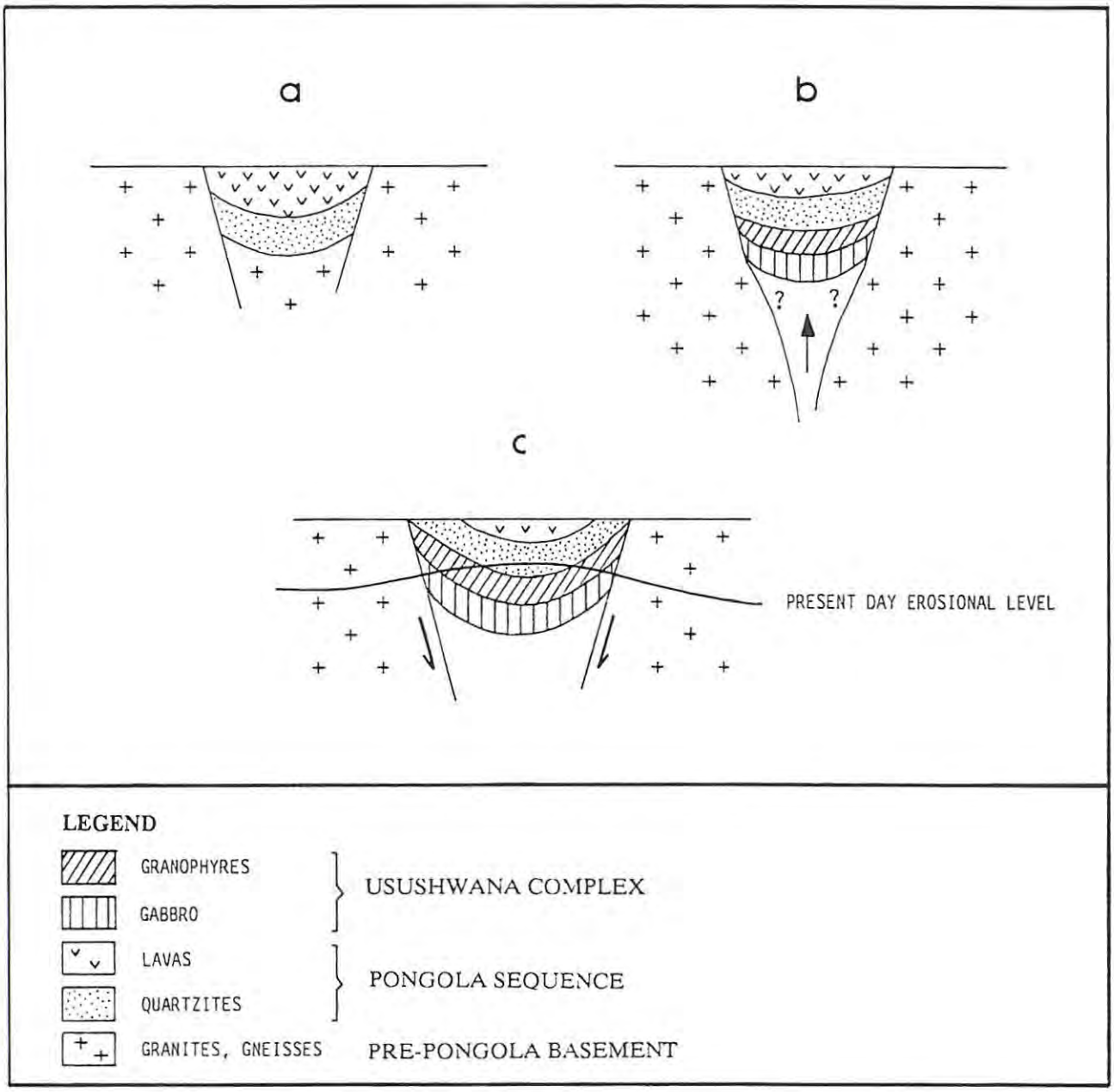

Fig. 11 - *Schematic mode of emplacement of the Usushwana Complex (modified after Hammerbeck, 1977). See text for explanation.*

4.8 SUMMARY

The Usushwana Complex in the Piet Retief-Amsterdam area represents an exposed segment of a layered intrusion. The average Sm-Nd age is 2.9 Ga (Hegner et al., 1984), and therefore the Complex represents one of the oldest layered intrusions of southern Africa. Its emplacement concluded a long period of magmatic activity, initiated by the Pongola volcanism, the emplacement of the Thole ultramafic sills and the extrusion of the Amsterdam lavas.

The Complex is elongated in a north-westerly direction, parallel to major faults and synformal axes. Gravity data indicate that it has the form of a dyke-like body, and extends to a depth of 3000 to 5500 m. Lithologically, the Usushwana Complex consists of a package of mafic rocks, overlain by granitoids, which intruded along the contact between the basement granite-gneisses and the overlying volcano-sedimentary successions of the Pongola Sequence or the Amsterdam Formation. The same vertical distribution of lithotypes was observed in both the Eastern and Western limbs of the Complex, and can be compared with that of the southern extensions of the intrusion (Smith, 1983, in Wilson, 1990). In general, all rock types of the Complex are highly weathered, and appear to have been subjected to low-grade metamorphism.

The stratigraphy of the exposed segment of the Usushwana Complex, as established from field observations in the study area, may be summarised as follows.

The basal portion of the Complex consists of coarse- to medium-grained, equigranular gabbros and quartz gabbros, with minor amounts of plagioclase-bearing pyroxenites. Intense shearing characterises the contact of these rock-types with the basement. A gradational upward change in lithologies was observed. The basal gabbros are overlain by more melanocratic and finer grained varieties, and grade into quartz-rich magnetite-bearing gabbros, due to a progressive increase in magnetite and quartz content. Layers and lenses of magnetitite (up to 10 m thick) are developed at this stratigraphic level. Ultramafic or

noritic rock-types are only sporadically present in the study area.

The granitoid suite which overlies the mafic portion of the Complex is composed of two major rock-types. The first is granodioritic in composition and typically amphibole-rich. A gradational relationship with the magnetite-bearing gabbros can be observed at several places, and supports a hypothesis that the granodiorite represents a differentiation product of the mafic magma. The second rock-type is a fine-grained granitic rock (referred to as microgranite), which generally occurs on top of the granodiorite. It may not be part of the intrusion, but could represent the melt fraction of the silicic roof rocks, thus constituting a roof facies of the Complex.

A lithological cyclicity was recognised along the Hlelo River Section. At this locality, two cyclic units are present: the first starts with quartz and magnetite-bearing gabbros, and then grades upwards into granodiorite; the second has magnetite-rich gabbros and magnetite layers at the base, which in turn are overlain by magnetite-bearing apatite quartz gabbros that grade into granodiorites.

The exposed mafic rocks of the Complex have generally a low sulphide content. Pyrite, chalcopyrite and minor pyrrhotite were observed in small amounts at different places, generally being more abundant in the lower part of the mafic sequence. Only one well-mineralised sulphide occurrence was identified in the study area (on the farm Blesbokspruit 515 IT).

Several features of the Usushwana Complex, as exposed in the study area, are of particular importance to the understanding of the processes operating during the evolution of the Complex:

a - the dominance of gabbroic rocks, all containing quartz;
b - the occurrence of Fe-rich lithotypes and magnetitites at stratigraphically higher levels;
c - the presence of a lithological cyclicity in the Hlelo River Section;
d - the abundance of xenoliths of all the host rocks of the Complex, many of which show evidence of corrosion;

e - the volumetric disproportion between the acid and the mafic suites.

By analogy with other layered intrusions, the features mentioned above support the following conclusions for the Usushwana Complex:

- only the uppermost and more evolved portion of the intrusion is now preserved at surface (a, b);
- differentiation and fractionation were important processes in the evolution of the Complex (b, c);
- more than one pulse of magma characterised the emplacement of the Complex (c);
- extensive interaction of the original mafic magma with the silicic roof rocks resulted in their assimilation and partial melting (d, e).

CHAPTER 5: PETROLOGY OF THE USUSHWANA COMPLEX

5.1 INTRODUCTION

The mineralogical and textural features of the Usushwana Complex in the study area are described and discussed in this chapter. The Hlelo River Section was considered particularly suitable for a detailed petrological investigation, because of the variety of rock-types, the observed lithological cyclicity and the presence of magnetitite layers. For comparison, the Sterkwater Section was selected from the Eastern limb of the intrusion. A list of the thin sections examined is given in Appendix A. The location of the samples can be deduced from figures 7 and 9.

Note: In the following descriptions, the composition of the intercumulus material, rather than its abundance (Irvine, 1982), has been taken as the discriminating element for the classification of the cumulate rocks, as originally suggested by Wager et al. (1960). The descriptions of the opaque phases are from polished sections.

5.2 PETROLOGY OF THE HLELO RIVER SECTION

5.2.1 1st CYCLIC UNIT

Gabbro and quartz gabbro

The basal portion of the Hlelo River Section consists of equigranular, mesocumulate- to orthocumulate-textured gabbros and quartz gabbros. Plagioclase and clinopyroxene in varying proportions are the dominant cumulus phases, while the intercumulus material is mainly represented by syntaxial overgrowths on plagioclase grains and by granophyric intergrowths of quartz and k-feldspar (Plate 8).

The plagioclase is distinctly cloudy due to alteration; it is highly sericitised and saussuritised, and sometimes almost entirely

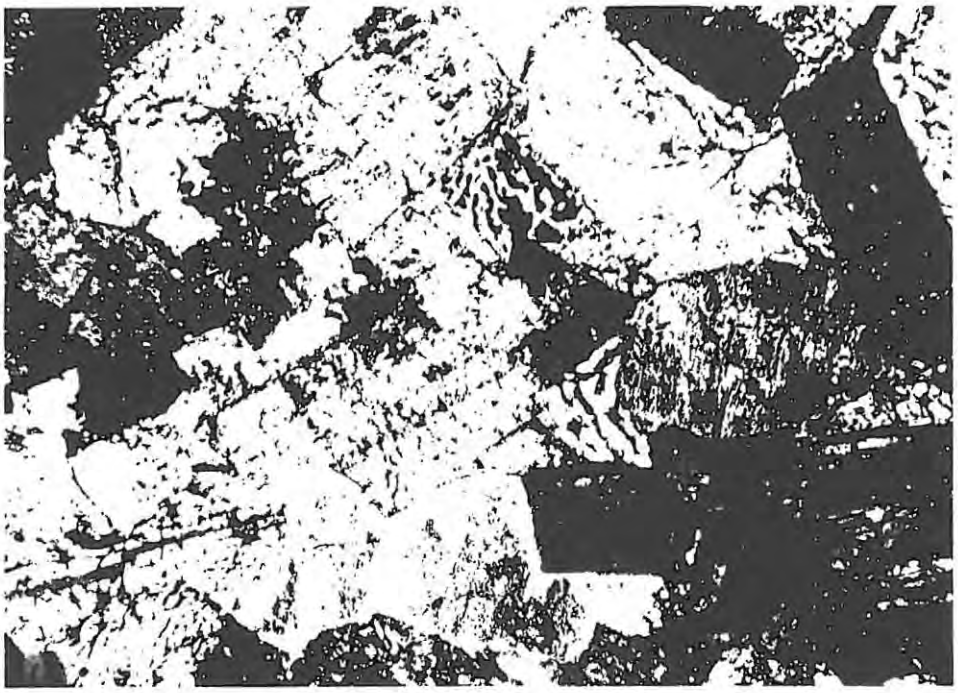

Plate 8 - *Orthocumulate basal gabbro. Note granophyric intergrowths and free quartz as intercumulus material. (Thin section U16a; + nicols; field of view = 4 mm).*

transformed into a mixture of epidote, zoisite, quartz, sericite and albite. Consequently, optical determinations could only be performed on a few grains. Core anorthite contents between 38 and 44% were indicated.

The clinopyroxene occurs as subhedral prismatic crystals of a Na-rich variety of augite (c/Z = 63°-65°). It is characteristically replaced by a fibrous, colourless to pale green amphibole, commonly described as uralite (actinolite pseudomorph, using the terminology of the Subcommittee on amphiboles, 1978) (Plate 9). A Mg-hornblende has been reported for amphiboles pseudomorphically replacing clinopyroxene (Somerset Dam intrusion, Queensland; Mathison, 1987). Bluish green to brown-green hornblende typically surrounds and partially replaces the clinopyroxene grains (Plate 10). The textures suggest that this type of hornblende formed from the residual liquid by reaction with the pyroxene during a late magmatic stage.

Plate 9 - *Pseudomorphic replacement of augite grains by fibrous amphibole (uralite) in the basal gabbros of the first cyclic unit.*
(Thin section U53; + nicols; field of view = 4 mm).

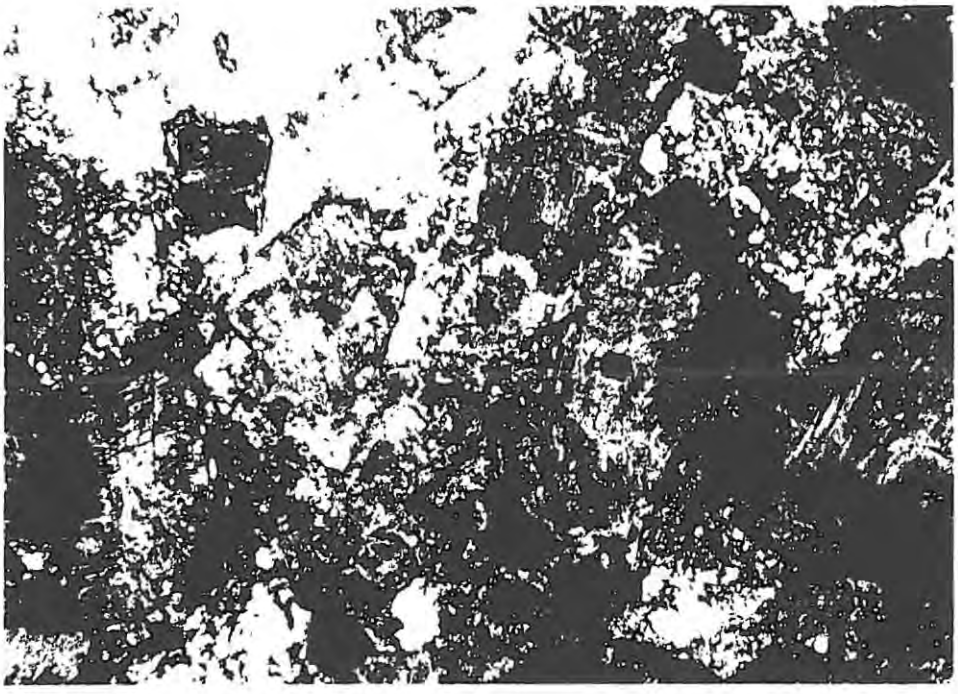

Plate 10 - *Bluish green to green hornblende forming rims around and partially replacing augite grains in the gabbros of the first cyclic unit.*
(Thin section U68; // nicols; field of view = 4 mm).

The interstices between the idiomorphic plagioclase and clinopyroxene grains are filled with lower temperature phases, whose modal content varies from 3% to more than 15%, progressively increasing with stratigraphic height (Fig. 12). Intercumulus minerals include zoned overgrowths to the plagioclase and residual quartz, the latter occurring either alone or more frequently intergrown with a perthitic alkali feldspar in the form of microgranophyre.

Accessory minerals are represented by abundant magnetite and ilmenite, biotite, scattered grains of apatite and minor amounts of primary hornblende. Magnetite and ilmenite occur as euhedral to anhedral or elongated (deformed) grains, which locally approach a cumulus status. They are characterised by incipient to extensive hydrothermal alteration to sphene and turbid leucoxene, respectively. Biotite occurs as tabular plates, and is pleochroic from pale yellow brown to dark brown, suggesting a relatively high iron content. It may be altered to chlorite directly or pass first from a brown to a green biotite and then to chlorite. Some of the biotite may be of a secondary nature, as in places it can be seen to replace the hornblende. Irregular aggregates of fine-grained biotite form after and surround the magnetite grains when in contact with plagioclase (Plate 11). Epitactic sagenitic rutile is frequently observed on the basal sections of biotite derived from the magnetite, and indicates the Ti-enrichment of the latter. Sphene and opaque minerals (pyrite and chalcopyrite) are only minor constituents.

Chlorite and serpentine are widespread, and their occurrence concomitantly with hornblende indicates that low-grade amphibolite facies conditions were reached during regional metamorphism (Winkler, 1979). The replacement of the primary mafic minerals is frequently associated with the segregation of secondary ("dusty") magnetite, which forms minute granules arranged typically in clusters or along fractures and cleavages.

Weathering resulted in the formation of Fe-hydroxides (lepidocrocite, goethite), mainly occurring within the mafic minerals and along fractures as flattened flakes and elongated fibres. Prismatic

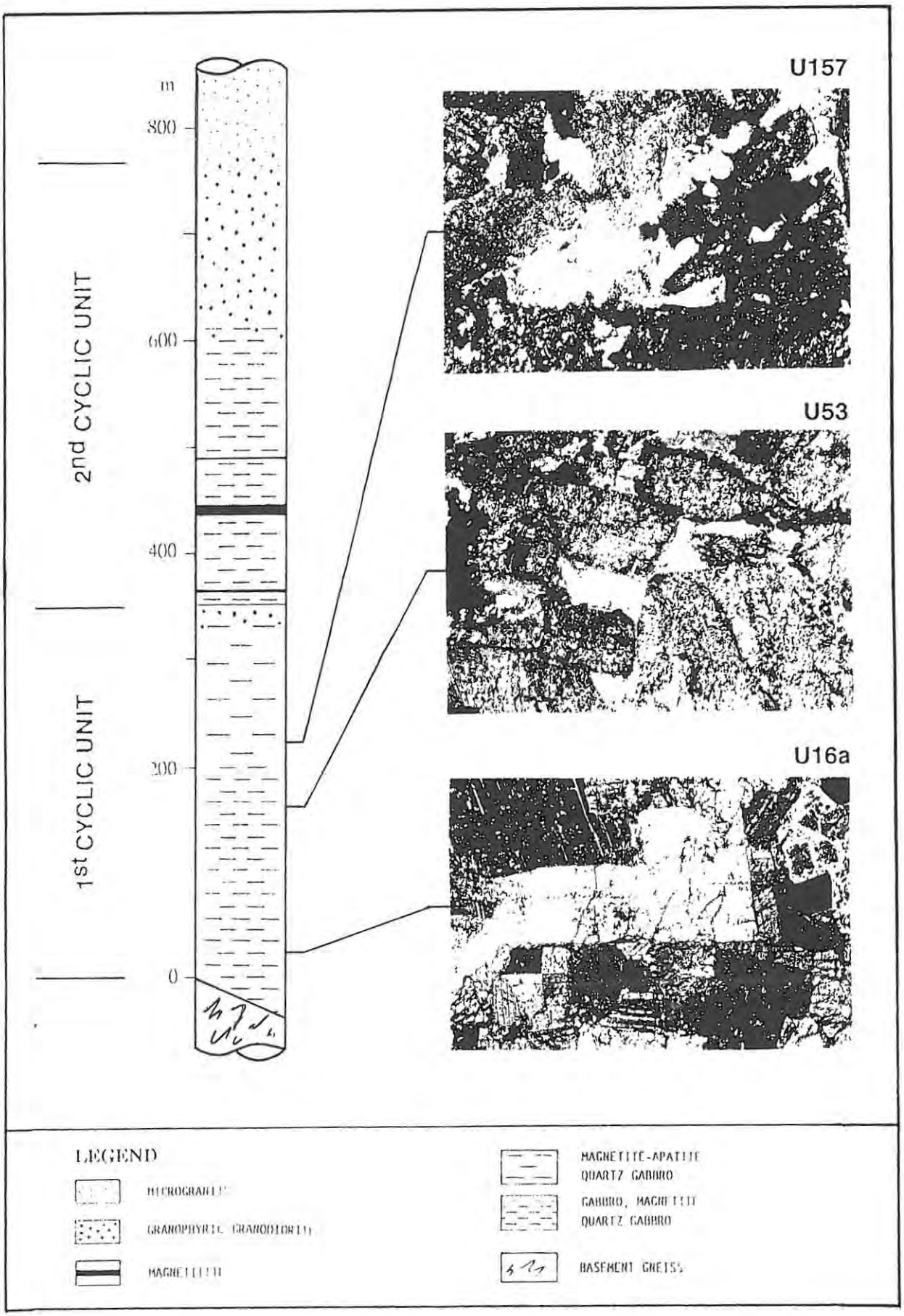

Fig. 12 - *Variations in the nature and amount of intercumulus material with stratigraphic height.*
(Thin sections U16a, U53, U157; + Nicols; field of view = 4mm).

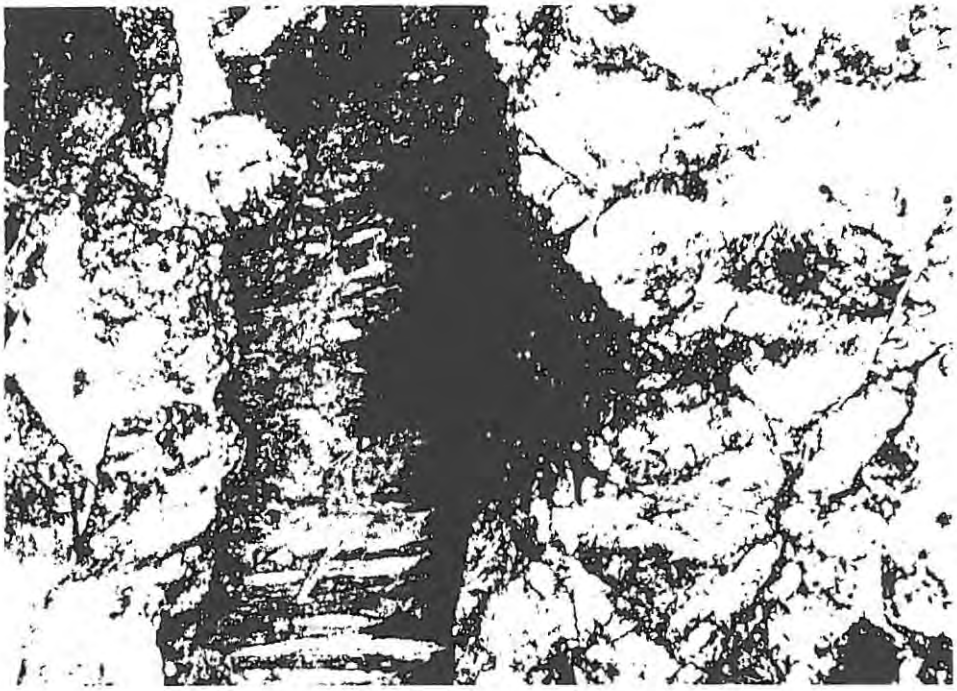

Plate 11 - *Titaniferous biotite rim developed around Fe-Ti oxides in contact with plagioclase.*
(Thin section 053; nicols; field of view 4 mm).

crystals, often slender to acicular, represent the oxidation products of chlorite. Minor haematite is also present. The oxidation of the magnetite grains is responsible for their extensive martitisation.

Much evidence for shearing has been observed. Deformation bands characterise the clinopyroxene and the biotite, while the quartz typically displays undulatory extinction. The plagioclase is frequently disrupted and undulatory extinction is observed in places. The effects of weathering and deformation described above are similar throughout all the Hlelo River Section.

Magnetite-bearing apatite quartz gabbro

The basal gabbros grade into a well-defined package of quartz gabbros, through an increase in the quartz, magnetite and apatite content. The quartz gabbros are characterised by a polymineral orthocumulate

Plate 12 - *Orthocumulate texture in the magnetite apatite quartz gabbros of the first cyclic unit. (Thin section 0154; + nicols; field of view 4 mm).*

texture, in which magnetite and apatite are additional cumulus phases to the plagioclase and the clinopyroxene (Plate 12). The order of crystallisation is inferred to have been plagioclase and apatite first, then magnetite and clinopyroxene, followed by the postcumulus minerals. In order of decreasing abundance, these are quartz, granophyric intergrowths, syntaxial overgrowths around the cumulus plagioclase, hornblende and biotite.

Optical determinations on the cumulus silicates were precluded by their extensive alteration. Saussuritisation and sericitisation of the plagioclase occur to a varying extent. All the pyroxenes have been completely replaced by an amphibole which is more strongly coloured than the pale uralite of the underlying basal gabbros. The pleochroism (X-yellow brown, Y bluish green, Z dark green) and the extinction angle ($c/Z = 13°$) are typical of an Fe-rich hornblende, which is considered to be of late magmatic origin. Crystals of zircon are frequently enclosed in the hornblende and the biotite, and typically

give rise to pleochroic haloes.

The apatite occurs predominantly in the form of slender euhedral needles, which may reach 0.3 mm in length. It may constitute up to 2% of the total mineral assemblage, but progressively decreases upwards. The apatite needles are frequently disrupted, and sulphides (pyrite and chalcopyrite) occur between the fragments. The magnetite may be present in amounts exceeding 10%, and occurs as euhedral to subhedral grains, which are less altered than those in the basal portion.

Low grade metamorphism resulted in a more extensive alteration of the feldspars and the hornblende, giving way to the formation of irregular aggregates of chlorite, epidote and actinolite. The latter two phases may occur either in single prismatic crystals or as radiating clusters.

Granophyric granodiorite

The proportion of granophyric intergrowths increases rapidly over the upper part of the oxide-rich gabbro as it grades into the overlying granophyric granodiorites (Fig. 13), which essentially consist of plagioclase, alkali feldspar and quartz (mostly in the form of granophyric intergrowths), with primary green hornblende as the dominant mafic phase. Accessory minerals include apatite, magnetite, biotite, sphene and zircon. Chlorite, epidote and serpentine, together with Fe-hydroxides are common secondary alteration and weathering products.

The plagioclase forms idiomorphic crystals of albitic composition, commonly zoned and usually altered to saussurite. Locally, it occupies the centres of the microgranophyric aggregates, which have highly irregular shapes and may replace the plagioclase itself. A small amount of alkali feldspar, as well as some quartz, may occur between the microgranophyre. Fe-rich hornblende ($c/Z = 17°$) occurs in irregular or elongated grains with frayed outlines, and displays a sieve structure. It is strongly pleochroic in dark olive green to blue

green, and interference colours are generally masked by body colours.

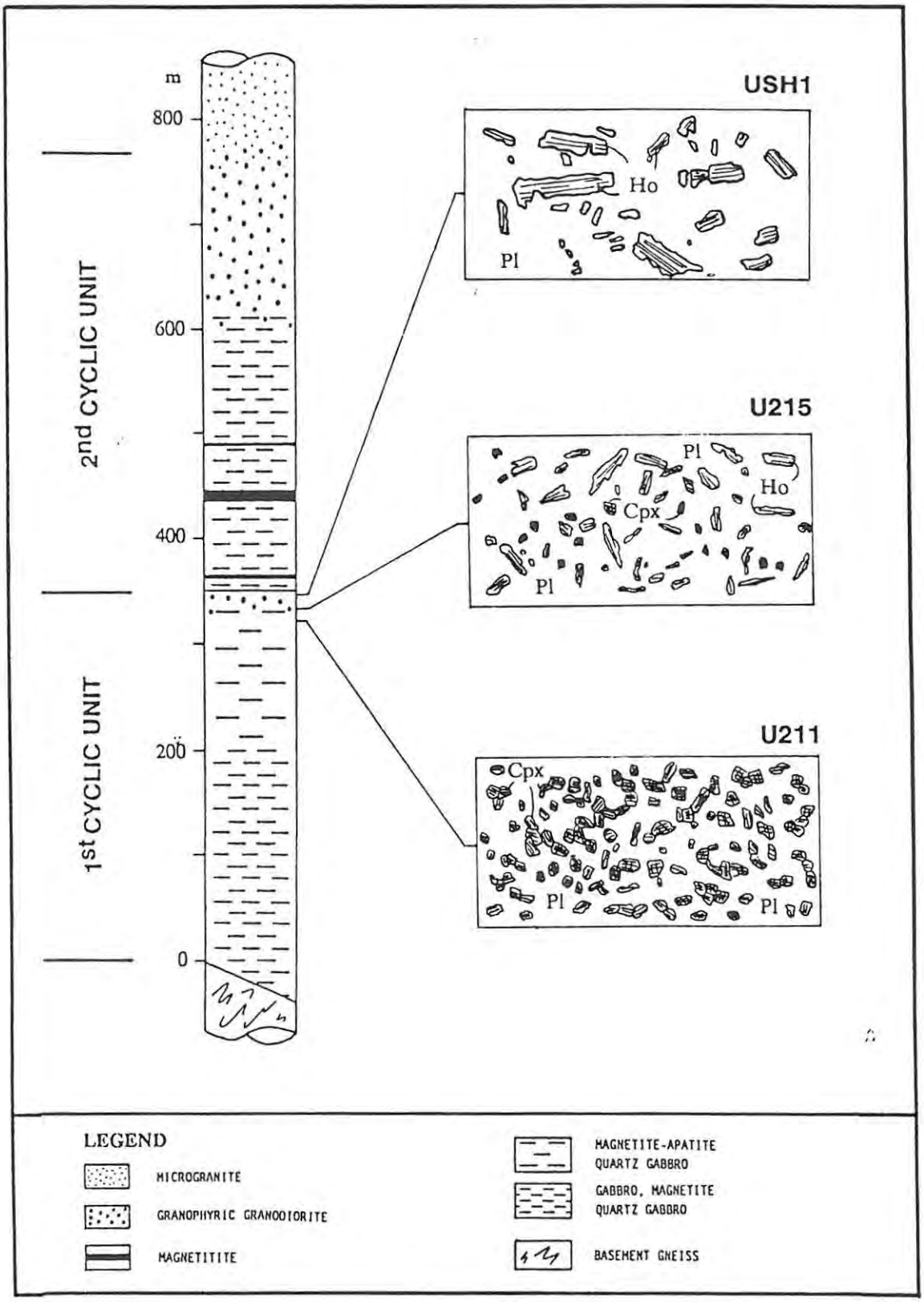

Fig. 13 - *Transition from gabbro to granodiorite.*
Pl=plagioclase; Cpx=clinopyroxene; Ho=hornblende.
(Thin sections U211, U215, USH1; field of view = 4 mm).

5.2.2 2nd CYCLIC UNIT

Petrographically, the second cyclic unit closely resembles the first, the major differences being due to the presence of magnetitite layers and the lack of a distinctive portion of magnetite-bearing apatite quartz gabbro.

Magnetite-bearing quartz gabbro

Similar features to the gabbroic basal portion of the Hlelo River Section are displayed by the orthocumulate quartz gabbros that occur at the base of the second cyclic unit. Plagioclase and clinopyroxene are the main cumulus phases, with minor magnetite and traces of cumulus apatite. Postcumulus minerals include microgranophyre, zoned overgrowths on plagioclase, magnetite and ilmenite, apatite, biotite, and hornblende.

Optically the plagioclase was determined to be a basic andesine (An = 46%), while the clinopyroxene has the composition of a Na-rich augite (c/Z = 55°÷60°). Usually uralite is pseudomorphous after the clinopyroxene, but with increasing stratigraphic height the latter appears to be more and more extensively replaced by hornblende. Irregular aggregates of epidote, chlorite and actinolite are considered to be derived from retrograde metamorphism of the hornblende. Locally, a pleochroic cream-emerald green (uniaxial) mica may be present; it is considered to be phengite, a high-silica variety of muscovite, which is reported to form in small amounts during low-grade metamorphism of mafic rocks (Winkler, 1979).

Magnetitite

The magnetitite consists of an adcumulate aggregate of polygonal magnetite grains (averaging 1 mm in size), separated by a selvage of fine-grained chlorite and minor biotite laths. The magnetite crystals are generally fractured and their boundaries are highly irregular, due

to alteration and replacement processes. In particular, sphene occurs along cracks and forms rims around the magnetite grains. The chlorite formed at the expense of the original silicates, during a metamorphic event. For a detailed description of the mineralogy of the magnetite ore, refer to Reynolds (1978a, 1981).

Granophyric granodiorite and granite

The granodiorites which overlie the magnetite-bearing quartz gabbros of the second cyclic unit generally consist of plagioclase set in a granophyric matrix (Fig. 14, sect. 409 and 464). The dominant mafic mineral is a primary deeply-coloured hornblende, which occurs in varying proportions as skeletal crystals or crystal aggregates (Plate 13). Magnetite, apatite, biotite, sphene and zircon are accessory minerals, while chlorite, serpentine and epidote are the common secondary alteration products. Variations in the amount of plagioclase change the rock from granodioritic to granitic; eventually at the top

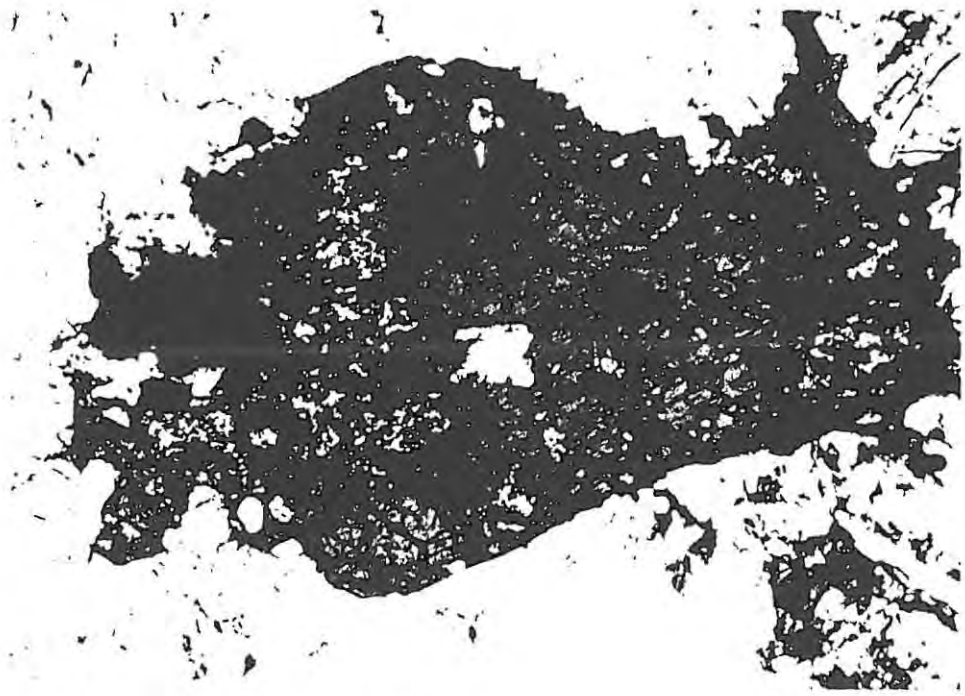

Plate 13 - *Basal section of a primary hornblende in the granophyric granodiorites of the second cyclic unit.*
(Thin section U144; // nicols; field of view = 4 mm).

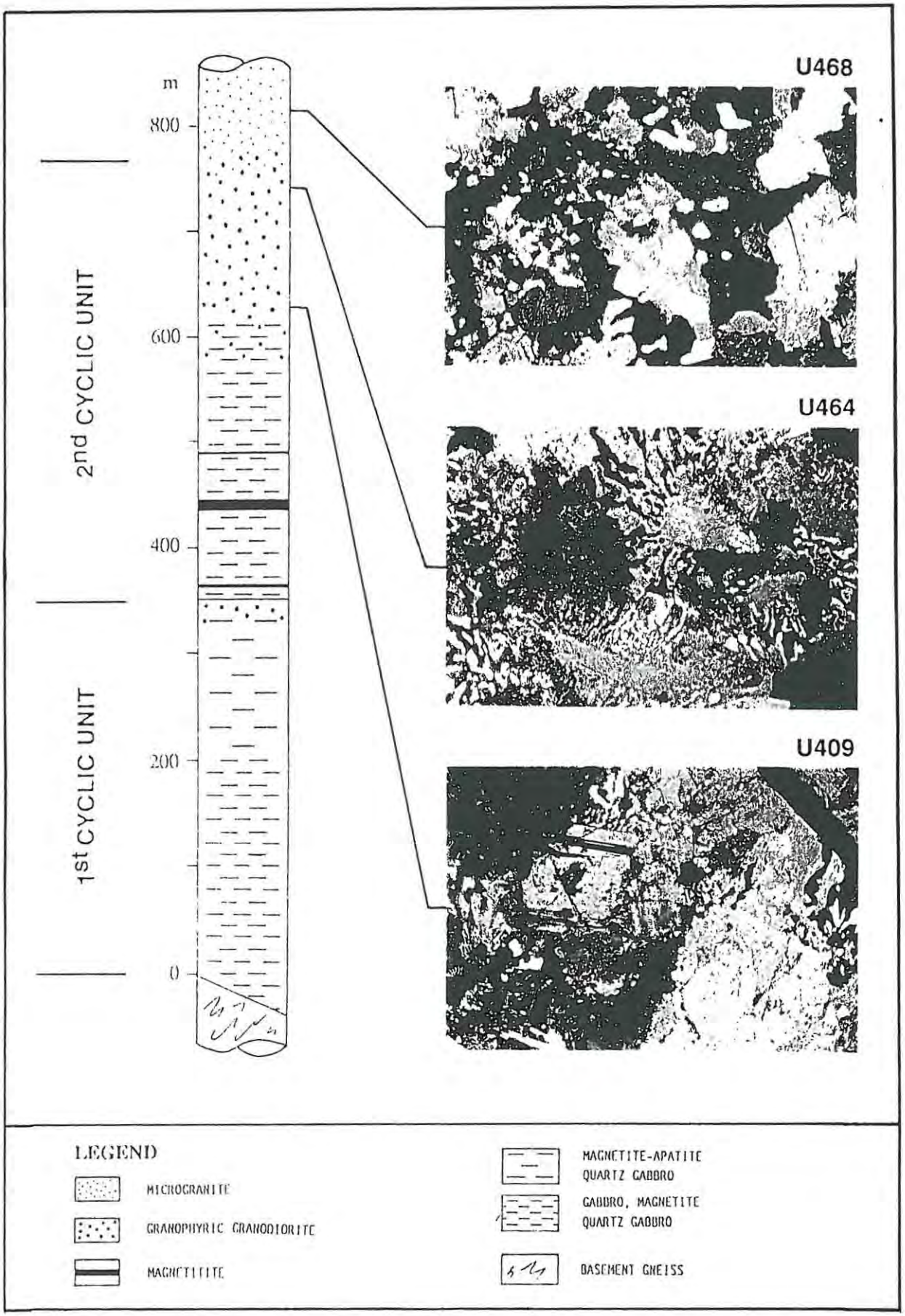

Fig. 14 - *Transition from granophyric granodiorite to microgranite. (Thin sections U409, U464, U468; + Nicols; field of view = 4mm).*

of the section the latter becomes dominant. This transition is also marked by the disappearance of the chlorite-actinolite-epidote aggregates and by the decrease in the amount of hornblende, with biotite progressively becoming the dominant ferro-magnesian constituent. Evidence of recrystallisation can be observed in the uppermost microgranites (Fig. 14, sect. 468), which are considered to represent the recrystallised country rocks of the Usushwana Complex.

In both the granophyric granodiorite and microgranite, the plagioclase is albitic in composition, and commonly acted as a centre of growth for the microgranophyric aggregates (Plate 14). The smaller aggregates have a radiating or a spherulitic structure, due to growth from the central plagioclase, but the larger ones have more irregular shapes. The replacement of the plagioclase by the microgranophyre is also a common feature (Plate 15). These textures are indicative of significant disequilibrium. The feldspars are variably altered, but a few are completely fresh. Free quartz is also present as corroded granular grains, which exhibit a strong undulatory extinction.

5.3 PETROLOGY OF THE STERKWATER SECTION

The Sterkwater Section can be broadly divided in three different portions, with gradual changes marking the transition between them. The basal part is represented by medium- to coarse-grained mesocumulate gabbros, with plagioclase and pyroxene forming the cumulus assemblage and only small amounts of recrystallised aggregates of quartz occurring as intercumulus phases. The basal gabbros grade upwards into orthocumulate quartz-rich gabbros, due to the increase in the amount of intercumulus material, which in the central portion consists mainly of granophyric intergrowths and syntaxial overgrowths on the existing cumulus plagioclase. Magnetite is scarcely represented in the basal portion, and only reaches a cumulus status in the upper part of the orthocumulate sequence. Granophyric granodiorites make up the uppermost portion of the succession. They typically consist of intergrowths of quartz and alkali feldspar, together with plagioclase, hornblende and minor

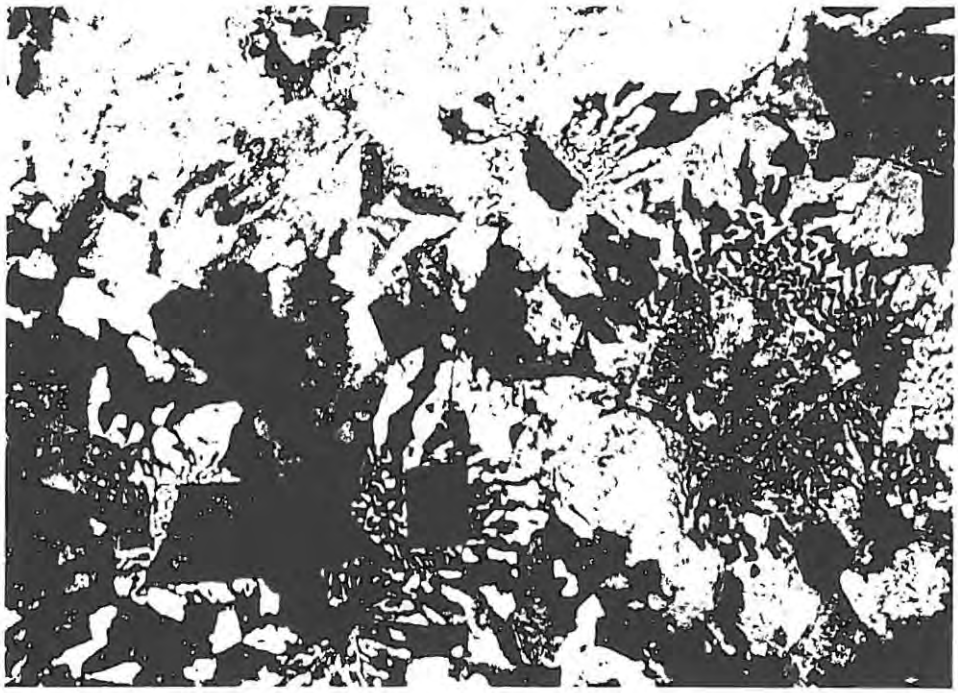

Plate 14 - *Altered euhedral to subhedral plagioclase grains in a granophyric matrix (granophyric granodiorites, second cyclic unit).*
(Thin section U409; + nicols; field of view = 4 mm).

Plate 15 - *Incipient replacement of plagioclase by granophyric intergrowths (granophyric granodiorites, second cyclic unit).*
(Thin section U409; + nicols; field of view = 1.5 mm).

magnetite. Microgranophyre can locally constitute the bulk of the rock (Plate 16).

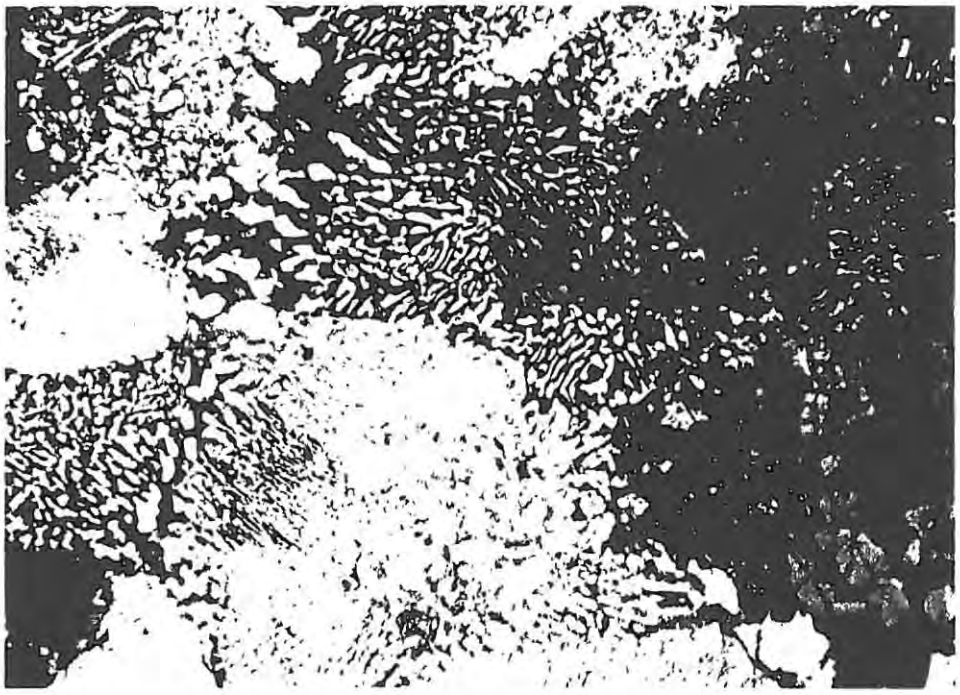

Plate 16 - *Pronounced granophyric texture in the granophyric granodiorite. Note corroded needles of amphibole (bottom right).*
(Thin section U621; + nicols; field of view = 4 mm).

Optical determinations showed that the plagioclase becomes more albitic throughout the whole sequence, although the trend is not smooth. Compositions range from An_{53} at the base of the succession to An_{36} in the uppermost gabbros. In the granodiorites, the anorthite content averages 28% and shows no significant trends. This could be partly ascribed to the limited numbers of sections examined. Hydrothermal alteration of the plagioclase occurs only to a limited extent in the basal portion, sericitisation and saussuritisation becoming more extensive in the upper part of the mafic sequence.

The pyroxene occurs as subhedral prismatic crystals, with relict exsolution textures, but amphibolitisation occurs to such an extent that determination of the pyroxene composition is precluded. For the

same reason, the occurrence of both clinopyroxene and orthopyroxene (suggested by the weathered surface of the samples) could not be confirmed. The process of amphibolitisation resulted in the formation of incomplete euhedral crystals along the edge of the pyroxene grains, which are consequently characterised by irregular outlines. Smaller crystals of amphibole are frequently observed along fractures and grain boundaries, as well as growing on plagioclase and pyroxene (Plate 17). These textures are clearly of a metamorphic origin, and possibly obliterated the presence (if any) of late magmatic rims of hornblende on the pyroxenes, as observed in the Hlelo River Section (see section 5.2.1). Optically this amphibole was determined to be hornblende, with c/Z varying between 14° and 18°, although not displaying any significant trend. However, an Fe-enrichment from the base to the top of the sequence is suggested by an increase in the pleochroic intensity, and is likely to reflect the original composition of pyroxenes. The transition from a Mg-rich hornblende to an Fe-rich variety is supported by a general decrease in the 2V

Plate 17 - *Metamorphic hornblende on uralitised augite grains. (Thin section U352; + nicols; field of view = 4 mm).*

values, which vary from 90° in the basal portion (with both positive and negative signs), to less than 60° in the orthocumulate gabbros. Any further determination of the optical characteristics of the hornblende higher up in the succession is impossible, as body colours mask the interference colours.

Fe-rich biotite of metamorphic origin and apatite are the most common accessory minerals. The biotite occurs in the mafic part of the sequence and progressively increases with the stratigraphic height. Apatite is only a minor constituent and becomes relatively abundant only in the granophyric granodiorites, where it appears to be enclosed by magnetite and plagioclase.

Chlorite and finely crystalline sphene (respectively formed after the biotite and the magnetite) are additional secondary products to the hornblende, though they are never present in significant amounts. The minor development of chlorite, compared with the abundance of hornblende, suggests that in the Sterkwater Section metamorphism reached the low-grade amphibolite facies.

Deformation has affected the plagioclase and the quartz. The former is frequently disrupted or step-faulted, while the latter typically has undulatory extinction and is usually recrystallised to polycrystalline aggregates with sutured contacts.

5.4 PETROLOGY OF MINOR USUSHWANA COMPLEX LITHOLOGIES

In the study area, feldspathic pyroxenite, two-pyroxene gabbro and websterite outcrop to a limited extent. The petrological description of these rock-types is given below.

Feldspathic pyroxenite

The feldspathic pyroxenite outcropping on the farm Strydkraal 477 IT is a coarse-grained clinopyroxene cumulate rock. Intercumulus quartz and plagioclase constitute 18% of the rock. The clinopyroxene has the composition of an aegirinic augite (c/Z = 69°) and is extensively replaced by a green hornblende (c/Z = 16°), which usually forms a darker rim around the pyroxene grains. Plagioclase is present as poikilitic crystals altered to sericite, clay minerals and minor epidote. Recrystallised quartz forms polycrystalline aggregates with sutured contacts and imperfect triple junctions. Accessory minerals are sphene (possibly deriving from the alteration of magnetite), apatite (totally or partially enclosed by the clinopyroxenes) and zircon (as abundant inclusions in the hornblende).

The presence of hornblende without chlorite indicates that metamorphic conditions reached the lower part of the amphibolite facies. Retrograde metamorphism of the hornblende resulted in the development of a sieve structure, due to the formation of actinolite and epidote.

Two-pyroxene gabbro and websterite

The two-pyroxene gabbro (section U347; Blesbokspruit, 515 IT) is a coarse-grained plagioclase-clinopyroxene-orthopyroxene cumulate rock, with only very small amounts of interstitial quartz and minor syntaxial overgrowths on the plagioclase. The plagioclase is a fresh basic labradorite (An = 67%), with sericitisation developed only locally. In contrast, extensive alteration to sericite and uralite affected both the clino- and the orthopyroxene. The former is an

aegirinic augite (c/Z = 75°), the latter has been reported to be a bronzite (Hammerbeck, 1977).

A local transition to a coarse-grained orthocumulate websterite may occur (section U531), following the disappearance of the plagioclase from the cumulus assemblage. In the websterite, the plagioclase occurs as poikilitic crystals enclosing the pyroxenes, and can constitute as much as 30% of the total mineral assemblage (Plate 18).

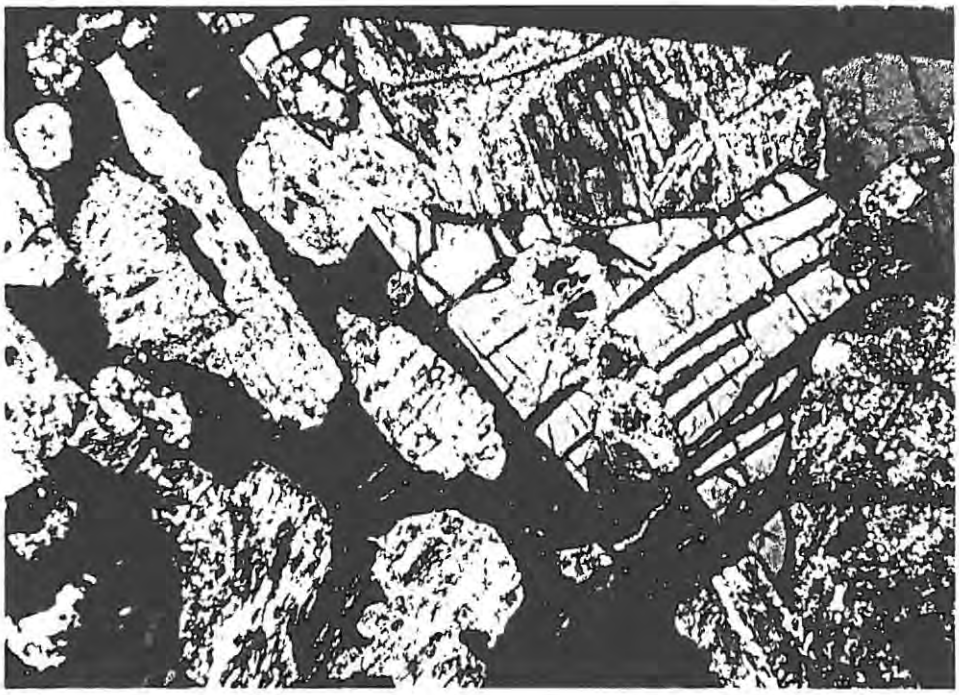

Plate 18 - *Intercumulus plagioclase surrounding altered cumulus pyroxene grains in the websterite (Blesbokspruit 515 IT). (Thin section U531; + nicols; field of view = 4 mm).*

5.5 SUMMARY AND DISCUSSION

Petrological studies of the exposed Usushwana lithologies have identified important mineralogical changes, which generally confirm field observations and support the recognition of differentiation trends within the Complex. Observations also suggest that contamination and assimilation processes were important during the crystallisation of the Usushwana rocks.

The Usushwana Complex, as exposed in the study area, represents a cumulate succession, capped by granophyric rocks, with differentiation resulting in an ordered stratigraphic sequence of progressively more evolved lithotypes. An inward dipping structure of the two limbs of the Complex is supported by the broadly similar mineralogical variations, with the more evolved members occurring in the inner part of the structure (see section 4.3).

The outcropping succession is made up of at least two imperfect cyclic units, consisting of dominant gabbros and quartz gabbros which grade upwards into granophyric granodiorites. The gabbroic rocks display mesocumulate to prevailing orthocumulate textures and, apart from the magnetitites, no adcumulates were observed in the exposed lithologies. The Usushwana Complex is unusual in containing a preponderance of orthocumulates; these are apparently not extensively developed in layered intrusions. In this respect, the Complex resembles the Skaergaard intrusion, which Wadsworth (1985) recognised to be predominantly composed of orthocumulates.

The mafic portion of each cyclic unit is characterised by the cumulus assemblage of plagioclase and clinopyroxene (augite), with variable amounts of granophyric intergrowths, syntaxial overgrowths on the cumulus plagioclase and free quartz as intercumulus phases. The occurrence of orthopyroxene, suggested by field observations (Sterkwater Section, see section 5.3), could not be confirmed, possibly due to the complete alteration of this phase. In the granophyric granodiorite, the mineral assemblage consists essentially of plagioclase set in a granophyric matrix, with primary hornblende as

the major mafic phase, and accessory apatite, magnetite, biotite, sphene and zircon.

Apatite occurs sporadically in the lower part of the mafic sequence, and only achieves a clear cumulus status at a higher level; in the granophyric granodiorite, it persists as an accessory phase. The general behaviour of apatite in the Usushwana Complex resembles that observed in other layered intrusions. The relatively abrupt appearance of this mineral in the cumulus assemblage, in contrast with the more gradual arrival of magnetite, is reported for the Skaergaard intrusion (Wager, 1960). The steady depletion of apatite after its initial arrival, and its low concentration above the Fe-Ti oxide-rich layers are common features to the Kiglapait intrusion (Morse, 1979), though in the Usushwana Complex the apatite is also found associated with magnetite gabbros.

Fe-oxides (magnetite and ilmenite) are consistently present throughout the sequence. The magnetite is a relatively minor constituent in the basal part of the lower unit (where it is apparently of intercumulus habit), and only becomes firmly established at approximately the same stage at which apatite reaches a cumulus status. Magnetitite layers and lenses are developed at various levels in the basal part of the upper cyclic unit.

Biotite is generally present, though it has no cumulus status in the intrusion, and occurs as isolated lath-like aggregates or as rims on the Fe-Ti minerals when in contact with the plagioclase. Biotite rims on opaque oxide minerals are apparently a characteristic signature of troctolites and olivine-rich gabbros (e.g. Morse, 1979; Whitney and McLelland, 1973). The involvement of olivine in the process has been considered indispensable to provide the necessary amount of Mg required by the reactions, the Mg content of the Fe-Ti oxides being judged insufficient in this regard (Whitney and McLelland, op.cit.). However, the olivine-free Usushwana rocks provide evidence that, even if poorly developed, oxide coronas of titaniferous biotite can form by reaction of plagioclase to Fe-Ti oxides. The absence of either spinel or garnet has generally been related to a reacting plagioclase more

sodic than An_{38-36} (Whitney and McLelland, 1983), and in the Usushwana rocks this might suggest a normal zoning in the marginal portions of plagioclase grains (see also section 6.2).

In the gabbroic rocks, sulphides (mainly pyrite and chalcopyrite) represent a late phase, as they are found along cracks and fractures within the earlier formed minerals (e.g. apatite, ilmenite).

Numerous observations point to extensive fluid-rock interaction during the late magmatic stage of crystallisation, under hydrothermal conditions. The deuteric uralitisation and the development of hornblende rims on the pyroxenes, the saussuritisation and sericitisation of the plagioclase (which were observed to occur at various degrees in the Usushwana rocks), are all controlled by the circulation of solutions and indicate that the mobile phase was saturated in H_2O and carried alkalis. Although the formation of these secondary minerals can be a characteristic effect of low-grade regional metamorphism, in the Usushwana rocks it cannot be correlated with certainty with any specific metamorphic event. The alteration of Fe-Ti oxides to sphene and turbid leucoxene can also be ascribed to the action of hydrothermal solutions (Heinrich, 1965). The magnetite-bearing, apatite gabbros are consistently more altered than the basal gabbros, and this feature is considered to reflect a greater amount of trapped fluid with stratigraphic height. The residual liquid was also progressively enriched in SiO_2, as indicated by the quartz-orthoclase intergrowths, which represent an intercumulus phase in the gabbros, increasing stratigraphically upwards and finally constituting the bulk of the granophyric granodiorite.

The existence of a differentiation trend is suggested by changes in the plagioclase and pyroxene composition. Variations in the plagioclase demonstrate a progressive fractionation from Ca- to Na-rich varieties. In the Sterkwater Section, plagioclase varies from An_{53} at the bottom to An_{27} at the top of the sequence. Similarly, in the Hlelo River Section, a change from basic andesine to albite was observed. On the basis of mineral composition and according to the directive of IUGS (Streckeisen, 1973), most of these rocks should be

classified more correctly as diorites. The hornblende replacing the pyroxenes (considered to reflect their original composition) displays an Fe-enrichment from the bottom to the top of the units, indicated by the increasing pleochroic intensity and decreasing 2V values (Gribble and Hall, 1985).

The Usushwana Complex was affected by a regional phase of metamorphism, an event common to most of the rocks of the Kaapvaal Craton. The mineral assemblage observed in the mafic lithotypes compares well with that marking low-grade metamorphic conditions. The widespread distribution of chlorite is diagnostic at this regard, and its association with hornblende (which can become locally predominant, as in the Sterkwater Section) indicates that the low-grade amphibolite facies range was reached (Winkler, 1979). The retrograde metamorphism of the hornblende (previously formed during the late magmatic replacement of the pyroxenes) resulted in the formation of epidote-chlorite-actinolite aggregates, which coexist with some biotite and a little muscovite (phengite).

Strain affecting the Usushwana rocks resulted in the plastic deformation of most of the minerals. Flexure and polygonisation induced undulatory extinction in the quartz grains; plagioclase exhibits tension slots and diaclases enclosing parts of the mineral characterised by undulated twin planes; pyroxene and biotite display deformation bands and kinks, while apatite needles are typically fragmented. In most cases, the observed parallel alignment of plagioclase and mafic minerals (giving rise to a well-defined lamination) cannot be considered as a primary texture, but is more likely to be related to a phase of intense shearing.

The Usushwana rocks are characteristically weathered, with the result that extremely fresh material is rarely available. Hydration and oxidation under sub-tropical climatic conditions (see section 2) resulted in the extensive development of limonite (goethite and lepidocrocite) and haematite.

The lithological change from mafic rocks to granophyres cannot simply

be related to fractionation processes, as some features indicate that contamination of the mafic magma and assimilation of the country rocks were important processes acting during the crystallisation of the Complex. Corroded quartz grains in the gabbroic rocks and strongly corroded stumps of plagioclase in the granodiorite could represent xenocrysts picked up from the country rocks, which resisted complete resorption in the magma. Some of the more acidic rocks (especially in the uppermost part of the sequence) display a heterogranular polygonal texture and quartz with "ameboid" appearance. It is likely that these textures are not related to normal crystallisation but rather to a partial melting and recrystallisation of a pre-existing rock which has been partially assimilated by the mafic magma.

By analogy with the stratigraphic variations of other layered intrusions, some of the observed mineralogical features can be taken as evidence that the Usushwana lithologies, as exposed in the study area, represent the roof facies of the Complex. This is clearly indicated by the overall cumulus mineralogy, in particular by the presence of apatite and Fe-Ti oxides, and the occurrence of intercumulus quartz (either associated with feldspar in granophyric intergrowths or as individual grains).

CHAPTER 6: MINERALOGY OF THE USUSHWANA COMPLEX

6.1 INTRODUCTION

In order to document cryptic variations of the main cumulus silicate phases within the Usushwana Complex, the stratigraphic succession exposed along the Hlelo River was investigated by means of electron microprobe. In particular, this study was aimed at establishing the petrographic significance of the granophyric rocks which cap every cyclic unit.

A total of 180 plagioclase and clinopyroxene analyses were performed on 14 polished thin sections. A minimum of 7 (maximum 14) different grains were analysed in each sample; only core regions were investigated, avoiding the more obviously marginal areas of the crystals. The average compositions for plagioclase and clinopyroxene are listed in Appendix C, while analytical details are provided in Appendix B. Microprobe data are generally in good agreement with the optical determinations.

6.2 PLAGIOCLASE VARIATION

Plagioclase is a common phase in all the rocks of the Hlelo River Section. Two different populations can be easily distinguished on the plagioclase ternary diagram (Fig. 15): the first is andesitic in composition and corresponds to the gabbroic rocks, the second is represented by the nearly pure albites of the granophyric lithotypes. Sample U262 is unusual in being a gabbro with the same plagioclase composition as that of the granophyres.

The overall range in the An-content of plagioclase [An= 100Ca/(Ca+Na+K)] is presented in figure 16a, where the average value and the range for each sample are plotted against the stratigraphic position (figure 16 also provides information about gaps in sampling, deformation and alteration, in order to facilitate assessment of the

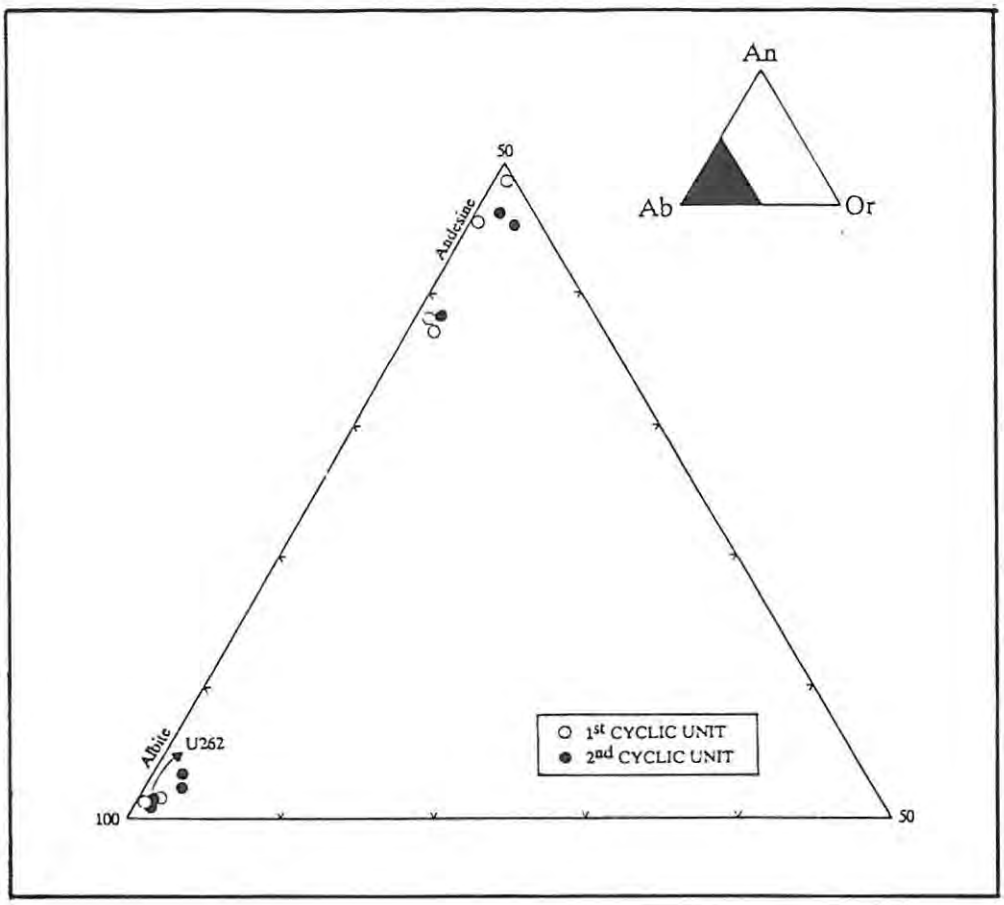

Fig. 15 - *Feldspar ternary diagram showing the average compositions of plagioclase in the Hlelo River Section.*

microprobe data). The compositional range of plagioclase in individual samples is relatively large, varying from as little as 0.38 mol % An to as much as 10.50 mol % An, with an average range of 6.5 mol % An. The greatest ranges have been observed in the mafic portion (e.g. sample U259: An_{min} 33.49 ÷ An_{max} 43.99), while the smallest variations are found in the granophyres (e.g. sample U409: An_{min} 0.75 ÷ An_{max} 1.13). Relatively wide compositional ranges of plagioclase are considered to be a typical feature of layered intrusions, and have been ascribed to partial re-equilibration during the early postcumulus stages of crystallisation, rather than representing a growth (zoning) effect (Wadsworth et al., 1982; Wadsworth, 1986). For this reason, it is considered that the most calcic composition in each sample is possibly more significant than the average core composition, as it may represent a remnant of the original cumulus material; both have been

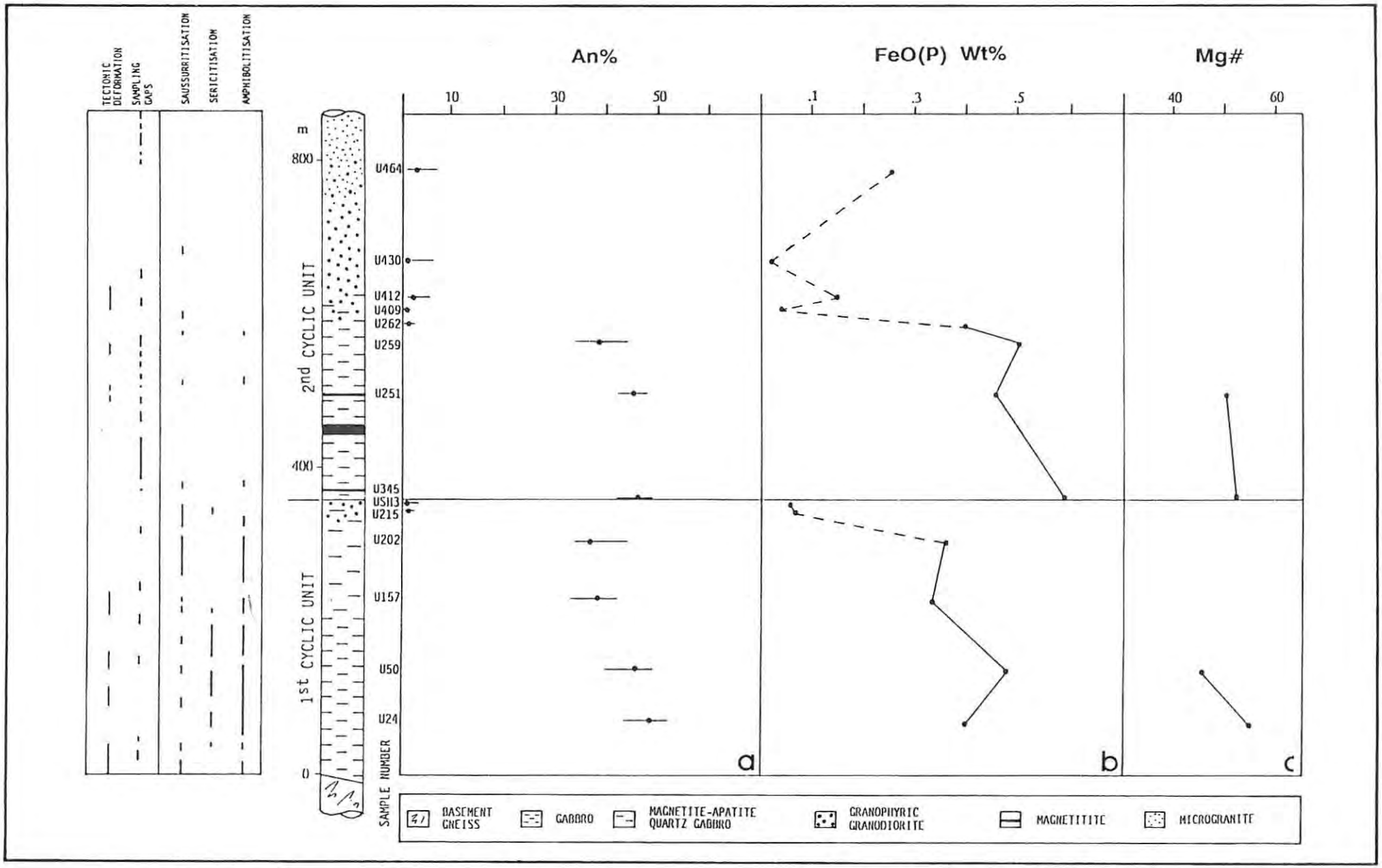

Fig. 16 - *Cryptic variations of cumulus silicate phases through the Usushwana Complex (Hlelo River Section):*
a) plagioclase - Anorthite content [An = 100Ca/(Ca+Na+K)];
b) plagioclase - FeO(P) content;
c) clinopyroxene - Mg# [100Mg/(Mg+Fe)]

consequently indicated in Appendix C and in figure 16a.

The cryptic variations depicted in figure 16a can be tentatively interpreted as indicative of a progressive fractionation trend within each cyclic unit, with a reversal occurring at the base of the upper one. A dramatic drop in the An-content is observed across the transition zone from the gabbroic rocks to the granophyres, and occurs over a narrow stratigraphic interval. The close-spaced sampling and the repetition of the same trend in both cyclic units argue against a compositional gap due to an incomplete record of the section. Despite field observations of a gradational contact between the gabbros and the granophyric granodiorites, the observed trend could indicate that the acidic rocks might not be part of the fractionation sequence, as already suggested on the basis of petrological features (see section 5.5).

In each unit, the decrease in An-content with stratigraphic height is accompanied by a general decrease in the FeO-content of the feldspar (Fig. 16b). The plagioclase grains of the second unit are more Fe-rich than their stratigraphic equivalents in the first unit, a feature taken to indicate a general Fe-enrichment stratigraphically upwards. Irregular Fe-concentrations are observed only in the uppermost part of the sequence. The relationship between Fe- and An-content is depicted in figure 17. Despite the wide scatter of datum points (especially on the An-rich side), this diagram shows quite distinctly that there is a compositional gap between the mafic and granophyric lithologies.

Due to extensive alteration, no detailed study of the zonation of the plagioclase was attempted. A limited number of analyses were performed on plagioclase rims, but they failed to reveal any meaningful pattern. For the same reason, it should be emphasised that the bulk An-content of the plagioclase could be slightly higher than the recorded values, as the extensive saussuritisation could have resulted in the Ca-depletion of plagioclase. Whitney and McLelland (1973) report on a Ca-impoverishment of the plagioclase (from $An_{60\div70}$ to $An_{20\div30}$), due to the formation of oxide coronas (see section 5.5). In the Usushwana rocks, this effect is considered to have been marginal; the incomplete

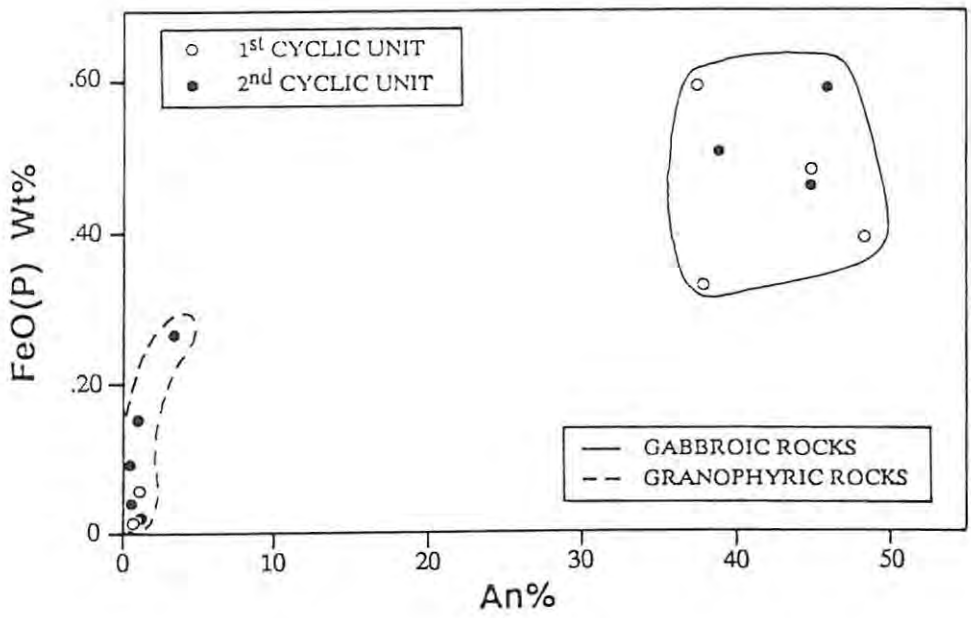

Fig. 17 - *Total iron [FeO(P)] versus An-content of plagioclase cores. Each datum point is the calculated average of 7 to 14 individual analyses.*

development of the coronas suggests that only the outer parts of the plagioclase grains were involved in this process.

6.3 CLINOPYROXENE VARIATION

The occurrence of clinopyroxene is confined to the mafic portion of the exposed sequence, where it appears to be of cumulus habit. Only a limited number of samples could be analysed due to the extensive amphibolitisation of the pyroxenes. Consequently, the conclusions drawn below must be taken as tentative.

In the new classification scheme for pyroxene (Subcommittee on pyroxenes, 1989), the datum points of the average compositions fall into the central part of the augite field (Fig. 18). Samples U345 and U251 (which belong to the lower part of the second cyclic unit) appear to be more calcic than the sample pair U24-U50 (which represents the basal portion of the first unit), but do not display any significant

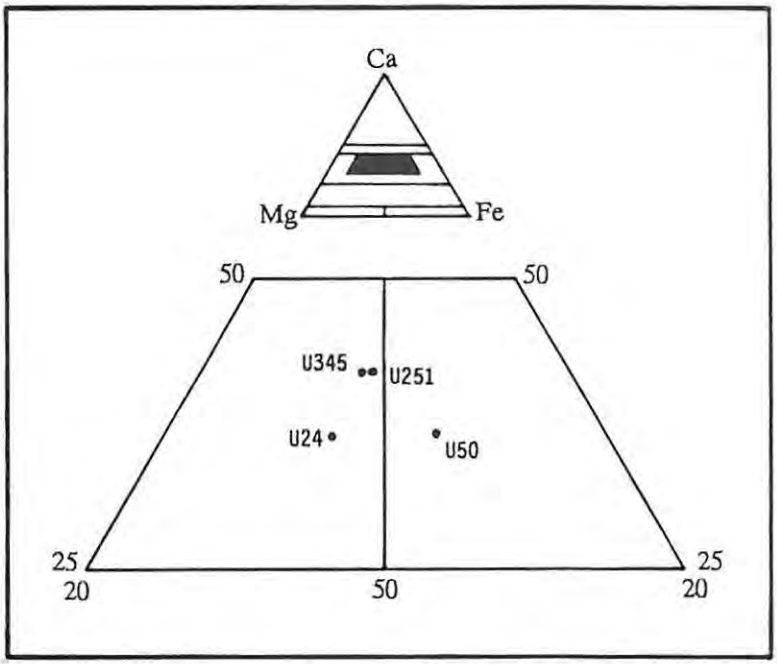

Fig. 18 - *Compositional range of clinopyroxene in the Hlelo River Section.*

trend with respect to the Fe content. On the contrary, samples U24-U50 show an Fe-enrichment from $Fs_{30.0}$ to $Fs_{35.9}$. The same pattern can be deduced from figure 16c, which depicts Mg# [Mg# = 100Mg/(Mg+Fe)] variations with height. It can be seen that there is an overall tendency for Mg# to parallel the An-pattern in both cyclic units. The less evolved composition of the pair U345-U251, compared to the Mg# of sample U50, may be considered additional evidence for a chemical reversal occurring at the base of the second unit.

The trend of clinopyroxene crystallisation associated with the fractionation of a mafic magma is illustrated in figure 19. The Bushveld Complex is taken as an example, but similar trends have been observed in many other layered sequences, e.g. in the Skaergaard intrusion (east Greenland; Nwe, 1976; Nwe and Copley, 1975), the Dufek Complex (Antarctica; Himmelberg and Ford, 1976) and the Birds River gabbro complex (South Africa; Eales and Booth, 1974). The crystallisation of clinopyroxene starts with the separation of a

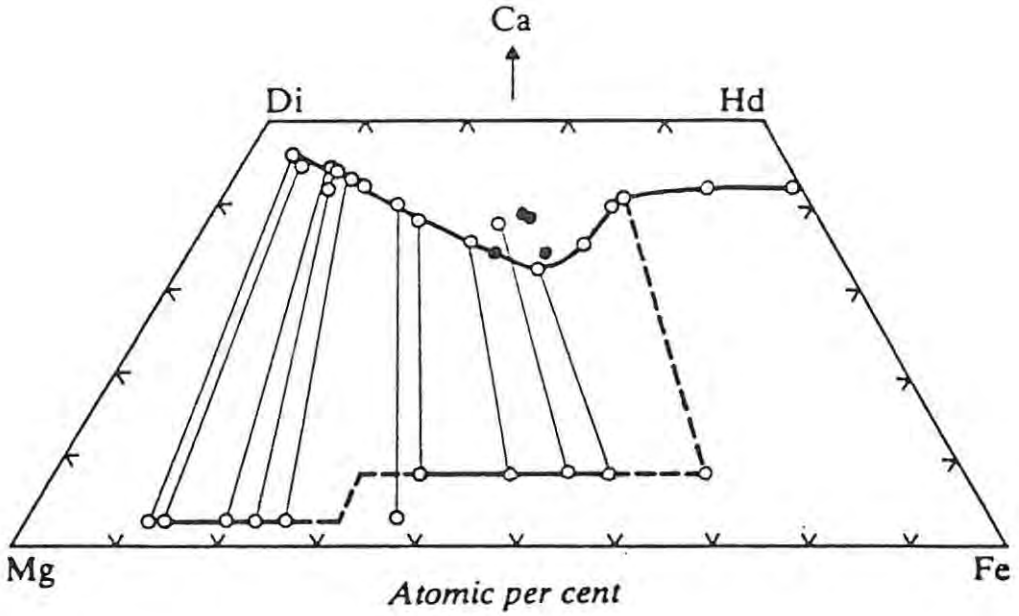

Fig. 19 - *Crystallisation trends of Ca-rich and Ca-poor pyroxenes. Open circles: Bushveld Complex (after Atkins, 1969); solid circles: Usushwana Complex (Hlelo River Section, this study). Compositions of the Usushwana pyroxenes from microprobe analyses.*

diopsidic pyroxene ($Ca_{45}Mg_{50}Fe_5$) which is usually associated with orthopyroxene. Compositions progressively evolve towards increasing contents of Fe, with the possibility of small reversals. The continuous change in the Mg:Fe ratio is accompanied by a decrease in the Ca content towards a minimum, represented by an augite of composition $Ca_{33}Mg_{31}Fe_{36}$. This stage corresponds to the limit of the two-pyroxene stability field. At this level, the trend of crystallisation changes abruptly and the earlier pattern of decreasing Ca content is reversed. The succeeding clinopyroxenes display significant compositional variation with Ca-enrichment and Mg-impoverishment ($Ca_{40.5}Mg_{18.7}Fe_{40.8}$). In the latter stages of fractionation, Fe-enrichment continues, while the Ca-content increases only marginally; the more evolved clinopyroxene has the composition of an Fe-rich hedenbergite ($Ca_{42.7}Mg_{0.5}Fe_{56.8}$).

In the Hlelo River Section, the clinopyroxene data compare well with relatively highly evolved compositions, at the fractionation stage

where the Ca-content approaches a minimum value (Fig. 19). The absence of orthopyroxenes in this sequence is not in contrast with the previous assessment, as this feature could be related to extensive alteration (orthopyroxenes are however inferred to be present in the Sterkwater Section, see section 5.3). A correlation between the higher Ca-content of clinopyroxenes and higher water-vapour pressures has been established by Deer and Abbot (1965), and may account for the Ca-enrichment of the clinopyroxenes in the second unit. The same effect is indicated by their restricted enrichment in Fe and supported by the formation of late hydrous phases in relatively large quantities (see section 5.5).

6.4 SUMMARY AND DISCUSSION

Microprobe analyses give insights into the mineral chemistry of the exposed portion of the Usushwana Complex (Hlelo River Section), and provide important information with regard to the existence of differentiation trends within the intrusion.

Given the mineralogical assemblage of the Usushwana lithotypes, the most sensitive compositional parameters for documenting stratigraphic cryptic variation are the Ca/Na ratio in plagioclase and the Mg/Fe ratio in clinopyroxene, respectively expressed as anorthite (An) and Mg number (Mg#). On the whole, the range in plagioclase composition is 47 mol % ($An_{48.41 \div 0.94}$). In the first cyclic unit, clinopyroxene compositions cover a wider range than the coexisting plagioclase ($Mg\#_{54.35 \div 45.41}$ - $An_{48.41 \div 45.33}$); similar ranges are recorded in the second unit ($Mg\#_{52.09 \div 51.34}$ - $An_{46.11 \div 45.26}$).

On the basis of microprobe results, the exposed succession cannot definitely be attributed to only fractionation processes (see chapter 8 for a thorough discussion of this problem). The separation of average plagioclase compositions into two distinct groups (as shown by the diagrams in figure 15 and 17) strongly suggests that the gabbroic and granophyric rocks of each cyclic unit do not belong to a single fractionation sequence. However, within the gabbroic portion of each

unit a certain degree of fractionation has taken place. When plotted against stratigraphic position (Fig. 16), plagioclase compositions display trends towards a lower An-content, with a resetting to higher values at the base of the second unit. Though limited in number, the analyses of clinopyroxene confirm this tendency, as they follow the plagioclase pattern sympathetically.

Based on the assumption that the exposed portion of the Complex represents the upper part of a mafic intrusion (see section 5.5), an attempt was made to compare the mineralogical and textural features of the Usushwana sequence with those of the final evolutionary stages of other layered intrusions (Fig. 20). Comparisons were made taking into account either the cumulus mineralogy or the compositional ranges of the principal minerals.

All the basic layered intrusions considered contain two coexisting pyroxenes in part of the sequence, and in all of these the Ca-poor pyroxene disappears during crystallisation. It is generally assumed that the Ca-poor pyroxene disappears concomitantly with the reappearance of Fe-rich olivine (e.g. Skaergaard, Bushveld; Wadsworth, 1986; Fongen-Hyllingen; Wilson et al., 1981). However, in several complexes, Ca-poor pyroxene ceases to crystallise but olivine does not reappear. Among these are the Insch (Scotland; Wadsworth, 1986), Mt Kilkenny (Western Australia; Jaques, 1976), Kap Edvard Holm (east Greenland; Deer and Abbot, 1965), Kapalagulu (western Tanzania; Wadsworth et al., 1982), Dufek (Antarctica; Ford, 1970), Lebombo (South Africa; Saggerson and Logan, 1970), and Losberg intrusions (South Africa; Danchin and Ferguson, 1970).

The crystallisation sequence of the Usushwana Complex does not appear to be perfectly matched elsewhere. In terms of cumulus mineralogy, the Complex falls into the second of the two groups considered above, but major differences are evident when considering the compositional ranges of individual phases, i.e. the Usushwana plagioclase is generally more sodic, while the clinopyroxene is usually enriched in Fe and depleted in Ca. In contrast, the Usushwana Complex shows some remarkable similarities to the Skaergaard (and to a lesser entent to

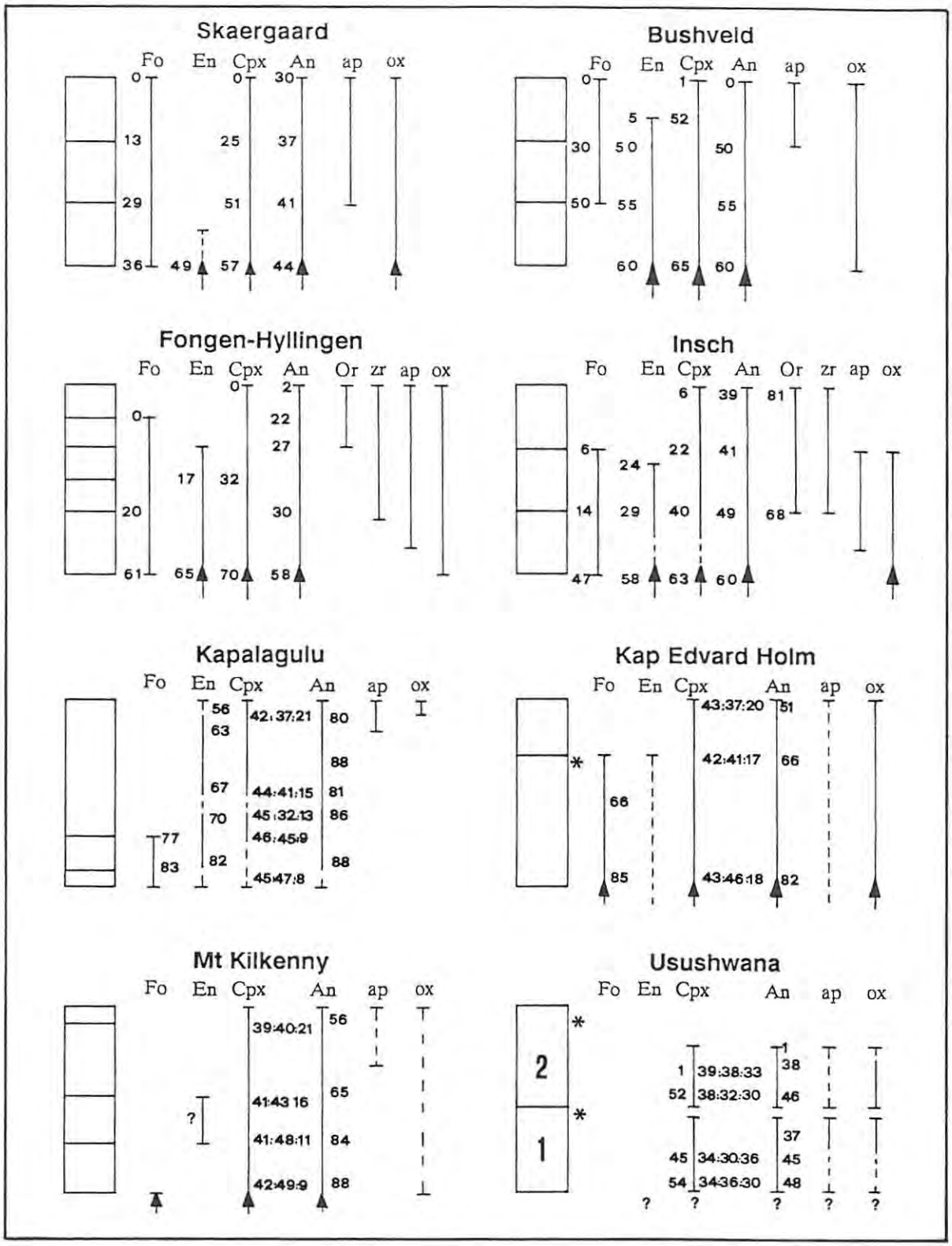

Fig. 20 - *Comparison of phase layering and cryptic layering patterns in the later fractionation stages of the Usushwana Complex and other mafic intrusions (see text for references).*

*Stratigraphic columns not to scale. Firm lines indicate cumulus ranges, with arrows showing continuity from lower parts of the sequences. Dashed lines indicate intercumulus occurrences. Clinopyroxene compositions reported as Mg# or Wo:En:Fs (both have been indicated from the Usushwana Complex). Fo=forsterite; En=enstatite; Cpx=clinopyroxene; An=anorthite; Or=orthoclase; zr=zircon; ap=apatite; ox=Fe-Ti oxides; *=granophyric layers or units. 1 and 2 refer to the cyclic units of the Usushwana Complex.*

the Bushveld) intrusion. It is noteworthy that these complexes are characterised by similar compositions of the cumulus assemblages at specific stages in the evolutionary process, as marked by the principal phase changes. In particular, the appearance of cumulus apatite corresponds to an An content of 41 and 38 mol % in the Skaergaard and Usushwana intrusion, respectively. Compared to the Skaergaard data, the covariation betweeen An in plagioclase and Mg# in clinopyroxene shows that the interval of Mg# is shifted towards more Fe-rich compositions, for a given range of coexisting plagioclase. Extremely Fe-rich clinopyroxenes have not been reported from the Hlelo Section, though this can be ascribed to the limited number of samples analysed, which is unrepresentative of all the sequence. The observed differences between the Usushwana and other intrusions can perhaps be accounted for by differences in parental magma compositions, P-T conditions, and by other factors such as contamination and the development of open-system conditions.

CHAPTER 7: WHOLE-ROCK GEOCHEMISTRY

7.1 INTRODUCTION

In this chapter the geochemical data derived from whole-rock XRF-analyses are presented and discussed. Twenty-three samples selected from the Hlelo River Section were analysed for a suite of 10 major and 16 trace elements. The analyses were carried out at the Department of Geology, University of Natal - Pietermaritzburg. Results and analytical details are attached in Appendix D and B respectively.

7.2 CHEMICAL VARIATIONS WITH STRATIGRAPHIC HEIGHT

7.2.1 MAJOR ELEMENTS

The chemical variations of major elements with stratigraphic height are depicted in figure 21 and summarised below.

Most of the major oxide plots define curves of increasing or decreasing content with height, with overall similar trends repeated in each cyclic unit. The first unit is characterised by more regular variations than the second, and gradual changes between the different lithologies (including that from gabbros to granophyric rocks) can be clearly observed. A step-like pattern is present in the second unit.

Throughout much of the intrusion, SiO_2 varies slightly. The gabbroic cumulates maintain a constant SiO_2 content of about 50%, because of the relatively high amounts of quartz included in the granophyric intergrowths. In the granophyres, the silica content increases markedly to 60-70%. K_2O displays a similar trend to silica and appears to be controlled by K-rich intercumulus phases, mostly the feldspar in the granophyric intergrowths and the biotite.

CaO decreases constantly throughout the first unit, but more irregularly in the second, where a step marks the transition to

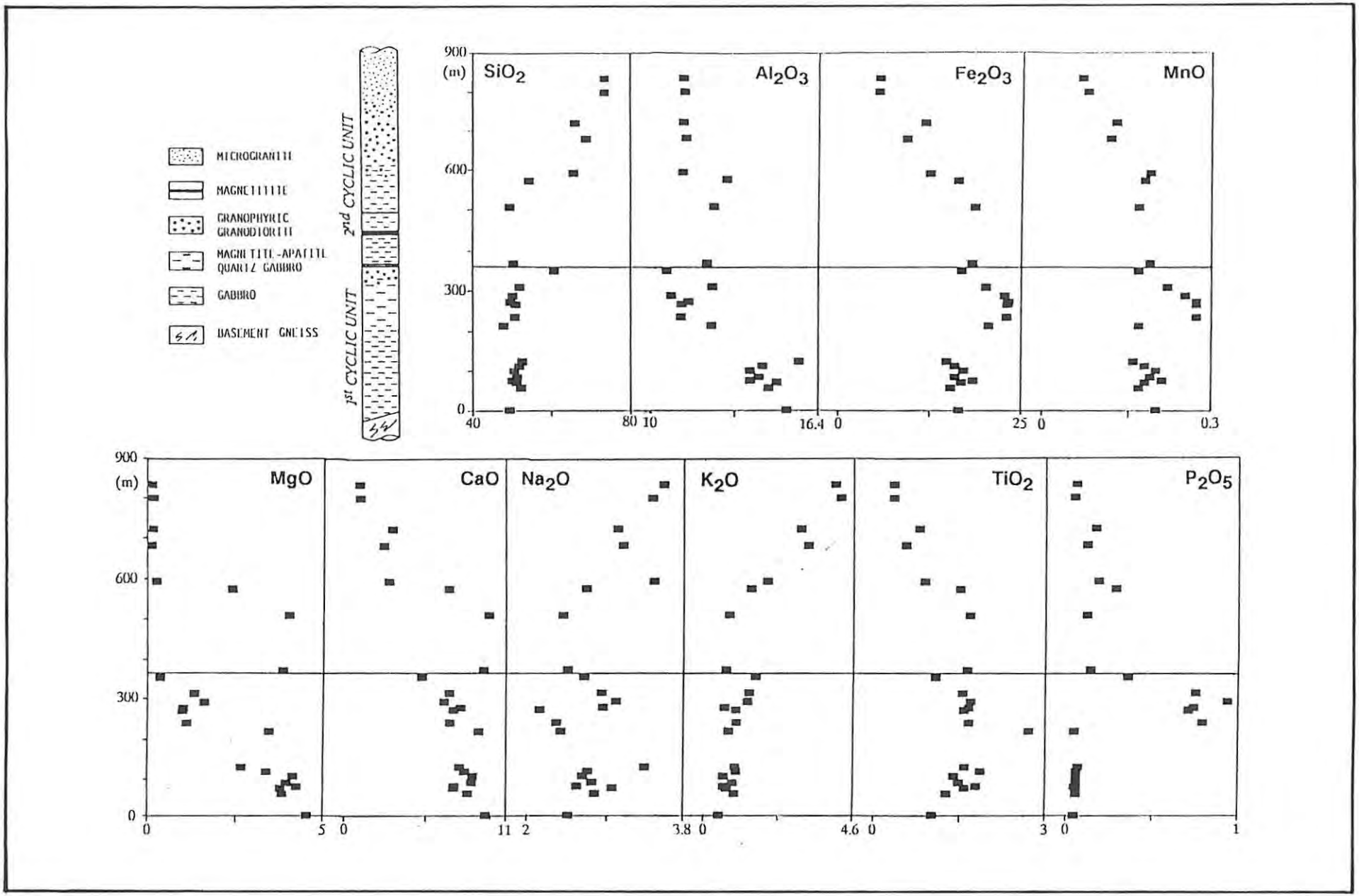

Fig. 21 - *Chemical variations of major elements with stratigraphic height (Hlelo River Section).*

granophyric rocks. A similar pattern was defined by the microprobe analyses of plagioclase, indicating therefore that the CaO variations are mostly governed by the modal amount of this mineral.

Na_2O should reflect the plagioclase trend and, with increasing fractionation (i.e. decreasing CaO values), it should become more enriched in the rock. This pattern is observed in the second unit, while levels of Na_2O in the first cycle are erratic, possibly due to its partial partition into the pyroxene.

Al_2O_3 tends to decrease with height, this variation being mostly dominated by the amount of plagioclase, and secondly by that of ferromagnesian minerals. Changes in the ratio of these phases are probably responsible for the different ranges of values in the first and second unit.

MgO abundances are mostly sensitive to the presence of mafic minerals (e.g. clinopyroxene). In the gabbroic rocks, decreasing levels of MgO with height are generally ascribed to progressive fractionation, as this feature reflects the decrease in the amount of clinopyroxene which characterises many fractionated sequences (Danchin and Ferguson, 1970).

Total Fe (as Fe_2O_3) and MnO contents vary sympathetically, their close coherence being a typical feature of mafic intrusions (Danchin and Ferguson, 1970). The MnO/Fe_2O_3 ratio remains almost constant over the entire sequence, averaging 0.011 (range 0.008 ÷ 0.015). Two minor cycles seem to occur in the basal gabbros and in the magnetite-bearing apatite quartz gabbros of the first unit. The trend is one of increasing values of Fe_2O_3 and MnO, followed by a decrease towards the upper part of these packages. Absolute maximum values are reached in the magnetite-bearing apatite quartz gabbro. The second unit is characterised by an overall decrease in the levels of Fe_2O_3 and MnO.

In mafic intrusions, TiO_2 usually displays a pattern of steady enrichment culminating in the precipitation of ilmenite, followed by a gradual decrease in the TiO_2 content of the successive differentiates

(Danchin and Ferguson, 1970). This trend does not seem to be matched in the Usushwana Complex. In the first unit, TiO_2 tends to increase from the base of the sequence, maintains fairly constant values in the magnetite-bearing apatite quartz gabbros and then decreases in the granophyric granodiorites. In the second unit it decreases regularly, reaching minimum values in the granophyres. However, modal variations of magnetite and ilmenite were not determined, therefore precluding the establishment of a precise relationship between the Ti variations and modal mineralogy.

P_2O_5 variations indicate that in the Hlelo River Section P behaves as a relatively incompatible element, remaining at constant low values until it becomes compatible in apatite; at this point very high concentrations are recorded in the rock. Concentrations then decrease in the granophyric rocks. The same trend is not repeated in the second unit, which displays only a slight decrease in the P_2O_5 content.

Variations in the compositions of gabbros from other parts of the Usushwana Complex were investigated by Hammerbeck (1977), by means of traverses on Sterkwater 472 IT and Piet Retief Townlands (see figure 2 for location). No marked differentiation was recognised by Hammerbeck (op.cit.) on plots of the major oxides against the position of the samples along the traverses, apart from a slight decrease in alumina and combined alkalis, and a concomitant increase in silica, total iron and magnesia. Though not pronounced, these trends are the same as those observed in the Hlelo River Section. Any further comparison is precluded by the fact that the true stratigraphic thickness cannot be established along these traverses.

Despite a relatively wide scatter of points, on an AFM ternary diagram (Fe_2O_3:MgO:Na_2O+K_2O; Fig. 22a) the gabbroic rocks cluster towards the Fe_2O_3 corner. The granophyric rocks, as a result of their low MgO contents, plot close to the iron-alkali join, in the range Fe_2O_3 = 41.5 - 78.6. The resulting differentiation trend might therefore be defined as one of Fe-enrichment in the gabbros, followed by a rapid descent towards the alkali corner of the diagram. The granophyric granodiorites of the first unit have a relatively high iron content

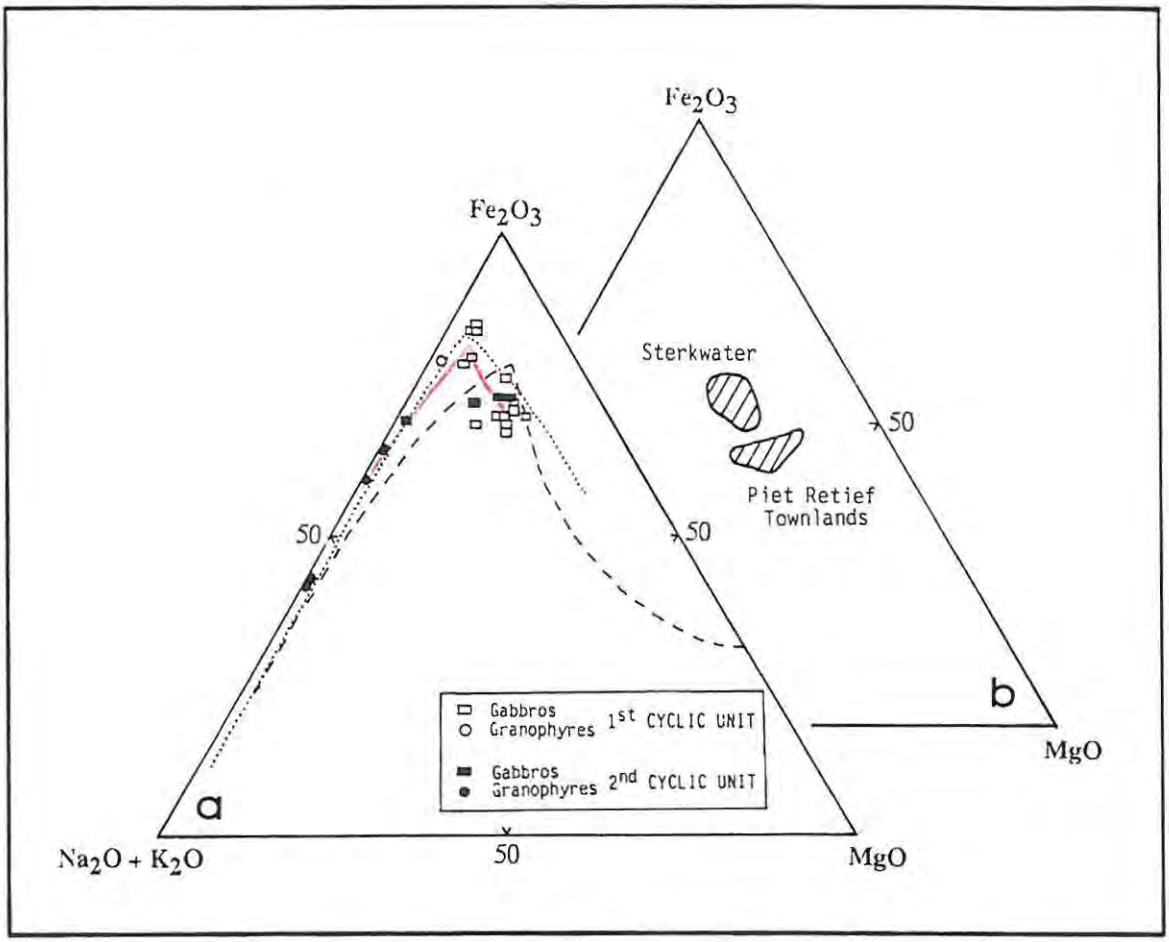

Fig. 22 - *a) Fractionation trends of the Usushwana Complex (red line), the Bushveld Complex (dashed line; after Danchin and Ferguson, 1970) and the Skaergaard intrusion (dotted line; after Nesbitt et al., 1970).*
b) Composition of rocks of the Usushwana Complex from Sterkwater 472 IT and Piet Retief Townlands 419 HT (modified after Hammerbeck, 1977).

(78.6), while the equivalent rocks of the second unit are depleted discontinuously in this element and possibly do not all belong to the differentiation pattern described above. A comparison with the Bushveld and Skaergaard trends (Fig. 22a) shows that the Ususwhana lithotypes resemble the more evolved differentiates and the silica-rich rocks of these complexes, and that a marked parallelism exists with the more Fe-rich Skaergaard intrusives. Figure 22b combines data from this study with those provided by Hammerbeck (1977) for other portions of the Complex. Though stratigraphic relations are uncertain, the gabbros on Piet Retief Townlands appear to be more mafic than those on the farm Sterkwater, and both are less differentiated than the Hlelo quartz-rich gabbros. From figure 22a and 22b, an indication

may be derived, that the Usushwana differentiation trend defined by the Hlelo data could be projected towards more primitive compositions in lower (not exposed) parts of the sequence.

7.2.2 TRACE ELEMENTS

The most significant trace element variations with stratigraphic height are depicted in figure 23, which indicates an overall increase in incompatible element concentrations upwards in the sequence and a concomitant decrease in compatible element abundances. A similar trend has been predicted for increasing stages of differentiation in layered intrusive complexes (Cawthorn and McCarthy, 1985).

Nb, **Y**, **Zr** and **Ba** tend to increase within a single unit, the uppermost granophyres of the second unit (microgranites) usually yielding the maximum concentrations. **Rb** has a similar trend, though points are more scattered and the granophyric granodiorites of the first unit have an unexpected low Rb content. For all the previously mentioned elements, sample U262 (which represents the transition between the gabbros and the granophyric granodiorites of the second unit) is characterised by anomalously high concentrations, and does not plot on the curve established by the other samples. Variations in the trapped liquid proportion from sample to sample have been considered to explain the random scatter in the incompatible element trends (Cawthorn and McCarthy, 1985).

La and **Sc** show an overall tendency to decrease with height in each unit and to follow sympathetically the Fe_2O_3 trend. **V** and **Sr** (the latter not depicted in figure 23) have a similar pattern.

The element **Cu** (not depicted in figure 23), useful as an indicator of S when present in anomalously high concentrations, ranges from 27.1 to 225.4 ppm (with an erratic peak at 424.5 ppm), and generally tends to decrease along the sequence. Cu, however, does not follow the S pattern sympathetically, suggesting the presence of other sulphur phases (e.g. pyrite).

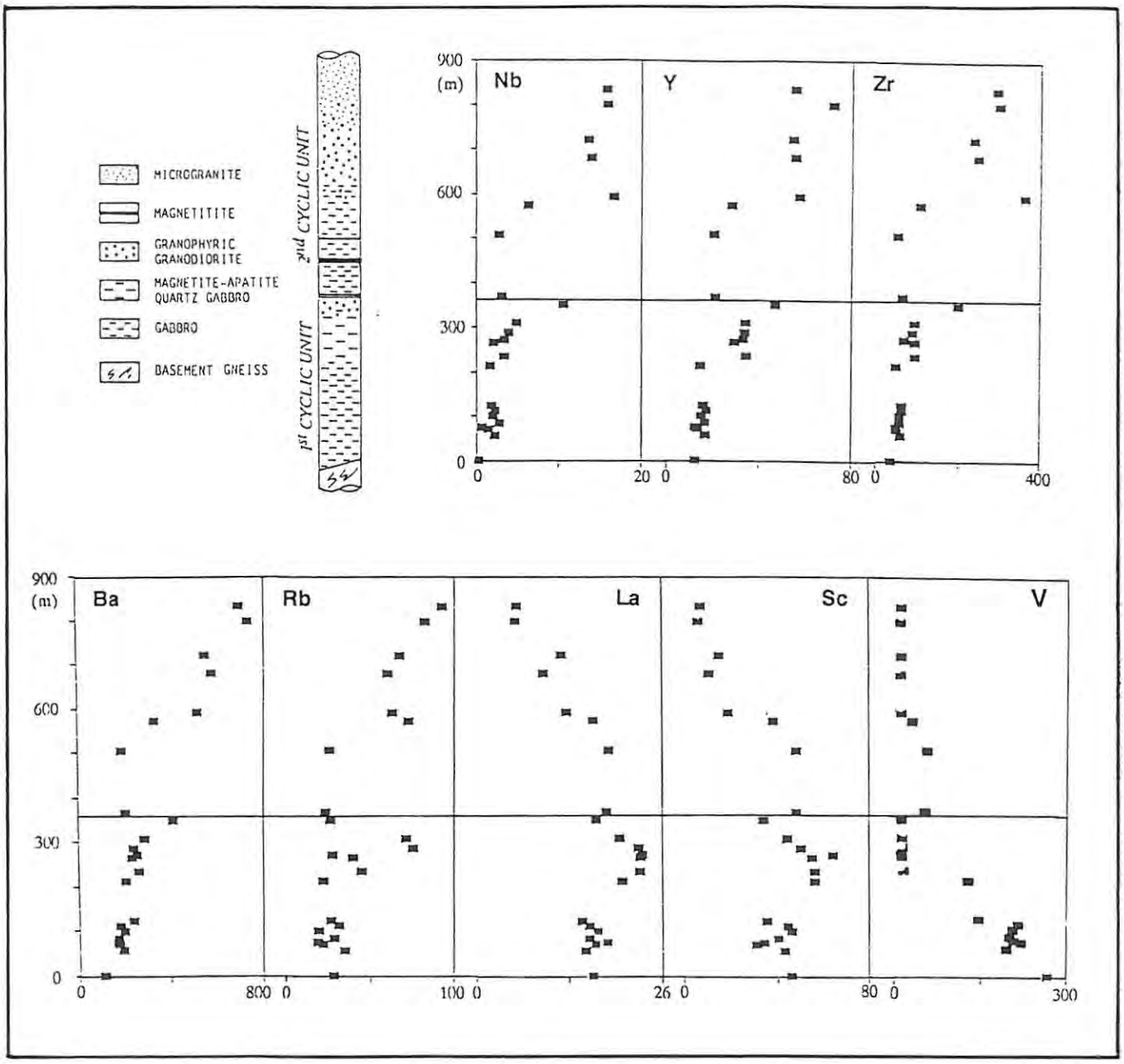

Fig. 23 - *Chemical variations of trace elements with stratigraphic height (Hlelo River Section).*

Compatible elements either display a wide scatter of data (e.g. Cr) or have minimal variations (e.g. Ni), so that no trends emerge. Ni tends, however, to concentrate in the basal gabbros of each unit, and so does Cu. Erratic values characterise the U, Th and Zn diagrams.

7.3 INTERELEMENT RELATIONSHIPS

7.3.1 MAJOR AND TRACE ELEMENTS VS MgO

MgO is considered to be a good index of differentiation, as it usually decreases from the most primitive to the most differentiated rocks (Danchin and Ferguson, 1970). Plots of major elements against MgO (Fig. 24) show a clustering into two distinct fields, corresponding to the gabbroic and granophyric lithotypes. The gabbros span a wide range of MgO contents (0.95 ÷ 4.32 wt.% MgO), but generally show limited variations in all the elements considered. The granophyric lithotypes have a narrow MgO range (0.09 ÷ 0.33 wt.% MgO), and display more pronounced enrichment or depletion in the plotted oxides. The gabbroic lithologies can be further subdivided: the magnetite-bearing apatite quartz gabbros lie within the range 0.95 ÷ 1.54 wt.% MgO, while the basal gabbros of each unit have more than 2.27 wt.% MgO. Sample U262 does not plot in the same group established by the gabbros, but appears to have the same geochemical signature as the overlying granophyres, a similarity already noted from microprobe data (see section 6.2).

Concentrations of K_2O show a strong negative correlation with MgO, while **CaO** has the opposite tendency. This trend reflects changes in lithology and modal compositions, in particular the variable ratio plagioclase-orthoclase in the rock. The relationship of SiO_2 to MgO is similar to that of K_2O, and is mostly controlled by the quartz content of the various lithologies.

An overall positive correlation with MgO is displayed by Fe_2O_3, with maximum values recorded in the magnetite-bearing apatite quartz gabbros. The Fe_2O_3 pattern is closely followed by **MnO**. Again, these trends can be explained by variations in modal compositions (ratio of feldspar to ferromagnesian phases). TiO_2 tends to correlate positively with MgO, with a sharp increase in the granophyres and a flatter trend in the gabbroic rocks.

No clear trends are revealed by plotting Al_2O_3 and P_2O_5 against MgO,

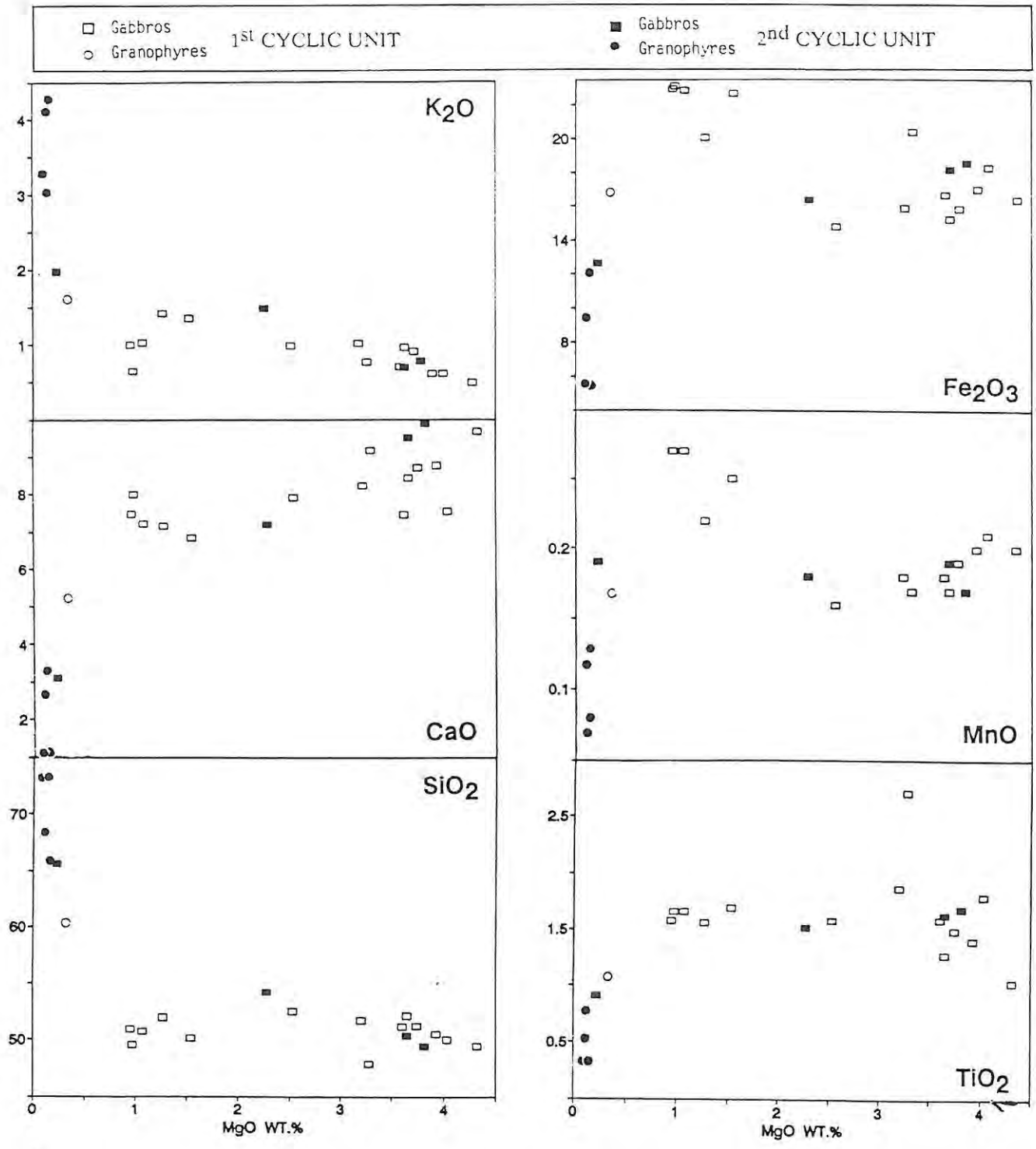

Fig. 24 - *Interelement relationships of selected major elements (all whole-rock data in wt%).*

though the granophyric rocks, as always, cluster in a separate field. Unexpectedly, the Na_2O values do not show a positive trend as does CaO, but a wide scatter of points marks the gabbroic rocks (these latter elements are not depicted in figure 24). This indicates that Na is not simply associated with feldspar, but enters the lattice of other minerals (e.g. clinopyroxene), as suggested by optical determinations (see section 5.2.2). Remobilisation during low-grade metamorphism could also account for the observed trend.

Most of the trace elements follow regular trends when plotted against MgO (Fig. 25), and display the same clustering of datum points observed for the major oxides. A negative relationship is evident for most of the incompatible elements (i.e. **La**, **Y**, **Nb**, **Zr**, and **Th**), and appears to be clearly related to their enrichment in the granophyric rocks. **Ba** behaves sympathetically to the previous elements. **Sc** and **Sr** show a positive correlation,while **Rb** data (not reported in figure 25) are more widely scattered. **Cu** shows a weak positive correlation with MgO, while levels of U, Cr, and V do not disclose any significant pattern.

7.3.2 TRACE ELEMENTS VS Zr

During fractional crystallisation, if two elements are equally incompatible, their concentration in the liquid will increase at the same rate, and hence their ratio will remain constant (Cawthorn and McCarthy, 1985). Therefore, on variation diagrams, rocks genetically related by this process should plot on a straight line passing through the origin. In figure 26, Zr was plotted against the other trace elements because of its nearly perfect incompatible behaviour and the wide range of concentrations in the analysed suite of rocks (36.7 - 364.7 ppm).

A positive correlation indicating a sympathetic enrichment is shown by **Nb**, **Y** (Fig. 26a, 26b), **La**, **Ba**, and **Th**, due to the lack of affinity for most of the phases fractionating in a basaltic system (Pearce and Norry, 1979). Nb and Y tend to partition into apatite, but the

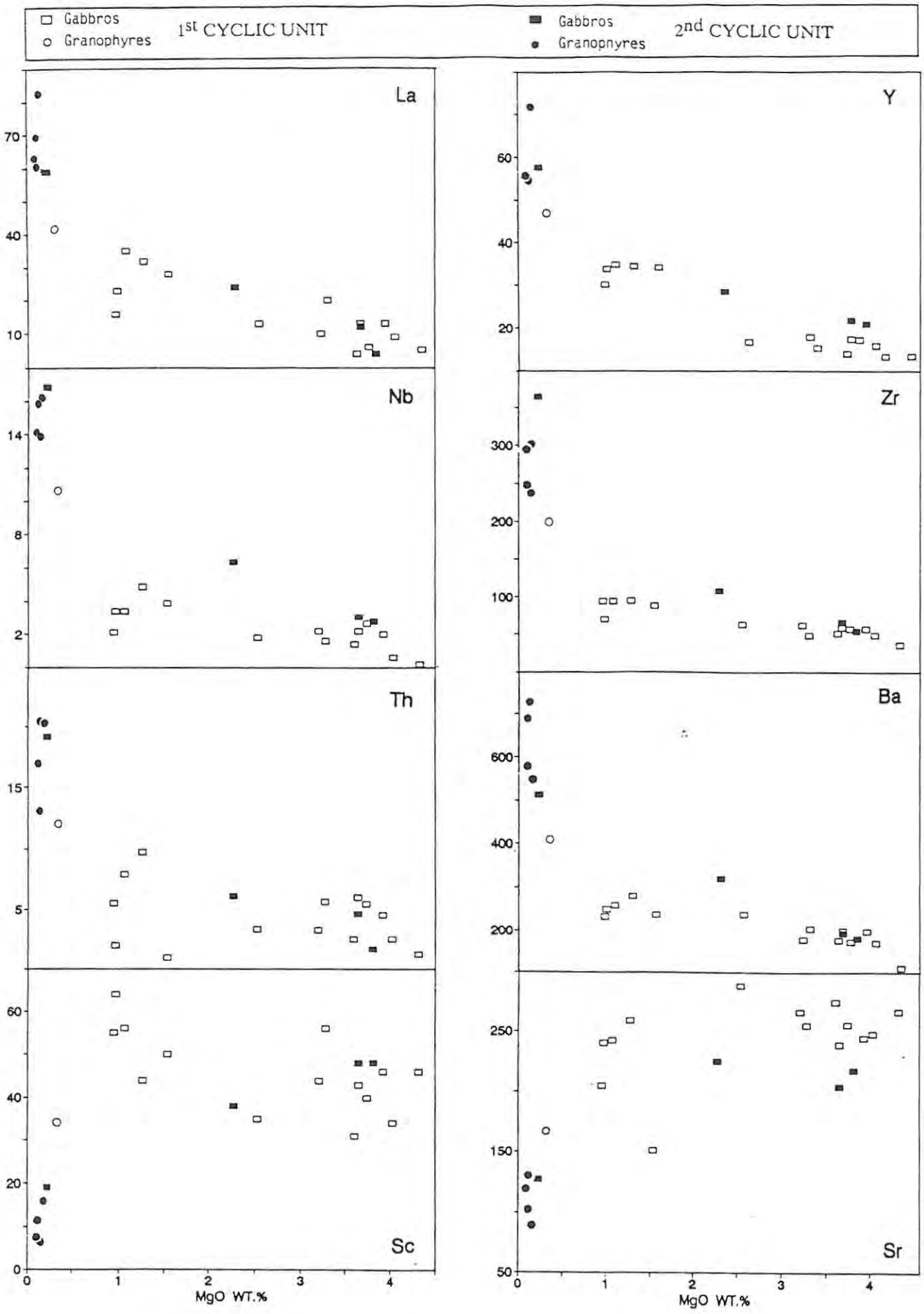

Fig. 25 - *Interelement relationships between selected trace elements (all in ppm) and MgO. (All whole-rock data).*

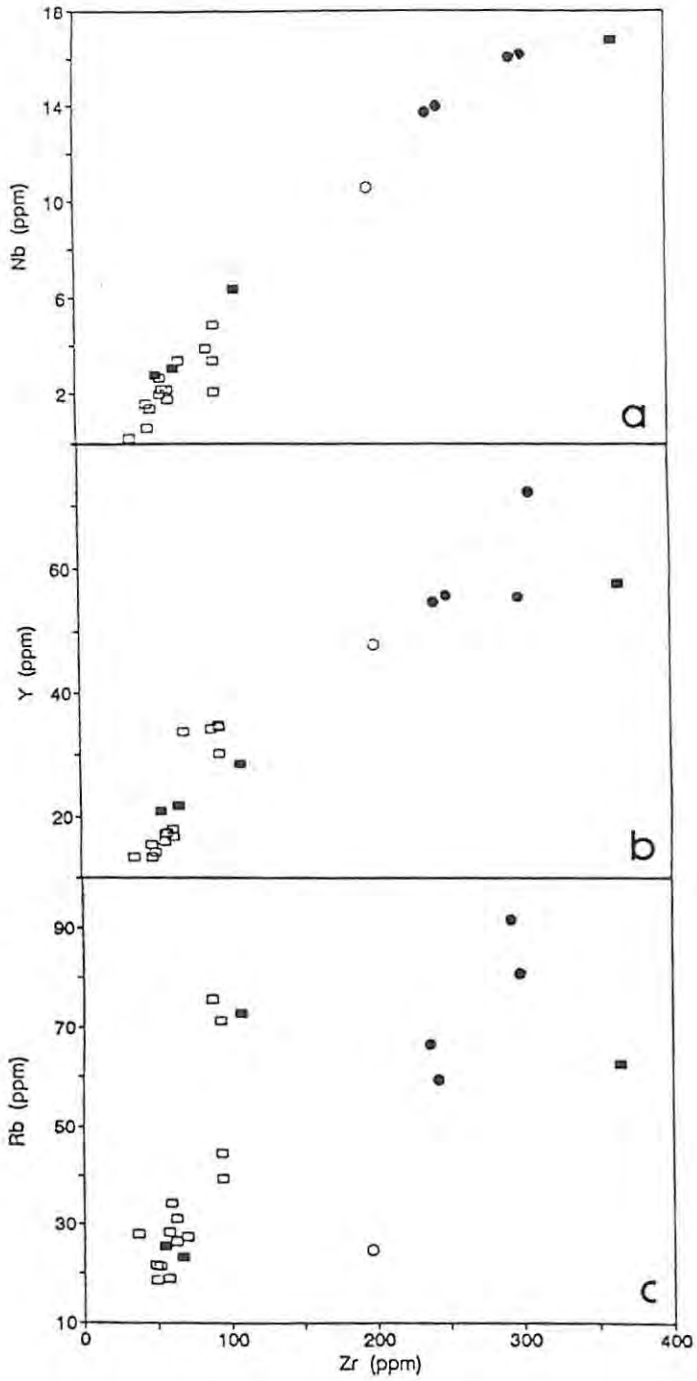

Fig. 26 - *Interelement relationships of selected trace elements: a) Nb vs Zr; b) Y vs Zr; c) Rb vs Zr. Symbols as in figure 25.*

straightforward trends defined by these elements suggest that their incompatible character was not affected by the crystallisation of apatite-rich horizons. In all the diagrams for the incompatible trace elements, the granophyric rocks plot on the line of constant ratio defined by the gabbros (with the exception only of sample U262), and therefore seem to be related to the latter by a process of fractional crystallisation. Though Rb is expected to behave incompatibly, its relationship to Zr is anomalous, being characterised by a relatively wide scatter of datum points (Fig. 26c). This is ascribed to the irregular behaviour of Rb or to remobilisation during metamorphism, rather than to the partitioning of Zr into the magnetite, as the last feature is not apparent from other variation diagrams.

Plotted against Zr, the elements Sr, Sc and, to a lesser extent, Cu and V, behave incompatibly, being depleted during fractional crystallisation. Cr, U, Zn, Ni, and S variation diagrams do not define any significant trend.

7.4 COMPARISON OF THE MAIN ROCK-TYPES

Average compositions of the main rock-types in different stratigraphic intervals were calculated, and are compared in Table II. This was done by averaging all samples of the same lithology within each unit. Sample U262, though described as a gabbro, proved to be geochemically similar to the granophyres and was therefore considered independently. The granophyric rocks of the second unit were split into two groups, representing samples taken near the contact with the gabbros (granophyric granodiorites) and from higher in the succession (microgranites).

The basal gabbros of the first and second unit are similar in their average compositions. In the first unit, the differences observed with the magnetite-bearing apatite quartz gabbros are easily explained as a result of either differentiation or modal variations (i.e. the higher Fe_2O_3, MnO and P_2O_5 averages reflect the increase in magnetite and apatite). Compared with the average composition reported by Le Maitre

Table II

Average chemical compositions (in wt.%) of the main rock-types of the exposed sequence of the Usushwana Complex.

1st UNIT

	gabbro	magn., ap. qtz gabbro	granophyric granodiorite
SiO_2	50.74	50.63	60.54
Al_2O_3	14.33	11.41	10.64
Fe_2O_3	16.81	22.36	16.85
MnO	0.18	0.26	0.17
MgO	3.59	1.16	0.33
CaO	8.43	7.34	5.28
Na_2O	2.74	2.65	2.66
K_2O	0.79	1.09	1.62
TiO_2	1.64	1.63	1.10
P_2O_5	0.06	0.79	0.36
TOTAL	99.31	99.32	99.55

2nd UNIT

	qtz gabbro	U262	granophyric granodiorite	microgranite
SiO_2	51.30	65.61	67.25	73.24
Al_2O_3	12.55	11.27	11.37	11.33
Fe_2O_3	17.79	12.64	10.69	5.60
MnO	0.18	0.19	0.12	0.07
MgO	3.24	0.22	0.11	0.12
CaO	8.87	3.11	3.07	1.13
Na_2O	2.52	3.46	3.07	3.50
K_2O	0.99	1.98	3.13	4.14
TiO_2	1.61	0.90	0.68	0.35
P_2O_5	0.18	0.19	0.14	0.05
TOTAL	99.23	99.57	99.63	99.53

(1976) for tholeiites, the Usushwana gabbros are depleted in Al, Mg and Ca, and enriched in Si and Fe.

The transition between gabbros and granophyric granodiorites in both cyclic units is characterised by a regular trend of SiO_2 and K_2O

enrichment, coupled with a depletion in Al_2O_3, Fe_2O_3, MnO, CaO, TiO_2 and P_2O_5. The changes in the average abundances from gabbros to granophyric granodiorites are less marked in the first unit than in the second (e.g. CaO ranges from 8.43 to 5.28 and from 8.87 to 3.07 in the first and second unit, respectively). Selected trace element averages for the main rock-types of different stratigraphic intervals are in general agreement with the observations based on major oxide data.

A markedly different whole-rock geochemistry distinguishes the granophyric granodiorites of the two units, as well as the gragranophyric granodiorites and the microgranites within the second unit (Table II). Significantly, lower contents of SiO_2, Al_2O_3, Na_2O, and K_2O, together with marked enrichment in other oxides, characterise the granophyric granodiorites of the first unit. In the second unit, the compositional changes between the granodiorites and the microgranites are not smooth and progressive, and major drops can be significantly observed (e.g. Fe_2O_3 drops from 10.69 to 5.60 from the granodiorites to the microgranites, while it decreases only from 12.64 to 10.69 from sample U262 to the granodiorites; Mn, Ca and P behave in a similar manner). Compared to the average composition for granodiorites (Le Maitre, 1976), similar rocks of the Usushwana Complex have higher contents of Fe and lower concentrations of Mg and Al; granophyres from the first and second unit are respectively depleted and enriched in K.

The above-mentioned differences may indicate that different processes were involved in the formation of the various granophyric types. It is considered that at least part of the granophyres (i.e. the granophyric granodiorites) are genetically related to the gabbroic rocks, of which they would represent silica-rich differentiates.

7.5 SUMMARY AND DISCUSSION

Whole-rock major and trace element data provide information on the possible magmatic processes that controlled the evolution of layered intrusive complexes, and that include differentiation, magma mixing, assimilation of country rocks, contamination and addition of new magma. This section deals in particular with the most important findings in relation to differentiation. The significance of other processes in the evolution of the Usushwana Complex is specifically addressed in chapter 8.

Generally, the differentiation of mafic magmas is manifested by two chemical trends. The first tends to enrich the liquid in iron relative to magnesium and is reflected by crystallising mafic minerals; the second is indicated by the progressive enrichment of alkali elements relative to calcium in the felsic minerals. In addition to these effects, a general increase in incompatible element abundances can be predicted as the differentiating liquid becomes enriched in these elements; compatible trace elements should decrease concomitantly.

Several lines of evidence suggest that differentiation was effective during the evolution of the Usushwana Complex. Furthermore, the Usushwana lithotypes are confirmed to represent late-stage differentiates, as demonstrated by a comparison with the Bushveld and Skaergaard trends on the AFM diagram.

Most element concentrations vary systematically with stratigraphic height. Similar patterns tend to be repeated in the first and second cyclic unit, thus confirming the distinction made previously on the basis of field relationships, cumulus mineralogy and compositional changes of different phases. The best indications of the stage of differentiation, compared to other chemical variants, are provided by concentrations of CaO, MgO and K_2O (among the major oxides), and by the incompatible elements (Nb, Y, Zr and Ba in particular). Interelement relationships support the expected fractionation trend.

Contrasting observations emerge when granophyric rocks are considered in relation to the differentiated gabbroic sequence. Datum points of gabbros and granophyric rocks tend to cluster into two distinct fields on the interelement diagrams (by analogy with some microprobe results, see section 6.2), suggesting an independent origin for the two lithotypes. However, granophyres in different stratigraphic positions have different geochemical signatures. The granodiorites of the first unit often have average compositions or plot in a position intermediate between the gabbroic rocks and the granodiorites of the second unit. In the latter, a gap between the microgranites and the granophyric granodiorites close to the contact with the gabbros is also frequently observed. In the gabbroic and granophyric rocks, similar ratios in incompatible elements suggest a common process of fractional crystallisation. The hypothesis favoured herein to explain these contrasting features is one that supports a genetic link between the gabbros and at least part of the granophyric rocks, i.e. the granophyric granodiorites of the first and second unit. Partial melting and recrystallisation of country rocks are thought to have been more relevant for the formation of the uppermost granophyres (i.e. microgranites); the role played by these processes is further discussed in chapter 8.

CHAPTER 8: PETROGENESIS OF THE USUSHWANA COMPLEX

8.1 INTRODUCTION

In this chapter, the different processes controlling the evolution of mafic layered complexes are considered. It is a widely accepted theory that the dominant process operating in the magma chamber of a mafic intrusion is igneous fractional crystallisation. Controversial aspects of this process include: the degree of differentiation and contamination before emplacement, the amount of assimilation of country rocks and the role of magma addition. The likelihood of these processes having occurred in the Usushwana Complex and their relevance to its evolution are discussed below in the light of field observations, microscopic evidence and analytical results.

8.2 NATURE OF THE PARENTAL MAGMA AND EVIDENCE FOR CONTAMINATION

Although a cumulate succession represents an excellent record of the crystallisation history of a layered intrusion, it does not preserve the chemical composition of the parental magma. In the absence of features such as chilled margins, feeder dykes or early cumulus assemblages (as in the case of the Usushwana Complex at its present level of exposure), it is difficult to make more than an estimate of the original liquid compositions. This attempt is based mainly on comparisons with other layered intrusions, for which more reliable data on the nature of the parental magma exist.

The differentiation pattern of the Usushwana Complex (see figure 22, chapter 7) depicts an initial enrichment in iron in the gabbros and a subsequent enrichment in alkalis in the granophyric rocks, and is consistent with the well established magmatic differentiation trend of tholeiitic stratiform complexes (Bowes et al., 1970; Nesbitt et al., 1970). Features which are also comparable with a tholeiitic parent and indicative of a strongly fractionated tholeiitic magma, include:
a - the occurrence of intercumulus quartz and the abundance of

granophyric intergrowths (Wadsworth et al., 1982);

b - the presence of granitoid (granophyric) differentiation products;

c - the overall cryptic variation patterns, in particular the compositional trend of Ca-rich pyroxenes (approaching a Ca minimum in the pyroxene ternary diagram) and the coexistence in the uppermost gabbros of Fe-enriched mafic minerals with plagioclase of oligoclase-andesine composition (Wilson et al., 1981).

Furthermore, a tholeiitic affinity has been indicated for the volcanic rocks of the Pongola Sequence, and these are considered to have been derived from the same source that generated the Usushwana magma (Hegner et al., 1984).

In addition, there is a great deal of evidence to suggest that contamination of the original tholeiitic magma has taken place in the Complex. Contamination is believed to have occurred either before or after the emplacement of the Complex, though the relative contributions are difficult to assess.

The Usushwana basic magma was apparently intruded along an unconformity between a basement complex of tonalites-trondhjemites, and a relatively undeformed cover of quartzites, andesitic and rhyolitic lavas (see chapter 3). All these dominantly felsic rocks could have represented a potential source for the contamination of the Usushwana magma. Different models have been proposed to describe the tectonic framework at the time of emplacement of the Complex (e.g. relatively newly established, stable continental crust; Armstrong et al., 1982; continental rift zones; Burke et al., 1985), but all agree that the tectonic setting was essentially continental. Hegner et al. (1984) suggested that basic magmas of mantle origin were emplaced as sills located at or near the base of the lower continental crust, and resided there for a prolonged period due to their density contrast with the overlying differentiated crust. Crustal assimilation could therefore have occurred, together with fractional crystallisation, until the contrast in density was reduced enough to allow the evolved melt to ascend. After emplacement at higher crustal levels, further contamination is considered to have occurred at the roof of the intrusion; this particular aspect is discussed in more detail in the

next section with reference to the genesis of granophyres.

Contamination by silicic rocks is additionally supported on the basis of bulk compositions and textural features. Chemical compositions of the gabbroic rocks show that the SiO_2 content is greater (by up to 5%) than expected from tholeiitic magmas formed in a continental setting (Wilson, 1990). A large proportion of quartz could have originated from contamination of the magma, as indicated, for instance, by the corroded quartz grains (see section 5.2.2) which would represent xenocrysts inherited from the country rocks. Potassium levels are also higher than average in primitive tholeiitic magma, as suggested by the abundance of granophyric intergrowths in most rock-types of the Complex. Direct evidence for contamination is provided by the abundance of xenoliths of all the host rocks of the Complex (quartzites in particular, because of their higher refractory nature), many of which appear to have been rounded and embayed by assimilation.

Further support for contamination is derived from geochemical studies and isotopic relationships (Hegner et al., 1984). Measurements on primary clinopyroxenes yielded an initial $^{87}Sr/^{86}Sr$ ratio of 0.703024 ± 24 (0.7031 ± 0.0028 according to Davies et al., 1970), considerably higher than the expected value of 0.701 for the 2.9 Ga old primitive mantle. A negative deviation of the initial Σ_{Nd} (-2.9 ± 0.2) from the chondritic Nd growth curve is also observed, and contrasts with the average range (0 ÷ +3) of Archaean rocks, for which a derivation from chondritic or LREE-depleted mantle has been indicated. Furthermore, the linear array of Sm-Nd datum points for the Usushwana gabbros gives an apparent age of ≈ 3.1 Ga, which is in conflict with geological evidence showing the Complex to intrude the 2.9 Ga old Pongola Sequence. The Sm-Nd data can be interpreted as a mixing line between the 2.87 Ga old Usushwana magma and older continental crust. The LREE-enriched REE pattern (Fig. 27), a negative Nb-Ti anomaly and the low but uniform ratio of Ti/Zr ≈ 46 indicate a source distinctly different from primitive mantle and reflect the characteristics of continental crust, therefore indicating a substantial amount of crustal contamination.

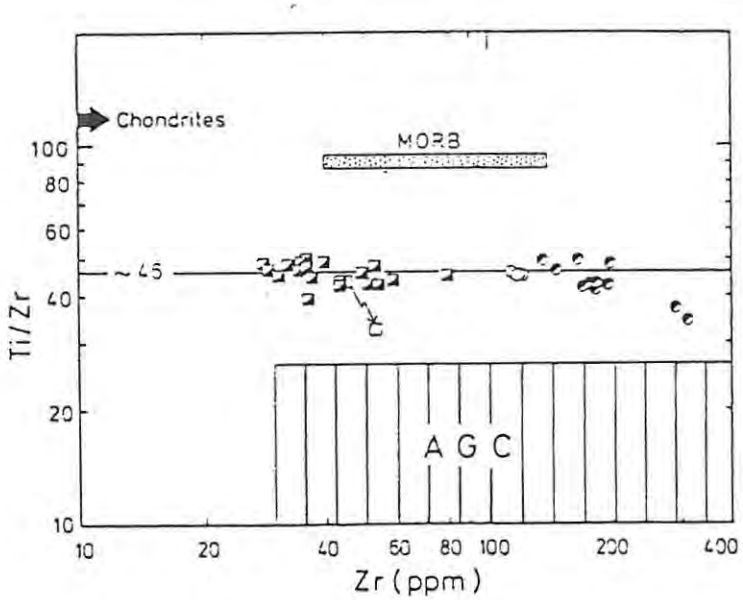

Fig. 27 - *Ti/Zr vs Zr variations for the Fe-enriched Pongola basalts (semi-filled circles), Pongola tholeiitic basalts (circles), Usushwana gabbros (open squares) and Usushwana pyroxenites (semi-filled squares). These values are between those for MORB (= Middle Ridge Ocean Basalts) and the main rock-types underlying the Usushwana Complex (AGC = Ancient Gneiss Complex). They can be interpreted to result from mixing of primitive magma with basement rocks (after Hegner et al., 1984).*

8.3 ORIGIN OF THE GRANOPHYRIC ROCKS

The origin of igneous rocks of highly contrasting chemistry but closely related in time and space, such as the gabbro-granophyre association of mafic layered intrusions, has been strongly debated for many years. Several models have been proposed to account for the presence of granophyres in these complexes. They can be broadly divided into two groups (Walraven, 1985):

a - magmatic origin, due to differentiation of the basic melt or to a separate intrusion of acid magma;

b - metamorphic origin, including in situ recrystallisation of sedimentary/volcanic country rocks and crystallisation from a melt produced by anatexis and remobilisation of country rocks. In both cases the basic magma is considered to have acted as the heat

source.

In the Usushwana Complex, various and contrasting aspects of the granophyres (e.g. field relations, petrology and geochemistry) point to a complex interaction between the mafic magma and the country rocks in the roof zone of the magma chamber. A composite process involving either differentiation from the mafic magma or partial melting and recrystallisation of the country rocks is invoked to account for the origin of the different granophyric rocks recognised in the Complex (i.e. the granophyric granodiorite and the microgranite, see section 5.2.2). The main arguments relevant to the origin of these lithotypes, as put forward in the previous chapters, are summarised below.

Spatial relations of the granophyres to the other rock-types of the Complex indicate that the former occur at the top of the gabbroic package, the only exception being represented by the granodiorites of the first unit in the Hlelo River Section and by small erosion relics (see attached map). The microgranite is always associated with the gabbroic rocks (but not vice-versa) and it appears to have its greatest areal development where the Complex was intruded along the contact between the basement and the Vaalkop rhyolites. In places the microgranite is seen to transgress across part of the gabbroic sequence (e.g. the magnetitite layers on Ishlelo 441 IT, see figure 5). A transition from gabbros to rocks texturally and mineralogically resembling the granodiorites was almost always observed, though the latter are often restricted to a narrow strip (only few metres in width) flanking the stratigraphically highest gabbros. When both granodiorites and microgranites are present, the former occupy an intermediate position between the gabbros and the microgranite. The large volume of acidic rocks is difficult to reconcile with a differentiation hypothesis, particularly for an intrusion the size of the Usushwana Complex (Hunter, 1970a).

Intrusive contact relations between the two granophyric rocks or with the supposed country rocks (the Vaalkop rhyolites in particular) were not observed, the different rock-types usually merging into one another and not always being easily distinguishable in the field. In

places, the gabbros have been reported to intrude the acidic rocks (Hammerbeck, 1977); acidic veins observed elsewhere in the gabbros have been interpreted as downward injections of remobilised granitic melt (see section 4.7).

Microscopic features (see chapter 5) are mostly consistent with a process of partial melting and recrystallisation of a pre-existing rock (partially assimilated by the mafic magma), as indicated by the quartz-feldspar intergrowths. These are interstitial between pyroxene and plagioclase in the basic rocks, becoming increasingly abundant upwards, until the rocks consist almost entirely of an intergrowth of quartz and feldspar, with hornblende as the predominant mafic mineral (granodiorites). In the uppermost part of the sequence (microgranites), only a small proportion of the quartz and feldspar is intergrown, and a large proportion of the rock has a granular texture, often showing evidence of recrystallisation. In the upper portion, the intergrowths are also noticeably irregular, indicating replacement of quartz by feldspar rather than simultaneous growth under equilibrium conditions. The same relations have been observed in the Diepkloof Granophyre of the Bushveld Complex, which is thought to have originated by melting of the roof rocks as a result of heating by the underlying basic magma (Walraven, 1985).

Microprobe analyses (see chapter 6) generally support the findings of microscopic studies, as plagioclase compositions display a major gap between the gabbroic and the granophyric rocks. This is unlikely to be related to an incomplete record of the stratigraphic sequence (due to the narrow sampling interval of 10 m), and therefore suggests a different origin for the two rock-types. Ca-poor compositions of the plagioclase in micropegmatitic rocks of the Sudbury intrusion have been attributed to reaction during the final stages of crystallisation of an initial Ca-rich plagioclase with interstitial water (Naldrett et al., 1970). This interpretation is not substantiated for the Usushwana Complex because of the absence of epidote, a mineral which should represent one of the reaction products. The corroded laths of plagioclase, acting as centres for the granophyric intergrowths, are more likely to represent grains incorporated from the roof rocks.

In contrast to most of the features described above, a number of aspects of both the major and trace element geochemistry (see chapter 7) suggests that a genetic relationship exists, at least between the granodiorites (particularly those of the first cyclic unit) and the gabbros, while the microgranites are more clearly geochemically distinguished from these lithotypes. Major elements do not show significant compositional gaps across the contact gabbro-granodiorite of the first unit, while discontinuities are observed in the second; similar behaviour is indicated by the trace element data. Interelement relationships indicate that the granophyric granodiorites with low silica content (first unit) have a closer affinity to the gabbros than the equivalent rocks of the second unit. A distinct geochemical signature for the granodiorites and the microgranites was also noted by Hammerbeck (1977), who reported significant differences in most of the major oxides (SiO_2, $FeO+Fe_2O_3$, Na_2O+K_2O and, to a lesser extent CaO). In contrast, a marked similarity has been observed between the microgranites and the Vaalkop rhyolites (Hammerbeck, op.cit.).

8.4 EVIDENCE FOR THE ADDITION OF NEW MAGMA

The process of replenishment of a magma chamber with fresh magma is considered to be a common feature in mafic layered complexes, and has been demonstrated in the Bushveld, Rhum and Kap Edvard Holm intrusions (Wager and Brown, 1968), as well as for the Fongen-Hyllingen (Wilson et al., 1981) and the Muskox intrusions (Irvine, 1980). Arguments favouring new magma addition are based on reversals in the normal differentiation trend or the behaviour of trace elements. In particular, "incompatible trace element abundances and ratios in cumulate rocks may be used to predict the levels at which new magma may be injected. Sudden and sustained changes in absolute abundances suggest new magma addition, while gradual increases are consistent with fractionation of a large body of magma" (Cawthorn, 1983).

In the Usushwana Complex, a reversal has been observed between the first and second cyclic unit (Hlelo River Section), which involves changes in mineral assemblages and compositions, as well as in the

major and trace element contents. Changes are more pronounced if the hypothesis is accepted that the granophyric granodiorites of the first unit are part of the differentiation sequence (e.g. in this case plagioclase compositions vary between 1.38 and 46.11% An).

The geochemistry of the major oxides and trace elements also indicates a break, with a resetting to values similar (or slightly more evolved) to those reported for the base of the first unit. The incompatible elements such as Zr, Y, Ba, La and K show a distinct hiatus at 360 m height in the intrusion (see figure 23, chapter 7), with enrichment factors of 1.4 to 2.4 across this interval (Nb displays a very high enrichment factor of 15.5, which decreases to 2.4 if the average of the first three basal samples is considered). In order to avoid the uncertainty of random variations in the proportions of trapped liquid, incompatible trace element ratios were plotted against stratigraphic height (Fig. 28). Sustained changes are not observed, although a general tendency to show a decrease can be seen between the first and the second unit. Zr was chosen because of its nearly perfect incompatible behaviour; ratios that use the Rb contents generally do

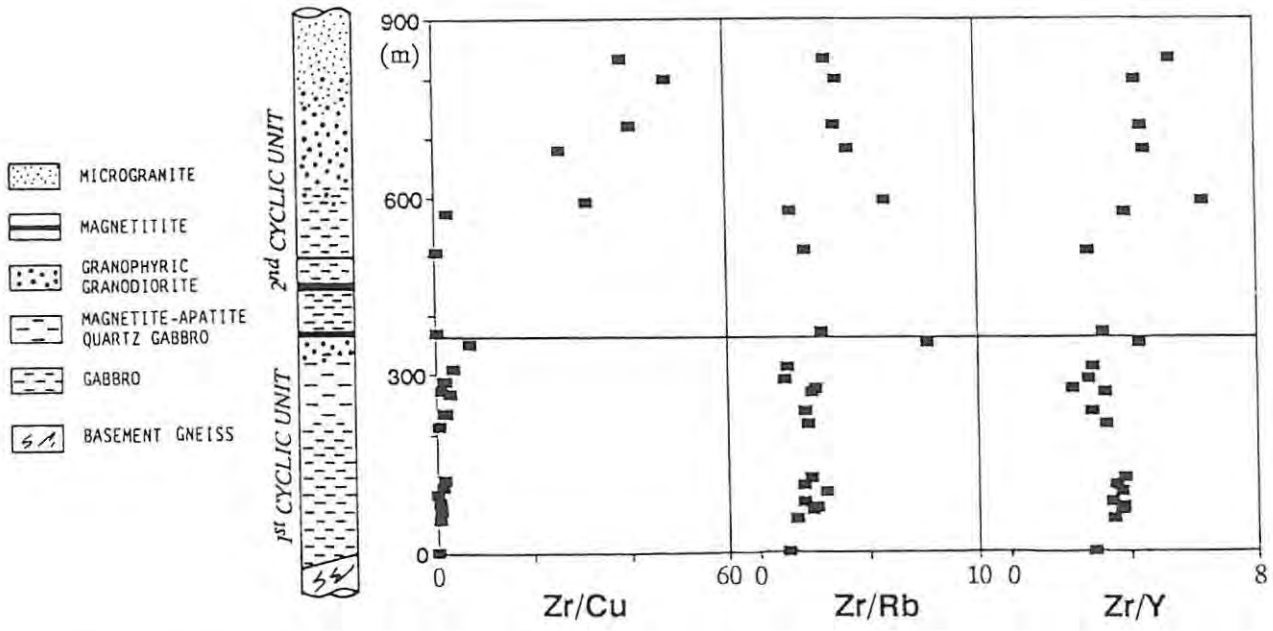

Fig. 28 - *Incompatible trace element ratios against stratigraphy (Hlelo River Section).*

not show meaningful variations with height, possibly reflecting the anomalous trend of this element (see section 7.2.2).

All the above-mentioned features are not consistent with fractional crystallisation from a single homogeneous magma, but are more likely to be related to a new pulse of liquid. Mixing with the differentiated residual magma residing in the chamber was probably limited due to density contrasts, as suggested by the sharp contact between the first and the second unit. The additional magma which gave rise to the second cyclic unit is considered to have been a more or less differentiated analogue of the first, as suggested by the repetition of overall compositional variations of plagioclase, and by the fact that the break observed in the single element plots does not correspond with a change in the ratio of different elements.

8.5 DISCUSSION

All the reported features argue strongly against a hypothesis that the chemically and mineralogically varied mafic and felsic rocks of the Usushwana Complex formed as a single comagmatic series. The suggested model involves differentiation of an already contaminated magma, which resulted in the production of small amounts of granophyric granodiorites as end-stage differentiates. This process is considered to have been enhanced by the assimilation/incorporation of acid material, derived by partial melting of the felsic country rocks at the roof of the magma chamber. Recrystallisation of these rocks gave rise to the microgranites.

Anatexis of a volcanic roof has been repeatedly proposed for the Bushveld Complex, where thermal modelling has indicated that a conspicuous thickness of rocks can melt in the presence of a fluid-rich gabbroic magma (Irvine, 1970; Von Gruenewaldt, 1972; Walraven, 1985). Despite the great difference in size and stratigraphic thickness between the Bushveld and the Usushwana Complex, similar conditions must have occurred in the latter, as indicated by the widespread evidence of a great deal of contamination. The enrichment

of the gabbroic Usushwana magma in fluids (see section 5.5) also favours this hypothesis. The Vaalkop rhyolites do not always form the roof of the Complex, but are considered to have had an original greater extension than is presently observed (see section 3.2.4). The absence of granophyric rocks in part of the Complex (see attached map and figure 5) indicate that the basic magma was, in places, an inadequate heat source, unable to raise the roof rocks to sufficiently high temperatures to provide large-scale recrystallisation. It is significant, in this regard, that granophyres are less developed where the roof of the Complex is composed of more refractory rocks (e.g. quartzites and basalts of the Pongola Sequence, dacites of the Amsterdam Formation).

The model proposed by Campbell and Turner (1986) is particularly appropriate to describe the process of assimilation at the roof of the magma chamber. These authors suggested that melting of the roof rocks in a basaltic magma chamber is induced by the latent heat of crystallisation released at the bottom of the chamber. This results in the formation of a lighter layer of melted material at the top, which tends to mix only slightly with the underlying basic magma. The double-diffusive interface separating the two melts, though allowing upward thermal transmission, would not permit efficient mass transport, therefore precluding extensive assimilation of melted roof material by the basaltic magma (unless a large number of blocks from the roof would fall through the upper layer and melt in the lower layer). At a later stage, the contaminated magma at the roof crystallises, and limited fractional crystallisation may follow assimilation. In the Usushwana Complex, this process would account for the formation of the granophyric granodiorite. The limited amount of mixing with the basaltic magma would explain both the observed chemical differences of the granophyric granodiorites with the gabbros and their closer affinity compared to the microgranite. The latter is considered to have been derived by limited partial melting and recrystallisation of country rocks. Evidence for contamination in the gabbroic rocks (as reported in the previous section) can easily be related to assimilation of crustal material prior to emplacement of the Complex.

Major changes in the mineral assemblages, plagioclase compositions, major and trace element contents occur between the first and the second cyclic unit. This break is consistent with the injection of a new pulse of magma at this horizon, possibly having a similar composition to that emplaced in the previous cycle.

CHAPTER 9: ECONOMIC MINERAL POTENTIAL OF THE USUSHWANA COMPLEX

9.1 INTRODUCTION

In this chapter, an assessment of the economic mineral potential of the Usushwana Complex in the study area is attempted. The likely occurrence of different kinds of mineralisation is discussed with particular reference to Cu-Ni sulphide, PGE (Platinum Group Elements), chromite, magnetite and gold ore. The available data from the literature and the results obtained during this study are compared with models proposed for other similar layered intrusions.

9.2 RELEVANT FEATURES FOR THE ASSESSMENT OF THE ECONOMIC MINERAL POTENTIAL OF THE USUSHWANA COMPLEX

Despite its great areal extent, the Usushwana Complex is relatively small volumetrically, compared to many other layered intrusions (e.g. Bushveld Complex, Skaergaard intrusion). A possible lateral extension under younger cover rocks is suggested by gravity and magnetic anomalies. The Usushwana Complex is either basin- or funnel-shaped, and locally resembles the structure of the Great Dyke. The contacts of the intrusion dip steeply inwards at 45°÷65° and inferred depths are between 3000 and 5500 m (see also below). The Usushwana magma reservoir must have been of considerable thickness in order to have provided sufficient heat to account for the great amount of contamination observed (though influx of fluids could have been important also).

Lithological, mineralogical and geochemical characteristics indicate that only the upper levels of the intrusion are currently exposed. There is no evidence of an ultramafic portion, at least in the outcropping section of the intrusion, the sequence comprising mostly gabbros and quartz gabbros with intercalated magnetitite layers. A few small, isolated outcrops of pyroxenite, noritic gabbro and websterite are present, but their stratigraphic position is generally uncertain.

Besides the magnetitites, bands of monomineralic rocks (e.g. anorthosites and chromitites) are not observed. Petrologically, it is unlikely that gabbroic rocks would develop over the entire stratigraphic interval indicated by gravity data (see section 4.3), and therefore a greater proportion of ultramafic rocks may be present at depth. However, studies of chemical trends in sections of exposed stratigraphy have shown that, although fractionation was operative during the evolution of the Usushwana magma, it appears to have been of little importance compared to the dominant role played by assimilation and contamination. In particular, the degree of fractionation in the gabbroic rocks is limited, especially when compared with the stratigraphic thickness over which it occurs; this might constrain the occurrence of ultramafic rocks at depth.

Known mineralised occurrences within the Usushwana Complex are restricted to sub-economic Cu-Ni sulphide concentrations and lenses of titaniferous magnetite. Apart from the sulphides observed on Blesbokspruit 515 IT (see section 4.6.5), no evidence was reported from the study area (other than sparsely disseminated pyrite in the gabbro). The most significant concentrations occur in Swaziland, where disseminated chalcopyrite and pyrrhotite are present in a medium- to coarse-grained pegmatitic gabbro. Traces of Au and platinoids have been reported from most samples (cf Winter, 1965, and Hunter, 1970a). On the whole, the succession hosting the mineralised horizons appears to be chemically less evolved than the sequence in the study area, including hypersthene gabbros and xenoliths of olivine gabbro. A magmatic origin by segregation of a sulphide immiscible liquid has been envisaged by Wilson (1990) on the basis of mineral phase relationships, while Winter (1965) suggested that sulphide formed at a later stage, concomitantly with the alteration of primary silicate minerals.

9.3 BASE METAL (Cu-Ni) SULPHIDE MINERALISATION

In a mafic magma, sulphur behaves as an incompatible element with respect to the silicate phases. When continuous fractionation of cumulus silicates leads eventually to sulphur saturation in the magma, low proportions of iron-rich sulphide can separate. These are commonly devoid of economically significant components, mainly because of very low concentrations in the parental magma (Cu) or because of depletion by early-formed silicate phases (Ni). The formation of economic concentrations of sulphides enriched in base metals (or, in certain cases, in PGE) can be achieved by:

- rapid cooling of the parental magma during the initial stages of emplacement (Haughton et al., 1974);

- mixing of two (or more) disparate magmas, one primitive and one more evolved, but both close to sulphide saturation (Irvine, 1977);

- contamination of basic magma with various types of material from external sources (Irvine, 1975; Naldrett and Macdonald, 1980); in particular, the interaction between a basic melt and silicic rock-types would modify the bulk composition of the magma and reduce the solubility of sulphur, therefore causing sulphide precipitation.

RAPID COOLING OF THE MAGMA

This process accounts for the minor enrichment of sulphides in the basal parts of layered intrusions. Sulphide formation in the basal portion of a mafic intrusion is usually associated with ultramafic rocks (e.g. Bushveld and Stillwater Complexes, Great Dyke). Occurrences of this kind cannot be expected given the present level of exposure of the Usushwana Complex (except perhaps in the Swaziland counterpart of the intrusion, where sulphide concentrations are reported in the lower layers); they are more likely to be found at depth, provided that ultramafic rocks are present.

MIXING OF MAGMAS

Mixing of magmas with different affinities can lead to the precipitation of sulphides by two contrasting processes. A batch segregation has been proposed for the compositionally uniform sulphide zones of the Merensky (Bushveld Complex; Sharpe, 1982; Naldrett et al., 1986) and J-M Reefs (Stillwater Complex; Todd et al., 1982; Raedeke and Vian, 1986). The mineralisation is considered to have resulted from fountain mixing of a hot primitive melt with cooler resident magma, with the density of the latter having been increased by extensive plagioclase crystallisation. Fractional segregation, followed by mechanical concentration within the cumulus pile, has been suggested for the Main Sulphide Zone of the Great Dyke, where the mineralisation is hosted by ultramafic rocks stratigraphically underlying the first appearance of cumulus plagioclase (Wilson et al., 1989). Mixing of a more fractionated magma (residing higher in the chamber and which had already started to crystallise plagioclase) with that at the base of the chamber would have induced the segregation of sulphides in quantities exceeding the normal cotectic proportions with silicate minerals.

Evidence for complex mixing processes is provided by rapid lithological changes of contrasting rock-types (e.g. from anorthosite to pyroxenite in the Merensky Reef, and from bronzitite to websterite and gabbro in the J-M Reef), together with erosional features and marked changes in the composition of cumulus phases (Wilson et al., 1989). The exposed monotonous and regular gabbroic succession of the Usushwana Complex in the study area does not seem to constitute a suitable environment for sulphide concentrations originating from the mixing of magmas. It is also considered improbable that occurrences of this kind can be found at depth, due to the limited rate of fractionation in the stratigraphic section.

CONTAMINATION OF BASIC MAGMA

Contamination of the basic magma by silicic rocks as the origin of

sulphide ores has been proposed for many layered intrusions. The model, as proposed by Naldrett and Macdonald (1980), is illustrated in figure 29. On the 1200°C isothermal section of the system FeO-FeS-SiO_2, a magma of composition A is a one-phase homogeneous liquid. Addition of SiO_2 could move the magma into the two-liquid field (composition B), resulting in the formation of a silicate-rich liquid (Y) and a co-existing immiscible sulphide liquid (X). The greater density of the latter would cause a mechanical separation of sulphides to form an enriched layer.

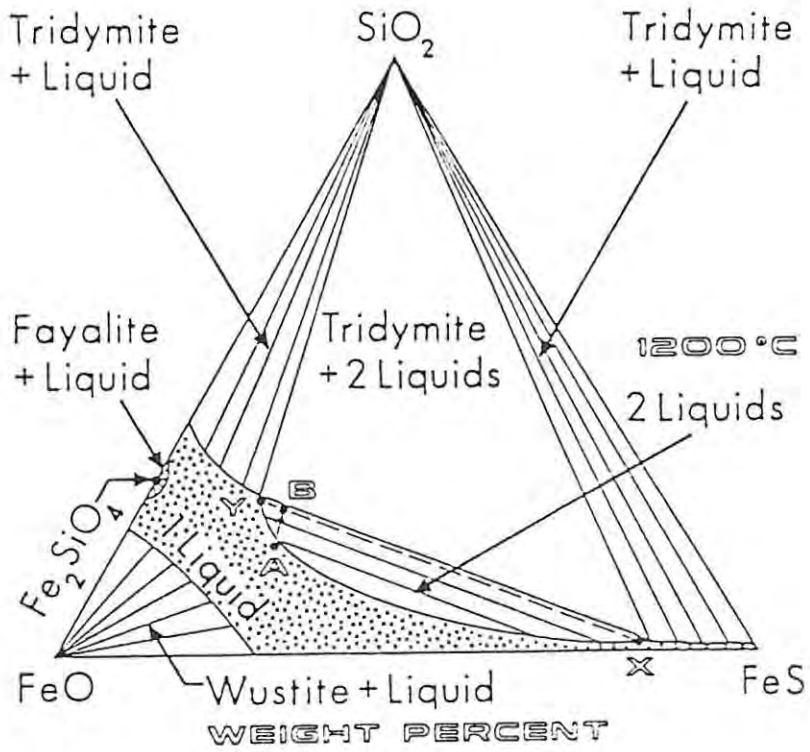

Fig. 29 - *The 1200°C isotherm of the Fe-S-O system illustrating, the effects of adding SiO_2 to a homogeneous sulphide-rich silicate liquid (after Irvine, 1975).*

This model appears to have important implications for the Usushwana Complex, where contamination played a dominant role in the evolution of the magma (see section 8.2 and 8.3). Comparisons can be made between the Complex and several mafic intrusions, showing strong

evidence for mineralisation having resulted from contamination processes, e.g. the Noril'sk-Talnak deposit (Siberian Platform; Naldrett, 1989), the Duluth Complex (north central USA; Naldrett, 1989) and the Sudbury deposit (Ontario; Naldrett and Macdonald, 1980). In these complexes, both massive and disseminated sulphide ores (mainly pyrrhotite, chalcopyrite, pentlandite and cubanite) occur in mafic and ultramafic rocks. Differentiation can be pronounced (Noril'sk) or limited (Sudbury), but the mineralisation is generally associated with early-formed cumulates of relatively primitive compositions. In the Noril'sk and Duluth deposit, as much as 60% (to 75%) of the sulphur is considered to have been derived from the country rocks (from evaporites and sulphide facies iron formation, respectively). In both intrusions, the ingestion of an external source of sulphur is considered to have been followed by its precipitation as magmatic sulphide (probably due to contamination by silicic country rocks), leading to the formation of economic ores.

A similar process is likely to have occurred in the Usushwana Complex, which has intruded a variety of silica-rich rock-types. Sulphide deposits may be expected at the contact between the mafic series and its country rocks, where chemical interaction between the two may have occurred. In this regard it is significant that the sample U259 (representing the transition gabbros-granophyric rocks) yielded the highest Cu and Ni contents in the stratigraphic section (see Appendix E). However, by analogy with the examples quoted above and as suggested by the lower S content of the exposed rocks (Hammerbeck, 1977), sulphide concentrations of economic interest are more likely to occur at deeper levels, in association with less evolved rock-types.

9.4 PGE MINERALISATION

Platinum Group Elements (PGE) occur in very low concentrations in unmineralised mafic and ultramafic rocks (e.g. average Pt content = 10 ppb; Macdonald, 1987a) and an enrichment factor of approximately 10^3 is required to reach mean economic grades (e.g. 5÷10 ppm Pt). In a mafic layered intrusion, PGE display a ubiquitous association with

sulphides, due to their strong partitioning into the latter relative to silicate phases (Naldrett and Duke, 1980). Other features common to the PGE occurrences in layered intrusions are (Campbell et al., 1983):

- the PGE-enriched sulphides are at or near the base of cyclic units, marked by the re-appearance of high temperature cumulus phases (chromite and olivine) and reversal in mineral fractionation trends;

- the coarse-grained, pegmatoidal rocks hosting the mineralisation generally occur above the stratigraphic level at which plagioclase first becomes a cumulus phase;

- local discordances ("potholes") are present in the footwall rocks.

Because of their peculiar association with sulphides, the same mechanisms described in the previous section for the precipitation of base metal sulphides can be considered viable for the formation of PGE concentrations. Two aspects are important, however, in the context of the Usushwana intrusion. Firstly, to have PGE enrichment at the currently preserved level, the magma must not have been previously depleted in PGE by an earlier sulphide-forming event. The Usushwana magma has been regarded as having been uniformly contaminated at the time of emplacement (Hegner et al., 1984). This could have induced the removal of significant proportions of sulphides in deeper magma chambers, therefore limiting the likelihood of finding PGE concentrations. Secondly, sulphide mineralisation containing the highest PGE grades is generally related to mixing of mafic and ultramafic magmas (Macdonald, 1987b; Barton et al., 1986); at present no indications exist for such an interaction having occurred in the Usushwana Complex.

In addition to the mechanisms considered previously, a hydrothermal model has been proposed (e.g. Ballhaus and Stumpfl, 1986) in which late-stage (deuteric) fluids are considered to provide an effective transport medium for PGE (mostly by means of halogen complexation). The fluids would percolate upwards in the cumulate succession and could interact with sulphide-rich layers, resulting in considerable

modification of the original mineralogy and chemistry, and in PGE incorporation into the sulphides. Fluid action in a late magmatic stage was extensive in the Usushwana Complex. However, it is considered improbable that these fluids could have carried significant amounts of PGE due to the likelihood of PGE depletion having occurred in earlier sulphide-forming events. Furthermore, analyses for Pd and Au in selected sulphide-rich rocks of the Usushwana Complex generally yielded low values, comparable with the average content of mafic rocks (see Appendix E).

9.5 CHROMITITES

In mafic intrusions, chromite deposits typically consist of thin, laterally extensive layers, ranging from less than 1 cm to more than 1 m in thickness, and containing between 50% and 90% of fine-grained cumulus chromite (Duke, 1983). Stratigraphically, the chromitite layers occur in the lower portions of layered intrusions, and are typically associated with ultramafic to mafic rocks (e.g. pyroxenite, anorthosite, dunite, hartzburgite, etc.). Several models have been proposed for the formation of chromitite. These include changes in the total pressure (possibly induced by the addition or removal of magma batches; Cameron, 1980), contamination of magma by assimilation of silicic country rocks (Irvine, 1975) and mixing of a primitive magma with an evolved liquid residing in the chamber (Irvine, 1977).

In the Usushwana Complex, the occurrence of chromitites at the present level of exposure cannot be supported, due to the general lack of ultramafic rocks. This is confirmed by the fact that traces of chromite were only found in concentrates panned from streams draining pyroxenitic rocks in Swaziland (Winter, 1965). It is considered more probable that chromitites may occur at depth, in association with less evolved rocks.

9.6 MAGNETITITES

The occurrence of discrete V-bearing titaniferous magnetite layers in the later crystallisation fractions of numerous layered mafic intrusions is a well documented feature (e.g. Reynolds, 1978a). These horizons are currently exploited for the production of vanadium and steel and represent potential sources for high titanium material and iron (Reynolds, 1978b).

Impersistent magnetitite layers are an important component of the upper part of the mafic member of the Usushwana Complex. Descriptions of the layers in the study area are given in sections 4.6.1 and 4.6.4. Similar occurrences are reported from south-east of Piet Retief (Smith, in Wilson, 1990) and several magnetitite layers are known in Swaziland (Winter, 1965; Hunter, 1970a). In the latter area, the best developed bands occur over a strike length of ≈ 2400 m and a stratigraphic thickness of about 600 m. Single bands do not exceed 1.5 m in thickness and appear to result from a gradual increase in the magnetite content of the gabbro, though the contacts of the bands are generally sharp. Enrichment in apatite has been noted in the gabbro at the base of this succession.

Bulk chemical compositions of the Usushwana magnetitite from several localities are given in Table III. The magnetitites have a high, though variable, titanium content (range 8-16% TiO_2) and remarkably consistent levels of V_2O_5 (average 0.21%). Iron contents are also variable (range 39-61% Fe_2O_3), the lowest values reflecting the presence of significant amounts of silicate impurities. Because of the moderate TiO_2 and very low V_2O_5 contents, the magnetitites of the Usushwana Complex cannot be regarded as a potential source for either these commodities. Furthermore, the deposits are of limited extent, the near-surface resources of the Piet Retief-Amsterdam area not exceeding 1 million tons (Hammerbeck, 1977).

The occurrence of the Usushwana titaniferous iron ores in the form of discrete layers within gabbroic host rocks, together with their chemistry and mineralogical relationships, has been considered

TABLE III

Composition of magnetitites from the Usushwana Complex.

	1	2	3	4	5	6	7
SiO_2	4.61	2.71	3.61	7.05	8.77	NR	NR
TiO_2	11.99	12.70	12.99	15.54	13.16	8.12	6.20
Al_2O_3	3.39	2.60	3.23	3.56	4.01	NR	NR
Fe_2O_3	51.24	53.71	61.19	39.56	39.60	NR	NR
FeO	25.04	25.40	17.75	29.14	28.78	NR	NR
MnO	NR	NR	0.38	0.26	0.52	NR	NR
MgO	0.56	0.43	0.77	0.82	0.08	NR	NR
CaO	0.05	0.05	NR	2.17	2.42	NR	NR
Na_2O	0.03	0.03	NR	0.22	0.05	NR	NR
K_2O	0.14	0.02	NR	0.19	0.40	NR	NR
Cr_2O_3	0.07	0.04	0.07	0.02	0.01	NR	NR
V_2O_5	0.25	0.30	0.29	0.22	0.05	0.17	0.21
P_2O_5	NR	NR	NR	0.17	0.06	NR	NR
TOTAL	97.37	97.22	100.28	99.02	97.91	-	-

1 - Ishlelo 441 IT, northernmost body; Hammerbeck, 1977.
2 - Ishlelo 441 IT, Hlelo River; Hammerbeck, 1977.
3 - Average of 4 samples in ferrogabbro, Ishlelo 441 IT; Reynolds, 1978a.
4,5 - Titaniferous magnetite in gabbros, south east of Mhlanbanyati, Swaziland; Hunter, 1970a.
6,7 - Magnetitite overlying melanocratic quartz gabbros on farm Bloemendal 10HU, south-east of Piet Retief; Smith, in Wilson, 1990.
NR = not reported.

consistent with their having formed during the later crystallisation stages of a highly fractionated basic intrusion (Reynolds, 1978a). Hammerbeck (1977) concluded that the precipitation of titaniferous magnetite would have followed the iron enrichment of the residual melt due to crystallisation of the quartz gabbro, and would have been enhanced by the increase in oxygen fugacity (f_{O2}) near the roof of the intrusion. The change in f_{O2} could have been brought about by contamination of the basic magma (Irvine, 1975), a process that is very likely to have occurred in the Usushwana Complex (see section 8.3). Changes in the structure of the magma, e.g. depolymerisation by components such as P_2O_5, is an alternative triggering mechanism for the formation of the magnetitite layers (Reynolds, 1985).

9.7 SKAERGAARD-TYPE Au MINERALISATION

In mafic layered intrusions, gold is known to occur in association with PGE and chromite mineralisation, from which it is generally recovered as a by-product (e.g. in the Merensky Reef and UG-2 chromitite layer of the Bushveld Complex). A new environment for Au mineralisation has recently been discovered in the Skaergaard intrusion. Stratabound, irregularly distributed Au concentrations (from 0.4 to 4.7 g/ton; average 1÷3 ppm) have been found to occur in a zone of highly disseminated sulphides (less than 1% by volume), consisting mainly of pyrite and pyrrhotite with small amounts of chalcopyrite and traces of PGE (3.1 ppm Pd and 1.4 ppm Pt) (Nielsen, 1989). The mineralised horizon is 2-5 m wide and is located in the upper part of the layered sequence, above the magnetitite layers but well below the roof zone (Nielsen, op.cit.).

An environment similar to that described above may be envisaged in the Usushwana Complex, whose exposed mafic rocks appear to be relatively high level intrusives and to have undergone considerable fractionation. Favourable sites for Skaergaard-type Au mineralisation in the Complex will be represented by those parts of the sequence where sulphur saturation has been attained, as Au has a strong chalcophile character and generally occurs in sulphide solid solution. Furthermore, Wilson (1990) pointed out that the Au partition coefficient between sulphide and silicate liquids is much less than that for PGE, and probably similar to that of base metals. Consequently, in a layered intrusion, Au could appear at higher levels than PGE concentrations. In the Great Dyke (Zimbabwe) maximum Au values are in fact displaced several metres above the PGE peaks (Wilson and Tredoux, 1990).

9.8 DISCUSSION AND SUGGESTIONS FOR EXPLORATION

Investigations of the Usushwana Complex in the study area did not reveal any significant indications of mineralisation at the present level of exposure. The general lack of mineralisation in the more evolved mafic rocks (gabbros and quartz gabbros) suggests that favourable conditions for the formation of ore deposits were not developed at this stage within the intrusion. Further assessment of the economic potential of the Complex is limited by the present insufficient knowledge of the lithologies, compositions and structure of the body at depth.

Two factors indicate that more primitive rocks are likely to be present at deeper levels. Firstly, the occurrence of ultramafics in other parts of the intrusion (i.e. Swaziland) testifies that magma compositions were variable, more so than is apparent from the monotonous gabbroic sequence exposed in the study area. Secondly, a thickness of 3000 to 5500 m (derived from modelling of gravity data) is unlikely to consist entirely of rocks of gabbroic composition - a reduced thickness with ultramafic rocks at depth seems a much more feasible model. A restricted degree of fractionation, however, was observed in the exposed gabbroic succession, indicating that this might not represent a single comagmatic series with the inferred ultramafics. The latter possibly correspond to a relatively earlier intrusive event.

Assuming a hypothesis that ultramafic rocks underlie the gabbroic sequence, the internal structure of the Usushwana Complex appears to be similar to that of many layered intrusions (e.g. the Great Dyke; Wilson, 1982) which have significant PGE, base metal sulphide and chromite mineralisation associated with the lower part of the stratigraphy. By analogy, therefore, it can be postulated that ultramafic rocks may lie at depth and be hosts to similar deposits.

Mineralised occurrences of the kind described above are generally related to internally controlled processes, but an important aspect in the assessment of the economic potential of the Usushwana Complex

concerns the possibility of mineralisation arising from external factors. In particular, contamination from the silicic country rocks has been recognised as one of the most important processes operating during the evolution of the Complex, and could have brought about the formation of either Cu-Ni sulphide or PGE mineralisation. As stated previously, mineralised occurrences are only sporadic at the present level of exposure, but the possibility exists that precipitation of sulphides could have occurred at deeper levels, corresponding to major onsets of contamination.

On the basis of the above assessments, it is suggested that to obtain a complete model of the structure of the body at depth, the following techniques should be employed:

- a ground-based gravity study on selected traverses. Density distributions should be based on normal gabbro as well as ultramafic rocks;

- exploration drilling, particularly aimed at gaining a better understanding of the entire lithological succession. This would reveal the occurrence of an underlying ultramafic sequence and would possibly delineate suitable environments for chromite, PGE and base metal sulphide mineralisation. The choice of a convenient site would depend on the results of the gravity survey, the sections where the Complex attains maximum depth being the most interesting.

The reported lack of surface expression of mineralisation, together with the petrological and geochemical information obtained during this study, points to an effective absence of ores within the outcropping section of the Complex. However, exposures of the intrusion in the study area are very poor, and the possibility of mineralisation occurring at relatively shallow levels beneath the overburden cannot be ruled out completely. Deposits that are more likely to occur at this level are Au, PGE, and base metal sulphides, brought about by episodes of contamination. A comprehensive soil and sediment sampling programme is suggested in order to ascertain the likelihood of such occurrences. The Hlelo River and the Blesbokspruit sections are the

base for orientation surveys, the first being well known petrographically and geochemically, the second hosting the only significant sulphide occurrence of the study area. Soil traverses at closely-spaced intervals are recommended for the latter locality, with soil samples analysed for selected precious metals.

In the light of the knowledge gained from this study and the statements made previously, it can be concluded that the Usushwana Complex does not represent an attractive target for mineral exploration at the present level of exposure, but a great potential exists for various ore deposits to occur at deeper levels.

CHAPTER 10: SUMMARY AND CONCLUSIONS

In this thesis, the Usushwana Complex (as outcropping in the Piet Retief-Amsterdam area, south-eastern Transvaal) is described and studied. The study involved an initial phase of regional mapping and detailed sampling of selected transverse sections of the Complex. A second phase included a petrological study of the various rock-types, a mineralogical investigation of the main cumulus silicate phases by electron microprobe and the whole-rock geochemistry of the silicate cumulates and granitoid rocks. The following aspects were specifically investigated:

a - stratigraphy of the Complex;

b - identification of differentiation trends;

c - relationship between mafic and granitoid rocks and origin of the latter;

d - economic mineral potential of the Complex.

From this study the following main conclusions can be drawn.

The Usushwana Complex, in the study area, represents a cumulate succession of gabbroic lithotypes capped by granophyric rocks. The mafic suite is characterised by meso- to orthocumulate quartz gabbros, with minor amounts of two-pyroxene gabbros and plagioclase-bearing pyroxenites. Similar trends have been observed in both the Western and Eastern limbs of the Complex, with basal coarse- to medium-grained equigranular quartz gabbros (and less frequently gabbros) overlain by more melanocratic and fine-grained varieties; discontinuous layers and lenses of magnetitite may be developed. Two major rock-types have been distinguished within the granitoid suite that overlies the mafic portion of the Complex: the first is an amphibole-rich granophyric granodiorite displaying a gradational relationship with underlying

quartz gabbros, the second is a fine-grained granitic rock (microgranite), which generally occurs on top of the granodiorite. A lithological cyclicity has been recognised along the Hlelo River Section. The first unit starts with gabbros and magnetite-bearing apatite quartz gabbros and then grades upwards into granodiorites; the second has magnetite-rich quartz gabbros and magnetite layers at the base, which in turn are overlain by magnetite-bearing gabbros that grade upwards into granodiorites.

Although there is poor evidence of small-scale layering within the Complex, it is suggested that the overall variation represented by the exposed succession formed stratigraphically (i.e. from base to top). Mineral composition and geochemical studies revealed the existence of differentiation trends consistent with a fractionation event that involved gabbroic liquids in the lower parts of the magma chamber (producing plagioclase of basic andesine composition) to small amounts of granodioritic magma at the roof (albitic plagioclase). Fractionation, however, was of minor importance in the formation of the various rock-types as several features indicate that assimilation and contamination played an important role. In particular, a complex interaction between magma and the acidic country rocks at the roof of the magma chamber is considered to have been responsible for the formation of the microgranites, which are thought to represent the products of partial melting and recrystallisation of the rocks hosting the Complex.

Mineralogical, textural and geochemical comparisons with other, better known, layered intrusions (e.g. Skaergaard and Bushveld Complexes) are indicative of a relatively advanced stage of fractionation, and therefore point to the exposed sequence of the Usushwana Complex in the study area representing the upper portion of the intrusion. This assessment is supported by the following features:

- the dominance of silica-rich mafic (gabbroic) rocks and the occurrence of Fe-rich lithotypes and magnetitites;
- the cumulus mineralogy (i.e. plagioclase, clinopyroxene, apatite, Fe-Ti oxides) and the compositional ranges of the principal phases (i.e. An 48.41-0.94%, $Mg\#_{Cpx}$ 54.35-45.41);

- the extensive action of fluids saturated in water;
- the enrichment in incompatible trace elements.

Significant mineralised occurrences have not been reported from the exposed portion of the Usushwana Complex. However, by analogy with other layered intrusions (e.g. Bushveld, Great Dyke, Skaergaard), favourable conditions for the formation of ore deposits are likely to have developed at lower stratigraphic levels. Base metal (Cu-Ni) sulphide, chromite and PGE mineralisation might occur in association with more mafic differentiates, whose presence is suggested by gravity and mineralogical data. Similar occurrences could have been brought about by major episodes of contamination. An environment favourable for Skaergaard-type Au mineralisation may also be envisaged for the Complex.

The findings of the different parts of this study support a model for the evolution of the Usushwana Complex comparable to that of other mafic layered intrusions. The potential therefore exists for the development of economic mineralisation within the Complex.

REFERENCES

ALLSOPP, H., ROBERTS, H.R., SCHREINER, G.D.L., and HUNTER, D.R. (1962). Rb/Sr age measurements on various Swaziland granites. *J.Geophysical Research*, **67** (13), 5307-5313.

ANHAEUSSER, C.R. (1973). The evolution of the early Precambrian crust of southern Africa. *Philos.Trans.R.Soc.Lond.* **A 273**, 359-388.

---------- (1986). The geology and evolution of the Barberton Mountain Land. *In*: Pearton, T.N. (Ed.), *The Barberton Mountain Land.* Excursion Guidebook. Geocongress '86, pp 1-22.

----------, and ROBB, L.J. (1981). Magmatic cycles and the evolution of the Archaean granitic crust in the eastern Transvaal and Swaziland. *Spec.Publ.Geol.Soc.Austr.* **7**, 457-467.

----------, and WILSON, J.F. (1981). The Granitic-Gneiss Greenstone shield. *In*: Hunter, D.R. (Ed.), *Precambrian of the Southern Hemisphere*, pp 423-499. Amsterdam: Elsevier.

ARMSTRONG, N.V., WILSON, A.H., and HUNTER, D.R. (1986). The Nsuze Group, Pongola Sequence, South Africa: geochemical evidence for Archean volcanism in a continental setting. *Precambrian Res.* **34**, 175-203.

ATKINS, F.B. (1969). Pyroxenes of the Bushveld intrusion, South Africa. *J.Petrol.* **10**, 222-249.

BALLHAUS, C.G., and STUMPFL, E.F. (1986). Sulfide and platinum mineralization in the Merensky Reef: evidence from hydrous silicates and fluid inclusions. *Contrib.Mineral.Petrol.* **94**, 193-204.

BARTON, J.M. (1981). The pattern of Archaean crustal evolution in southern Africa as deduced from the evolution of the Limpopo Mobile Belt and the Barberton granite-greenstone terrain. *Spec.Publ. Geol.Soc.Austr.* **7**, 21-31.

----------, HUNTER, D.R., JACKSON, M.P.A., and WILSON, A.C. (1980). Rb-Sr age and source of the Bimodal Suite of the Ancient Gneiss Complex, Swaziland. *Nature* **283** (5749), 756-758.

----------, CAWTHORN, R.G., and WHITE, J. (1986). The role of contamination in the evolution of the Platreef of the Bushveld Complex. *Econ.Geol.* **81**, 1096-1104.

BEUKES, N.J., and CAIRNCROSS, B. (1991). A lithostratigraphic-sedimentological reference profile for the Late Archaean Mozaan Group, Pongola Sequence: application to sequence stratigraphy and correlation with the Witwatersrand Supergroup. *S.Afr.J.Geol.* **94** (1), 44-69.

BOWES, D.R., SKINNER, W.R., and WRIGHT, A.E. (1970). Petrochemical comparison of the Bushveld Igneous Complex with some other mafic complexes. *Spec.Publ.geol.Soc.S.Afr.* **1**, 425-440.

BURKE, K., KIDD, W.S.F., and KUSKY, T.M. (1985). The Pongola structure of southeastern Africa: the world's oldest preserved rift. *J.Geodynamics* **2**, 35-49.

CAMERON, E.N. (1980). Evolution of the Lower Critical Zone, Central Sector, Eastern Bushveld Complex, and its chromite deposits. *Econ.Geol.* **75**, 845-871.

CAMPBELL, I.H., and TURNER, J.S. (1986). A laboratory investigation of assimilation at the top of a basaltic magma chamber. *J.Geology* **95**, 155-172.

----------, NALDRETT, A.J., and BARNES, S.J. (1983). A model for the origin of the platinum-rich sulphide horizons in the Bushveld and Stillwater Complexes. *J.Petrol.* **24**, 133-185.

CAWTHORN, R.G. (1983). Magma addition and possible decoupling of major- and trace- element behaviour in the Bushveld Complex, South Africa. *Chem.Geol.* **39**, 335-345.

----------, and McCARTHY, T.S. (1985). Incompatible trace element behaviour in the Bushveld Complex. *Econ.Geol.* **80**, 1016-1026.

CHENEY, E.S., ROERING, C., and WINTER, H. de la R. (1990). The Archean-Proterozoic Boundary in the Kaapvaal Province of Southern Africa. *Precambrian Res.* **46**, 329-340.

COMPSTON, W., and KRONER, A. (1988). Multiple zircon growth within early Archaean tonalitic gneiss from the Ancient Gneiss Complex, Swaziland. *Earth Planet.Sci.Lett.* **87**, 13-28.

CONDIE, K.C., and HUNTER, D.R. (1976). Trace element geochemistry of Archaean granitic rocks from the Barberton region, South Africa. *Earth Planet.Sci.Lett.* **29**, 389-400.

DANCHIN, R.V., and FERGUSON, J. (1970). The geochemistry of the Losberg intrusion, Fochville, Transvaal. *Spec.Publ.geol.Soc.S.Afr.* **1**, 689-714.

DAVIES, R.D., ALLSOPP, H.L., ERLANK, A.J., and MANTON, W.I. (1970). Sr-isotopic studies on various layered mafic intrusions in southern Africa. *Spec.Publ.geol.Soc.S.Afr.* **1**, 576-593.

DEER, W.A., and ABBOT, D. (1965). Clinopyroxenes of the gabbro cumulates of the Kap Edward Holm complex, east Greenland. *Mineralog.Mag.* **34**, 177-193.

----------, HOWIE, R.A., and ZUSSMANN, J. (1966). *An introduction to the rock-forming minerals*. Longman Group Limited, London, 528 pp.

DROOP, G.T.R. (1987). A general equation for estimating Fe^{3+} concentrations in ferromagnesian silicates and oxides from microprobe analyses, using stechiometric criteria. *Mineralog.Mag.* **51**, 431-435.

DUKE, J.M. (1983). Ore deposit models #7. Magmatic segregation deposits of chromite. *Geoscience Canada* **10**, 15-24.

EALES, H.V., and BOOTH, P.W.K. (1974). The Birds River gabbro complex, Dordrecht district. *Trans.geol.Soc.S.Afr.* **77**, 1-15.

FORD, A.B. (1970). Development of the layered series of capping granophyre of the Dufek intrusion of Antarctica. *Spec.Publ.geol. Soc.S.Afr.* **1**, 492-510.

GLIKSON, A.Y. (1972). Early Precambrian evidence of a primitive ocean crust and island nuclei of sodic granite. *Geol.Soc.Am.Bull.* **83**, 3323-3344.

GRIBBLE, C.D., and HALL, A.J. (1985). *A Practical Introduction to Optical Mineralogy.* George Allen & Unwin, London, 240 pp.

HAMILTON, P.J., EVENSEN, N.M., O'NIONS, R.K., SMITH, H.S., and ERLANK, A.J. (1979). Sm-Nd dating of Onverwacht Group volcanics, southern Africa. *Nature* **279**, 298-300.

HAMMERBECK, E.C.I. (1977). *The Usushwana Complex in the southeastern Transvaal with special reference to its economic mineral potential.* Unpubl.Ph.D. thesis, Univ.Pretoria, South Africa, 219 pp.

---------- (1982). The geology of the Usushwana Complex and associated formations - south-eastern Transvaal. **Memoir 70** *Geol.Surv. and Dep.Mineral Energy Aff., South Africa*, 119 pp.

HAUGHTON, D.R., ROEDER, P.L., and SKINNER, B.J. (1974). Solubility of sulphur in mafic magmas. *Econ.Geol.* **69**, 451-467.

HAUGHTON, S.H. (1969). Geological history of Southern Africa. *Geol.Soc. S.Afr., Johannesburg*, 528 pp.

HEGNER, E., KRONER, A. and HOFMANN, A.W. (1984). Age and isotopic geochemistry of the Archaean Pongola and Usushwana suites in Swaziland, southern Africa: a case for crustal contamination of mantle-derived magma. *Earth Planet.Sci.Lett.* **70**, 267-279.

HEINRICH, E.Wm (1965). *Microscopic identification of minerals*. McGraw-Hill, Inc.-New York, 398 pp.

HIMMELBERG, G.R. and FORD, A.B. (1976). Pyroxenes of the Dufek intrusion, Antarctica. *J.Petrol.* **17**, 219-243.

HUMPHREY, W.A., and KRIGE, L.J. (1931). The geology of the country south of Piet Retief. *Expl.Sh.geol.Surv.S.Afr.* **68** (Piet Retief), 66 pp.

HUNTER, D.R. (1951). *In*: A.Rep.geol.Surv.Dep.Swaziland (1950), 40-41.

---------- (1970a). The geology of the Usushwana Complex in Swaziland. *Spec.Publ.geol.Soc.S.Afr.* **1**, 645-660.

---------- (1970b). The Ancient Gneiss Complex in Swaziland. *Trans.geol.Soc.S.Afr.* **73**, 107-150.

---------- (1973). The granitic rocks of the Precambrian in Swaziland. *Spec.Publ.geol.Soc.S.Afr.* **3**, 131-148.

---------- (1974a). Crustal Development in the Kaapvaal Craton, I. The Archean. *Precambrian Res.* **1**, 259-294.

---------- (1974b). Crustal Development in the Kaapvaal Craton, II. The Proterozoic. *Precambrian Res.* **1**, 295-326.

IRVINE, T.N. (1970). Heat transfer during solidification of layered intrusions. I. Sheets and sills. *Canadian J.Earth Sci.* **7**, 1031-1061.

---------- (1975). Crystallization sequences in the Muskox intrusion and other layered intrusions. II. Origin of chromitite layers and similar deposits of magmatic ores. *Geochimica and Cosmopolita Acta* **39**, 991-1020.

---------- (1977). Origin of chromitite layers in the Muskox intrusion: a new interpretation. *Geology* **5**, 273-277.

---------- (1980). Magmatic infiltration metasomatism, double-diffusive fractional crystallization, and adcumulus growth in the Muskox Intrusion and other layered intrusions. *In*: R.B. Hargraves (Ed.), *Physics of magmatic processes*, pp 325-383. Princeton, N.J.: Princeton University Press.

---------- (1982). Terminology for layered intrusions. *J.Petrol.* **23** (2), 127-162.

JAQUES, A.L. (1976). An Archean tholeiitic layered sills from Mt Kilkenny, Western Australia. *J.geol.Soc.Austr.* **23** (2), 157-168.

JOUBERT, P. (1981). The Namaqualand metamorphic Complex. *In*: D.R. Hunter (Ed.), *Precambrian of the southern hemisphere*, pp 671-705. Amsterdam: Elsevier.

KRONER, A. (1985). Evolution of the Archaean continental crust. *Ann. Rev.Earth Planet.Sci.* **13**, 59-74.

----------, and COMPSTON, W. (1988). Ion microprobe ages of zircons from early Archean granite pebbles and greywacke, Barberton Greenstone Belt, southern Africa. *Precambrian Res.* **38**, 367-380.

LE MAITRE, R.W. (1976). The chemical variability of some common igneous rocks. *J.Petrol.* **17**, 589-637.

MACDONALD, A.J. (1987a). The platinum group element deposits: classification and genesis. Ore deposit models #12. *Geoscience Canada* **14**, 155-166.

---------- (1987b). PGE mineralisation and the relative importance of magmatic and deuteric processes: field evidence from Lac des Iles deposit, Ontario, Canada. *Geoplatinum '87*. Milton Keynes, U.K., April 23-24, 1987, abstract.

MATHISON, C.I. (1987). Cyclic units in the Somerset Dam layered gabbro intrusion, south-eatsern Queensland, Australia. *Lithos* **20**, 187-250.

MATTHEWS, P.E. (1981). Eastern or Natal sector of the Namaqua-Natal Mobile Belt in southern Africa. *In*: D.R. Hunter (Ed.), *Precambrian of the southern hemisphere*, pp 705-715. Amsterdam: Elsevier.

McLENNAN, S.M., and TAYLOR, S.R. (1983). Geochemical evolution of Archean shales from South Africa. I. The Swaziland and Pongola Supergroup. *Precambrian Res.* **22**, 93-124.

MORSE, S.A. (1979). Kiglapait Geochemistry II: Petrography. *J.Petrol.* **20** (3), 591-624.

NALDRETT, A.J., (1989). Ores associated with flood basalts. *Reviews in Economic Geology* **4** (Ore deposition associated with magmas), 103-118.

----------, and DUKE, J.M. (1980). Platinum metals in magmatic sulphide ores. *Science* **208**, 1417-1424.

----------, and MACDONALD, A.J. (1980). Tectonic settings of some Ni-Cu sulphide ores: their importance in genesis and exploration. *Geol.ass.Canada, Special Paper* **20**, 633-657.

----------, BRAY, J.G., GASPARRINI, E.L., PODOLSKY, T., and RUCKLIDGE, J.C. (1970). Phase layering and cryptic variations in the Sudbury Nickel Irruptive. *Spec.Publ.geol.Soc.S.Afr.* **1**, 532-546.

----------, GASPARRINI, E.C., BARNES, S.J., VON GRUENEWALDT, G., and SHARPE, M.R. (1986). The upper critical zone of the Bushveld Complex and a model for the origin of Merensky-type ores. *Econ.Geol.* **81**, 1105-1117.

NESBITT, R.W., GOODE, A.D.T., MOORE, A.C., and HOPWOOD, T.P. (1970). The Giles Complex, Central Australia: a stratified sequence of mafic and ultramafic intrusions. *Spec.Publ.geol.Soc.S.Afr.* **1**, 547-564.

NIELSEN, T.F.D. (1989). Gold mineralisation in the Skaergaard intrusion. *Geol.Surv.Greenland.* **Open File Series No 89/7**, 144 pp.

NWE, Y.Y. (1976). Electron-probe studies of the earlier pyroxenes and olivines from the Skaergaard intrusion, east Greenland. *Contrib. Mineral.Petrol.* **55**, 105-126.

----------, and COPLEY, P.A. (1975) Chemistry, subsolidus relations and electron petrography of pyroxenes from the late ferrodiorites of the Skaergaard intrusion, east Greenland. *Contrib.Mineral. Petrol.* **53**, 37-54.

PEARCE, J.A., and NORRY, M.J. (1979). Petrogenetic implications of Ti, Zr, Y and Nb variations in volcanic rocks. *Contrib.Mineral.Petrol.* **69**, 33-47.

PLUMB, K.A., and JAMES, H.L. (1986). Subdivision of Precambrian time: recommandations and suggestions by the Subcommission on Precambrian Stratigraphy. *Precambrian Res.* **32**, 65-92.

PODMORE, F. (1970). The shape of the Great Dyke in Rhodesia as revealed by gravity surveying. *Spec.Publ.geol.Soc.S.Afr.* **1**, 610-620.

RAEDEKE, L.D., and VIAN, R.W. (1986). A three dimensional view of mineralization in the Stillwater J-M Reef. *Econ.Geol.* **81**, 1187-1195.

REIMER, T.O., CONDIE, K.C., SCHNEIDER, G., and GEORGI, A. (1985). Petrography and geochemistry of granitoid and metamorphite pebbles from the early Archean Moodies Group, Barberton Mountainland/South Africa. *Precambrian Res.* **29**, 383-404.

REYNOLDS, I.M. (1978a). *A mineralogical investigation of coexisting iron-titanium oxides from various igneous rocks, with special reference to some South African titaniferous ores.* Unpubl.Ph.D. Dissertation, Rhodes University, Grahamstown, South Africa, 632 pp.

---------- (1978b). Mineralogical studies of south african titaniferous iron ores: their application to extractive metallurgy. *Trans.geol.Soc.S.Afr.* **81**, 233-240.

---------- (1981). The mineralogy and petrography of some titaniferous ores from the Usushwana Complex. *Trans.geol.Soc. S.Afr.* **84**, 261-269.

---------- (1985). The nature and origin of titaniferous magnetite layers in the Bushveld Complex: a review and synthesis. *Econ.Geol.* **80**, 1089-1108.

SAGGERSON, E.P., and LOGAN, C.T. (1970). Distribution controls of layered and differentiated mafic intrusions in the Lebombo volcanic sub-province. *Spec.Publ.geol.Soc.S.Afr.* **1**, 721-734.

SHARPE, M.R. (1982). Noble metals in the marginal rocks of the Bushveld Complex. *Econ.Geol.* **77**, 1286-1295.

SMITH, R.G. (1983). *The geology of the Usushwana Complex southeast of Piet Retief.* Unpubl.Hons.Dissertation. Univ. Natal. Pietermaritzburg, South Africa, 71 pp.

SOUTH AFRICAN COMMITTEE FOR STRATIGRAPHY (SACS), (1980). *Stratigraphy of South Africa. Part 1 (Comp. L.E. Kent). Lithostratigraphy of the Republic of South* Africa, *South West Africa/Namibia and the Republics of Bophutatswana, Transkei and Venda.* Handb.geol.Surv.S.Afr., **8**, 690 pp.

STRECKEISEN, A.L. (1973). Classification and nomenclature recommended by the I.U.G.S., Subcommission on the Systematics of Igneous Rocks-Geotimes **18**,26-30.

SUBCOMMITTEE ON PYROXENES (1989). Nomenclature of pyroxenes. *Can. Mineralogist* **27**, 143-156.

SUBCOMMITTEE ON THE AMPHIBOLE GROUP (1978). Nomenclature of amphiboles. *Can.Mineralogist* **16**, 501-520.

TANKARD, A.J., JACKSON, M.P.A., ERIKSSON, K.A., HOBDAY, D.K., HUNTER, D.R., and MINTER, W.E.L. (1982). *Crustal evolution of Southern Africa*. New York, Heidelberg, Berlin: Springer-Verlag, 523 pp.

TEGTMEYER, A.R., and KRONER, A. (1987). U-Pb zircon ages bearing on the nature of early Archean Greenstone Belt evolution, Barberton Mountainland, southern Africa. *Precambrian Res.* **36**, 1-20.

TODD, S.G., KEITH, D.W., LE ROY, L.W., SCHISSEL, D.J., MANN, E.L,M and IRVINE, T.N. (1982). The J-M platinum palladium Reef of the Stillwater Complex, Montana: 1. Stratigraphy and petrology. *Econ.Geol.* **77**, 1454-1480.

VAN EEDEN, O.R. (1972). The geology of the Republic of South Africa, an explanation of the 1:1 000 000 map, 1970 edition. *Spec.Publ. Geol.Surv.S.Afr.* **18**, 74 pp.

VAN VUUREN, C.J. (1965). *Die geologie van'n gebied suid van Amsterdam, Oos-Transvaal.* Unpubl.M.Sc. thesis, Univ.Orange Free State, South Africa, 93 pp.

VON GRUENEWALDT, G. (1972). The origin of the roof-rocks of the Bushveld Complex between Tauteshoogte and Paardeckop in the eastern Transvaal. *Trans.geol.Soc.S.Afr.* **75**, 153-172.

WADSWORTH, W.J. (1985). Terminology of postcumulus processes and products in the Rhum layered intrusion. *Geolog.Mag.* **122** (5), 549-554.

---------- (1986). Silicate mineralogy in the later fractionation stages of the Insch intrusion, NE Scotland. *Mineralog.Mag.*, **50**, 583-595.

----------, DUNHAM, A.C. and ALMOHANDIS, A.A. (1982). Cryptic variations in the Kapalagulu layered intrusion, Western Tanzania. *Mineralog.Mag.* **45**, 227-236.

WAGER, L.R. (1960). The major element variation of the layered series of the Skaergaard intrusion. *J.Petrol.* **1**, 364-398.

----------, and BROWN, G.M. (1968). *Layered igneous rocks*. Edinburgh: Oliver & Boyd, 588 pp.

----------, BROWN, G.M., and WADSWORTH, W.J. (1960). Types of igneous cumulates. *J.Petrol.* **1**, 73-85.

APPENDIX A

LIST OF THIN SECTIONS

Thin sections are listed in stratigraphical order and for each locality (refer to figure 2 and 5). The interval including thin sections U112a-U153 is a partial repetition of the basal portion (thin sections U3-U68).

Abbreviations used in the table are:

Eq. = equigranular
Ineq. = inequigranular
gr. = grained
qtz = quartz
magn. = magnetite
ap. = apatite

WALRAVEN, F. (1985). Genetic aspects of the granophyric rocks of the Bushveld Complex. *Econ.Geol.* **80**, 1166-1180.

WATCHORN, M.B. (1980). Fluvial and tidal sedimentation in the 3000 Ma Mozaan basin, South Africa. *Precambrian Res.* **13**, 27-42.

WHITNEY, P.R., and Mc LELLAND, J.M. (1973). Origin of coronas in metagabbros of the Adirondack Mts., N.Y. *Contrib.Mineral.Petrol.* **39**, 81-98.

---------- (1983). Origin of biotite-hornblende-garnet coronas between oxides and plagioclase in olivine metagabbros, Adirondack Region, New York. *Contrib.Mineral.Petrol.* **82**, 34-41.

WILSON, A.H. (1982). The geology of the "Great Dyke", Zimbabwe: the ultramafic rocks. *J.Petrol.* **23**, 240-292.

---------- (1990). *The geology of the Usushwana Igneous Suite and an assessment of its economic potential, with particular emphasis on base metals and platinum group element mineralization*. Unpubl. report, Anglo American Company, 43 pp.

----------, NALDRETT, A.J., and TREDOUX, M. (1989). Distribution and control of platinum group element and base metal mineralization in the Darwendale subchamber of the Great Dyke, Zimbabwe. *Geology* **17**, 649-652.

----------, and TREDOUX, M. (1990). The Geology of the Great Dyke, Zimbabwe: compositional and textural cyclic units in the P1 pyroxenite of Cyclic Unit 1 of the Darwendale Subchamber, and implications for crystallization and mineralization in narrow flared layered intrusions. *Econ.Geol.* **85**, 556-584.

WILSON, R.J., ESBENSEN, K.H., and THY, P. (1981). Igneous petrology of the synorogenic Fongen-Hyllingen layered basic complex, South-Central Scandinavian Caledonides. *J.Petrol.* **22** (4), 584-627.

WINDLEY, B.F. (1973). Crustal development in the Precambrian. *Philos. Trans.R.Soc.Lond.* **A 273**, 321-341.

WINKLER, H.G.F. (1979). *Petrogenesis of metamorphic rocks.* Springer-Verlag, New York, 316 pp. Fifth Edition.

WINTER, P.E. (1965). The Usushwana Complex. *Bull.geol.Surv.and Mines Dep.Swaziland* **5**, 29 pp.

ISHLELO 441 IT

No.	Description	No.	Description
U3	Strained gabbro	U191	Eq. medium-gr. magn.-bearing, ap. qtz gabbro
U8	Eq. medium-gr. gabbro	U202	Eq. medium-gr. magn.-bearing, ap. qtz gabbro
U13	Eq. coarse-gr. gabbro	U204	Eq. medium-gr. magn.-bearing, ap. qtz gabbro
U14	Eq. medium-gr. qtz gabbro	U211	Eq. medium-gr. magn.-bearing, ap. qtz gabbro
U16a	Eq. medium-gr. gabbro	U215	Ineq. medium-gr. granophyric granodiorite
U18	Eq. medium-gr. gabbro	USH1	Ineq. coarse-gr. granophyric granodiorite
U24	Eq. medium-gr. gabbro	USH2	Ineq. coarse-gr. granophyric granodiorite
U34	Strained medium-gr. gabbro	USH3	Ineq. coarse-gr. granophyric granodiorite
U37	Eq. coarse-gr. gabbro	USH4	Ineq. coarse-gr. granophyric granodiorite
U39	Eq. coarse-gr. gabbro		
U45	Eq. medium-gr. qtz gabbro	U345	Eq. medium-gr. magn.-bearing qtz gabbro
U47	Eq. coarse-gr. gabbro	U244	Eq. fine-gr. magnetitite
U50	Eq. coarse-gr. gabbro	U250	Eq. medium-gr. magn.-bearing qtz gabbro
U53	Eq. coarse-gr. qtz gabbro	U251	Eq. medium-gr. magn.-bearing qtz gabbro
U59	Eq. medium-gr. qtz gabbro	U259	Eq. medium-gr. magn.-bearing qtz gabbro
U68	Eq. medium-gr. gabbro	U262	Eq. medium- to coarse-gr. qtz gabbro transitional to a granodiorite
U112a	Eq. impure magnetitite	U405	Eq. medium-gr. granophyric granodiorite
U118	Eq. medium-gr. qtz gabbro	U409	Eq. medium-gr. granophyric granodiorite
U120	Strained medium-gr. qtz gabbro	U412	Eq. medium-gr. granophyric granite
U122	Strained medium-gr. qtz gabbro	U419	Eq. medium-gr. granophyric granite
U127a	Strained medium-gr. qtz gabbro	U424	Eq. medium-gr. granophyric granite
U138	Eq. coarse-gr. qtz gabbro	U430	Eq. medium-gr. granophyric granite
U140	Strained coarse-gr. qtz gabbro	U434	Eq. medium-gr. granophyric granite
U147	Eq. coarse-gr. qtz gabbro	U438	Eq. medium-gr. granophyric granite
U153	Eq. medium-gr. qtz gabbro	U444	Eq. coarse-gr. granophyric granodiorite
		U447	Eq. coarse-gr. granophyric granodiorite
U157	Eq. medium-gr. magn.-bearing, ap. qtz gabbro	U453	Eq. medium-gr. granophyric granodiorite
U163	Eq. medium-gr. magn.-bearing, ap. qtz gabbro	U459	Eq. medium-gr. granophyric granodiorite
U169	Eq. medium-gr. magn.-bearing, ap. qtz gabbro	U464	Eq. medium-gr. granophyric granite
U177	Eq. medium-gr. magn.-bearing, ap. qtz gabbro	U468	Eq. medium-gr. granophyric granite
U187	Eq. medium-gr. magn.-bearing, ap. qtz gabbro	U473	Eq. cataclastic granophyric granite
U189	Eq. medium-gr. magn.-bearing, ap. qtz gabbro	U476	Eq. medium-gr. granophyric granite

STERKWATER 472 IT

No.	Description	No.	Description
U352	Eq. medium-gr. gabbro	U390	Eq. medium-gr. magn.-bearing gabbro
U356	Eq. medium-gr. gabbro	U394	Eq. medium-gr. magn.-bearing gabbro
U364	Eq. medium-gr. gabbro	U396	Eq. medium-gr. magn.-bearing gabbro
U368	Eq. medium-gr. gabbro	U398	Eq. medium-gr. granophyric granite
U372	Eq. medium-gr. gabbro	U621	Eq. medium-gr. granophyric granodiorite
U376	Eq. medium-gr. gabbro	U625	Eq. medium-gr. granophyric granodiorite
U388	Eq. medium-gr. magn.-bearing gabbro	U629	Eq. medium-gr. granophyric granodiorite

BLESBOKSPRUIT 515 IT			
No.	Description	No.	Description
U347 U531	Eq. coarse-gr. Two-pyroxene gabbro Ineq. coarse-gr. websterite		

DERBY 444 IT			
No.	Description	No.	Description
U329 U336 U337 U339	Gabbroic sill Gabbroic sill Troctolite (sill) Troctolite (sill)	U340 U619 U620	Eq. medium-gr. gabbro Ineq. medium-gr. granodiorite Eq. fine-gr. granite

STRYDKRAAL 477 IT			
No.	Description	No.	Description
U486	Eq. coarse-gr. feldspatic pyroxenite		

APPENDIX B

1) Operating conditions for the Jeol CXA-733 Superprobe

All electron microprobe data were determined on a Jeol CXA-733 Superprobe, operating at 15 kV and a beam current of 25 nA, using a Duncumb-Reed atomic number correction scheme. The standards used for calibration are: Jadeite (Rhodes), Orapa ilmenite, Wollastonite (JVPL), and Orthoclase (JVPL). For all the analyses a defocused 10 μm beam was used. The counting times were set 30 seconds for peak and 10 seconds for background position.

2) Analytical details for the X-ray fluorescence spectrometry

Element	Tube	KV	Ma	Analytical line	Analysing crystal	Collimator	Counter	Peak 2θ	Count Time Sec.	Background 2θ	Count Time Sec.	Standard	Blanks	Detection limits	Analytical accuracy
SiO_2	Cr	50	50	Ka	Pet	Coarse	Flow	109.165	60	106.000	30	SiO_2 100% NIMD 37.02%		0.004%	0.2%
Al_2O_3	Cr	50	50	Ka	"	"	"	145.040	60	139.160	30	NIML 13.90%	SiO_2	0.005%	0.5%
Fe_2O_3	Au	50	50	Ka	Lif200	Fine	"	57.525	40	Blank standards used to calibrate background.		NIML 10.28%	SiO_2 and $60CaO+40SiO_2$	0.001%	0.5%
MnO	Au	50	50	Ka	Lif200	"	"	62.990	40			NIML 0.78%	SiO_2 and $60CaO+40SiO_2$	0.001%	0.5%
MgO	Cr	50	50	Ka	PX-1	Coarse	"	23.300	60	25.300	30	W-1 6.55%	SiO_2	0.011%	0.3%
CaO	Cr	50	50	Ka	pet	Fine	"	45.240	40	Blank standards		NIML 3.32%	SiO_2 and $40Fe_2O_3 60SiO_2$	0.0003%	0.2%
K_2O	Cr	50	50	Ka	Pet	"	"	50.720	40	used to calibrate		W-1 0.65%	SiO_2 and $60CaO+40SiO_2$	0.0003%	0.2%
TiO_2	Cr	50	50	Ka	Pet	"	"	36.720	40	background		W-1 1.05%	SiO_2 and $60CaO+40SiO_2$	0.0004%	0.2%
P_2O_5	Cr	50	50	Ka	Ge	Coarse	"	141.040	60	138.000 143.000	30 30	BR 1.10%	SiO_2	0.001%	0.2%
Na_2O	Cr	50	50	Ka	PX-1	Fine	"	28.170	60	30.000	30	BR 3.12%	SiO_2	0.018%	2%
Sc	Cr	50	50	Ka	Lif200	"	"	97.730	60	95.850 98.555	30 30	BCR 33 ppm	SiO_2 and $CaCO_3$	0.3 ppm	10%
Ba	Cr	50	50	La	Lif220	"	"	115.275	60	114.500 116.500	30 30	W-1 160 ppm	SiO_2 and MgO	1 ppm	± 20%
Zn	Au	50	50	Ka	Lif200	"	"	41.795	60	39.65 46.70	30 30	NIMP 100 ppm	SiO_2 and $CaCo_3$	0.3 ppm	± 10%
Cu	Au	50	50	Ka	Lif200	"	"	45.040	60	39.65 46.70	30 30	W-1 110 ppm	SiO_2 and $CaCo_3$	0.2 ppm	± 10%
Ni	Au	50	50	Ka	Lif200	"	"	48.690	60	46.70 50.00	30 30	BR 260 ppm	SiO_2 and $CaCo_3$	0.1 ppm	± 10%
Cr	Au	50	50	Ka	Lif200	"	"	69.375	60	68.10 70.80	30 30	JB1 400 ppm	SiO_2	0.6 ppm	10%
V	Au	50	50	Ka	Lif220	"	"	123.220	60	117.10 123.80	30 30	W-1 260 ppm	SiO_2	0.5 ppm	± 10%
La	Au	50	50	Ka	Lif220	"	"	138.920	60	132.60 141.80	30 30	BR 80 ppm	SiO_2	1.5 ppm	15%
Zr	Rh	50	50	Ka	Lif220	"	Scint	32.045	60	29.30 34.89	30 30	AGV 230 ppm	SiO_2	0.3 ppm	3%
Sr	Rh	50	50	Ka	Lif220	"	"	35.830	60	34.89 36.90	30 30	W-1 190 ppm	SiO_2	0.2 ppm	3%
Nb	Rh	50	50	Ka	Lif220	"	"	30.420	60	29.45 34.80	30 30	GSP 23 ppm	SiO_2	0.1 ppm	3%
Y	Rh	50	50	Ka	Lif220	"	"	33.855	60	29.45 34.80	30 30	NIMG 145 ppm	SiO_2	0.3 ppm	3%
Rb	Rh	50	50	Ka	Lif220	"	"	37.960	60	34.80 41.10	30 30	NIMG 320 ppm	SiO_2	0.4 ppm	2%
U	Rh	50	50	Ka	Lif220	"	"	37.300	100	36.90 41.10	30 30	NIMG 15 ppm	SiO_2	0.1 ppm	20%
Th	Rh	50	50	Ka	Lif220	"	"	39.250	100	36.90 41.10	30 30	GSP 105 ppm	SiO_2	0.5 ppm	20%

APPENDIX C

In the following pages the compositions of plagioclase and clinopyroxene which were determined by the author are listed. All the minerals analysed are of cumulus habit. Analyses are included that gave a total in the range of 99.0-100.6%. A minimum value lower than that usually considered (i.e. 99.4%) was accepted; in fact all the phases are extensively altered to hydrated products and this is considered to have resulted in low totals, since combined water was not determined. The average core compositions are based on a minimum of 7 microprobe analyses per rock.

Total number of microprobe analyses completed:

phase	number of samples	number of analyses
plagioclase	14	135
clinopyroxene	4	45

The mineral formulae have all been calculated to the appropriate number of oxygens, following the convention of Deer et al. (1966). In both plagioclase and pyroxene analyses, the Fe^{3+} content was recalculated according to the equation proposed by Droop (1987).

Notes

A) Plagioclase

(P): value from microprobe analyses
(C): recalculated value assuming stoichiometry
n : number of analyses used to calculate average composition
An : cationic ratio of 100Ca/(Ca + Na + K)
Ab : cationic ratio of 100Na/(Ca + Na + K)
Or : cationic ratio of 100K/(Ca + Na + K)

B) Clinopyroxene

(P): value from microprobe analyses
(C): recalculated value assuming stoichiometry
n : number of analyses used to calculate average composition
Mg#: cationic ratio of 100Mg/(Mg + Fe)
Wo : cationic ratio of 100Ca/(Mg + Fe + Ca)
En : cationic ratio of 100Mg/(Mg + Fe + Ca)
Fs : cationic ratio of 100Fe/(Mg + Fe + Ca)

MICROPROBE DATA: Composition of plagioclase (Hlelo River Section).

Sample No.	U24	U50	U157	U202	U215	USH3	U345	U251	U259	U262	U409	U412	U430	U464
Wt%														
SiO2	55.63	56.65	58.22	58.00	67.98	69.64	56.61	57.07	58.35	67.68	67.71	67.45	68.50	68.13
Al2O3	26.92	26.33	25.25	25.38	19.68	19.08	26.01	26.04	25.84	19.54	19.45	19.76	18.97	19.29
Fe2O3	0.41	0.54	0.36	0.69	0.08	0.01	0.65	0.47	0.45	0.44	0.05	0.17	0.02	0.26
FeO(P)	0.39	0.48	0.33	0.62	0.07	0.06	0.59	0.46	0.50	0.40	0.04	0.15	0.02	0.26
FeO	0.02	0.00	0.01	0.00	0.00	0.05	0.00	0.04	0.09	0.00	0.00	0.00	0.01	0.02
CaO	10.44	9.73	8.13	8.17	0.37	0.27	10.26	9.55	8.00	0.33	0.21	0.50	0.34	0.75
Na2O	6.02	6.41	7.17	7.18	12.00	10.87	6.42	6.02	6.95	11.81	12.21	11.61	11.80	11.35
K2O	0.20	0.11	0.15	0.30	0.09	0.05	0.30	0.54	0.25	0.09	0.09	0.43	0.05	0.33
Total(P)	99.59	99.72	99.25	99.66	100.19	99.96	100.18	99.69	99.89	99.83	99.71	99.90	99.68	100.10
Total(C)	99.64	99.77	99.29	99.73	100.19	99.97	100.24	99.74	99.93	99.87	99.71	99.91	99.68	100.13
Cations	(based on 32	oxygens)												
Si	10.0414	10.1983	10.4835	10.4038	11.8208	12.2668	10.1468	10.3060	10.4579	11.8326	11.8088	11.7861	11.9976	11.9198
Al	5.7277	5.5871	5.3587	5.3650	4.0336	3.9615	5.4941	5.5427	5.4583	4.0261	3.9972	4.0690	3.9155	3.9777
Fe3+	0.0558	0.0730	0.0482	0.0940	0.1000	0.0013	0.0876	0.0635	0.0612	0.0580	0.0062	0.0224	0.0026	0.0350
Fe2+	0.0033	0.0000	0.0017	0.0000	0.0000	0.0075	0.0000	0.0065	0.0137	0.0000	0.0000	0.0000	0.0008	0.0036
Ca	2.0193	1.8771	1.5686	1.5703	0.0698	0.0505	1.9699	1.8470	1.5373	0.0607	0.0392	0.0941	0.0641	0.1413
Na	2.1057	2.2392	2.5047	2.4972	4.0454	3.7011	2.2321	2.1088	2.4144	4.0035	4.1287	3.9330	4.0084	3.8496
K	0.0467	0.0253	0.0346	0.0696	0.0205	0.0112	0.0695	0.1256	0.0572	0.0191	0.0199	0.0955	0.0110	0.0731
n	14	11	9	8	11	10	9	9	7	8	10	10	9	9
An	48.41	45.33	38.18	37.91	1.69	1.38	46.11	45.26	38.40	1.5	0.94	2.28	1.55	3.44
Ab	50.47	54.06	60.98	60.40	97.82	98.31	52.26	51.68	60.16	98.03	98.58	95.41	98.18	94.78
Or	1.12	0.61	0.84	1.68	0.49	0.31	1.62	3.05	1.44	0.47	0.48	2.31	0.27	1.78
An MAX	52.46	55.34	42.00	43.84	2.65	3.87	49.00	47.54	43.99	2.65	1.13	5.57	6.26	11.93
An MIN	43.58	39.53	32.72	33.69	0.98	0.79	41.95	41.81	33.49	0.84	0.75	1.16	0.25	1.19
Standard	deviation:													
Wt%														
SiO2	0.86	0.81	0.77	0.45	0.28	1.33	0.69	0.60	0.61	0.44	0.40	0.51	0.56	1.09
Al2O3	0.39	0.60	0.49	0.39	0.15	0.39	0.69	0.25	0.48	0.24	0.16	0.26	0.11	0.27
Fe2O3	0.20	0.09	0.10	0.06	0.04	0.08	0.11	0.17	0.22	0.65	0.02	0.20	0.03	0.49
FeO(P)	0.15	0.08	0.09	0.05	0.04	0.05	0.10	0.04	0.12	0.59	0.02	0.18	0.02	0.43
FeO	0.08	0.00	0.00	0.00	0.00	0.05	0.00	0.12	0.22	0.00	0.00	0.00	0.01	0.05
CaO	0.59	0.79	0.45	0.43	0.12	0.16	0.48	0.42	0.47	0.13	0.02	0.34	0.38	0.76
Na2O	0.38	0.54	0.35	0.29	0.13	1.78	0.27	0.21	0.57	0.35	0.18	0.45	0.16	0.44
K2O	0.11	0.07	0.10	0.16	0.09	0.02	0.10	0.22	0.16	0.10	0.09	0.61	0.02	0.44

MICROPROBE DATA: Composition of clinopyroxene (Hlelo River Section).

Sample No.	U24	U50	U345	U251
Wt.%				
SiO2	49.90	49.76	49.54	50.11
TiO2	0.44	0.59	0.44	0.44
Al2O3	1.41	1.44	1.48	1.47
Cr2O3	0.00	0.02	0.01	0.01
Fe2O3	2.14	0.62	2.53	2.05
FeO(P)	19.51	21.50	19.39	19.26
FeO	17.58	20.94	17.11	17.42
MnO	0.40	0.39	0.44	0.42
NiO	0.00	0.01	0.01	0.03
MgO	11.71	9.79	10.43	10.31
CaO	15.67	15.55	17.39	17.67
Na2O	0.24	0.24	0.25	0.26
Total(P)	99.28	99.29	99.38	99.97
Total(C)	99.49	99.35	99.63	100.18
Cations (based on 6 oxygens):				
Si	1.9329	1.9523	1.9259	1.9373
Ti	0.0129	0.0173	0.0127	0.0126
Al	0.0642	0.0666	0.0680	0.0667
Cr	0.0001	0.0005	0.0002	0.0003
Fe3+	0.0624	0.0183	0.0739	0.0596
Fe2+	0.5697	0.6870	0.5566	0.5632
Mn	0.0130	0.0130	0.0146	0.0138
Ni	0.0001	0.0004	0.0004	0.0010
Mg	0.6760	0.5723	0.6040	0.5940
Ca	0.6505	0.6540	0.7243	0.7318
Na	0.0181	0.0182	0.0194	0.0196
n	9	10	13	13
Mg#	50.47	45.41	52.09	51.34
Wo	31.86	34.19	38.43	38.74
En	33.11	29.90	32.05	31.45
Fs	27.89	35.91	29.52	29.81
Standard deviation:				
Wt.%				
SiO2	0.25	0.22	0.51	0.54
TiO2	0.07	0.04	0.06	0.05
Al2O3	0.41	0.16	0.09	0.05
Cr2O3	0.02	0.01	0.01	0.02
Fe2O3	0.57	0.61	0.01	1.12
FeO(P)	0.93	1.04	1.11	0.46
FeO	0.80	1.13	1.70	0.90
MnO	0.05	0.03	0.04	0.04
NiO	0.01	0.01	0.00	0.01
MgO	0.67	0.25	0.47	0.45
CaO	0.93	0.84	0.99	0.84
Na2O	0.06	0.02	0.01	0.02

APPENDIX D

All whole-rock XRF have been carried out at the Geology Department of the University of Natal, Pietermaritzburg. Analytical details are provided in Appendix B2. All data were recalculated to 100% L.O.I.-free. Fe_2O_3 has been stated assuming a constant ratio of $FeO/Fe_2O_3 = 10$. The Mg# is the atomic ratio of $Mg/(Mg + Fe^{2+})$.

The abbreviations for the normative minerals are as follows:

AP	apatite	DIFS	diopside-ferrosilite
IL	ilmenite	DIWO	diopside-wollastonite
OR	orthoclase	HYEN	hypersthene-enstatite
AB	albite	HYFS	hypersthene-ferrosilite
AN	anorthite	Q	quartz
MT	magnetite	FO	forsterite
DIEN	diopside-enstatite	FA	fayalite

WHOLE-ROCK XRF-ANALYSES (Hielo River Section).

Sample No.	U1	U14	U20	U22	U26	U33	U40	U43	U68	U157	U163	U169	U187	U202	U215	U345	U251	U259	U262	U430	U444	U464	U468
wt.%																							
SiO2	49.43	52.15	51.17	49.99	51.24	50.53	51.73	52.48	47.91	50.71	50.92	49.51	50.11	51.92	60.54	50.38	49.42	54.18	65.61	68.62	65.78	73.23	73.26
Al2O3	15.26	14.56	14.87	13.85	14.17	13.83	14.31	15.73	12.36	11.18	11.21	11.46	10.80	12.40	10.64	12.19	12.47	12.99	11.27	11.41	11.31	11.35	11.31
Fe2O3	16.45	15.34	16.75	18.38	15.94	17.10	15.96	14.87	20.51	22.88	22.97	23.16	22.69	20.10	16.85	18.29	18.66	16.41	12.64	9.45	11.94	5.53	5.67
MnO	0.20	0.17	0.18	0.21	0.19	0.20	0.18	0.16	0.17	0.27	0.27	0.27	0.25	0.22	0.17	0.19	0.17	0.18	0.19	0.12	0.13	0.08	0.07
MgO	4.32	3.65	3.60	4.03	3.74	3.92	3.20	2.53	3.28	1.07	0.95	0.97	1.54	1.27	0.33	3.65	3.81	2.27	0.22	0.09	0.13	0.14	0.10
CaO	9.66	8.44	7.46	7.53	8.70	8.76	8.22	7.90	9.17	7.23	7.48	7.98	6.83	7.17	5.28	9.51	9.89	7.20	3.11	2.78	3.37	1.15	1.12
Na2O	2.48	2.78	2.98	2.58	2.75	2.64	2.70	3.36	2.39	2.34	2.15	2.87	3.02	2.86	2.66	2.47	2.41	2.68	3.46	3.10	3.04	3.44	3.57
K2O	0.49	0.97	0.71	0.62	0.91	0.62	1.02	0.98	0.77	1.03	1.00	0.65	1.36	1.42	1.62	0.70	0.79	1.48	1.98	3.25	3.01	4.23	4.06
TiO2	1.0307	1.2717	1.5906	1.7947	1.4920	1.4023	1.6714	1.5843	2.7122	1.6614	1.5720	1.6588	1.6934	1.5587	1.0955	1.6371	1.6885	1.5176	0.9016	0.5655	0.7971	0.3498	0.3491
P2O5	0.05	0.06	0.06	0.05	0.06	0.06	0.06	0.07	0.05	0.79	0.71	0.74	0.94	0.75	0.36	0.14	0.12	0.29	0.19	0.12	0.17	0.05	0.06
TOTAL	99.36	99.40	99.38	99.04	99.21	99.07	99.25	99.65	99.32	99.15	99.24	99.26	99.23	99.66	99.56	99.42	99.19	99.57	99.17	99.50	99.68	99.55	99.57
L.O.I	1.65	1.08	0.58	0.63	1.06	1.43	0.96	1.14	0.85	0.68	0.63	0.46	0.68	1.18	0.90	0.56	0.95	1.04	1.01	0.87	1.29	0.61	0.62
Mg#	0.36	0.34	0.32	0.32	0.34	0.33	0.30	0.27	0.26	0.09	0.08	0.08	0.13	0.12	0.04	0.30	0.31	0.23	0.04	0.02	0.02	0.05	0.04
Trace elements																							
ppm																							
Cr	3	3	2	3	4	4	5	2	6	3	4	1	4	5	4	2	1	2	3	3	2	3	3
V	737	473	537	504	486	501	525	347	303	12	7	3	9	6	3	109	117	52	4	0	4	2	4
La	5	13	4	9	6	13	10	13	20	35	16	23	28	32	41	12	4	24	59	63	60	82	69
Sc	46	43	31	34	40	46	44	35	56	56	55	64	50	44	34	48	48	38	19	11	15	6	7
Ba	112	192	175	170	172	197	177	238	203	257	230	247	236	279	405	198	181	320	512	577	546	730	691
Nb	0.2	2.2	1.4	0.6	2.7	2.0	2.2	1.8	1.6	3.4	2.1	3.4	3.9	4.9	10.7	3.1	2.8	6.4	16.8	14.1	13.6	16.1	16.0
Y	13.3	17.4	14.1	13.3	17.2	15.9	17.9	16.7	15.4	34.8	30.2	33.7	34.2	34.5	47.1	21.8	21.0	28.6	57.7	55.7	54.8	72.3	55.7
Rb	28.0	34.4	21.4	18.7	28.3	18.9	31.0	26.4	21.8	44.7	39.4	27.4	75.7	71.3	26.0	23.3	25.4	72.8	62.8	60.2	67.4	82.5	93.0
Zr	36.7	58.9	51.2	49.1	57.5	57.7	62.6	62.9	48.6	94.2	94.3	70.0	68.9	94.7	199.6	66.9	55.0	108.7	364.7	248.1	238.4	301.3	295.3
Sr	267.1	239.3	274.6	248.4	255.7	244.8	266.6	288.6	255.1	242.2	204.7	240.2	151.2	259.4	168.0	205.0	218.0	225.0	127.0	120.2	128.5	87.7	102.3
U	1.0	1.3	1.2	0.4	1.7	0.0	0.3	1.8	2.8	2.9	2.8	0.0	0.0	3.7	0.8	0.0	0.2	1.9	3.0	2.6	2.2	2.9	3.4
Th	1.2	6.0	2.5	2.5	5.4	4.5	3.2	3.3	5.6	7.9	5.5	1.9	0.9	9.7	12.1	4.6	1.6	6.1	19.2	17.1	13.1	20.1	20.5
Zn	86.1	89.2	95.3	102.4	74.5	97.2	96.8	93.3	88.3	138.9	103.7	94.3	106.3	97.9	111.2	97.4	97.7	107.3	153.4	105.0	109.4	98.6	99.5
Cu	225.4	123.9	70.2	68.6	123.4	424.5	54.6	44.2	113.9	49.4	33.1	63.0	48.3	27.1	28.9	213.2	103.2	42.0	11.6	9.6	5.9	6.3	7.6
Ni	21.0	12.4	4.2	5.8	5.2	15.2	8.5	5.3	0.0	0.0	0.0	0.0	0.0	0.0	0.0	70.0	69.1	2.7	0.0	0.0	0.0	0.0	0.0
S	551	679	843	894	1411	1430	1353	374	1821	121	57	0	23	0	130	4115	947	2553	684	39	0	0	0
CIPW-norm																							
wt.%																							
AP	0.12	0.14	0.14	0.12	0.14	0.14	0.14	0.17	0.12	1.87	1.68	1.75	2.23	1.78	0.85	0.33	0.28	0.69	0.45	0.28	0.4	0.12	0.14
IL	1.96	2.41	3.02	3.4	2.83	2.66	3.55	3	5.15	3.15	2.99	3.15	3.22	2.96	2.08	3.11	3.21	2.86	1.71	1.07	1.51	0.66	0.66
OR	2.9	5.73	4.2	3.66	5.38	3.66	6.03	5.79	4.55	8.21	5.91	3.84	8.04	8.39	9.57	4.14	4.67	8.8	11.7	19.21	17.79	25	23.99
AB	20.98	23.52	25.21	21.83	23.27	22.34	22.84	28.43	20.22	19.8	18.19	24.28	25.55	24.2	22.51	20.9	20.39	22.68	29.27	26.23	25.72	29.11	30.21
AN	29.06	24.39	25.1	24.38	23.64	24.06	23.92	24.95	20.73	15.9	17.99	16.47	11.9	16.81	12.31	20.11	20.88	19.02	9.38	7.62	8.33	3.04	2.85
MT	1.97	1.84	2	2.2	1.91	2.05	1.91	1.78	2.46	2.74	2.75	2.77	2.72	2.41	2.02	2.19	2.23	1.96	1.51	1.13	1.43	0.66	0.68
DIEN	2.58	2.28	1.45	1.62	2.54	2.47	2.02	1.5	2.61	0.54	0.47	0.61	0.81	0.67	0.19	3.13	3.33	1.37	0.07	0.04	0.07	0.05	0.03
DIFS	5.4	5.11	3.55	3.87	5.73	5.77	5.16	4.57	8.16	6.31	6.25	7.87	6.45	5.7	5.22	8.3	9.62	5.22	2.19	2.5	3.36	1.05	1.05
DIWO	7.74	7.14	4.81	5.28	7.89	7.94	6.88	5.76	10.21	6.18	6.05	7.63	6.62	5.79	4.82	10.92	11.44	6.18	2.01	2.25	3.04	0.98	0.97
HYEN	8.04	6081	7.51	8.42	6.77	7.29	5.95	4.8	5.56	2.12	1.89	1.81	3.02	2.49	0.63	5.96	6.16	4.28	0.48	0.18	0.26	0.3	0.22
HYFS	16.8	15.31	16.41	20.17	15.24	17.05	15.2	14.65	17.37	24.58	24.92	23.42	24.07	21.24	17.68	15.83	15.93	16.36	14.97	10.48	12.85	6.53	6.71
Q	0	3.3	2.42	2.39	2.3	2.07	4.2	2.91	0.31	6.05	8.08	3.57	2.58	5.44	20.14	2.57	0.59	9.25	24.67	27.65	23.83	31.56	31.54
FO	0.1	0	0	0	0	0	0	0	0	0	0	0	0	0	0	0	0	0	0	0	0	0	0
FA	0.22	0	0	0	0	0	0	0	0	0	0	0	0	0	0	0	0	0	0	0	0	0	0
TOTAL	97.86	97.99	97.84	97.35	97.73	97.49	97.79	98.3	97.44	97.46	97.16	97.18	97.2	97.86	98.02	97.49	97.72	97.72	98.42	98.64	98.59	99.05	99.05

APPENDIX E

Base and precious metal analyses were carried out at the Anglo-American Research Laboratories (Pretoria), using a combination of ICP (inductively coupled plasma) emission and atomic absorption spectrometry.

The lower limits of determination are as follows:

Cu	2 ppm
Ni	2 ppm
Pb	3 ppm
Zn	2 ppm
Co	3 ppm
Ag	0.5 ppm
As	6 ppm
Cd	1 ppm
Bi	5 ppm
Sb	2 ppm
Au	2 ppb
Pd	2 ppb

BASE AND PRECIOUS METAL DATA

Sample No	Cu ppm	Ni ppm	Pb ppm	Zn ppm	Co ppm	Ag ppm	As ppm	Sb ppm	Cd ppm	Bi ppm	Au ppb	Pd ppb
HLELO RIVER SECTION (Ishlelo 441 IT)												
U22	83.0	18.0	<0.9	35.0	35.0	1.3	1.7	6.4	<0.1	3.3	1.0	-1.0
U29	45.0	30.0	7.0	46.0	21.0	<0.5	<2.0	<2.0	<1.0	<5.0	2.0	2.0
U33	38.0	16.0	<0.9	91.0	36.0	1.5	1.5	5.5	<0.1	1.4	0.0	0.0
U36	14.0	4.6	7.4	101.0	5.6	1.0	2.0	5.0	<0.1	0.8	2.0	2.0
U58	839.0	28.0	<0.9	81.0	85.0	1.5	1.6	6.1	<0.1	3.7	0.0	-1.0
U87	54.0	19.0	10.0	70.0	34.0	<0.5	<2.0	<2.0	<1.0	<5.0	1.0	-1.0
U88	43.0	42.0	5.0	72.0	39.0	<0.5	<2.0	<2.0	<1.0	<5.0	2.0	0.0
U120	27.0	4.6	<0.9	97.0	7.9	1.2	2.1	5.7	<0.1	<0.7	1.0	2.0
U133	97.0	11.0	<0.9	52.0	47.0	1.3	0.6	2.7	<0.1	<0.7	0.0	1.0
U157	62.0	<2.0	3.0	97.0	42.0	<0.5	4.0	<2.0	<1.0	<5.0	2.0	0.0
U164	50.0	<2.0	6.0	59.0	40.0	<0.5	2.0	<2.0	<1.0	<5.0	1.0	0.0
U194	34.0	<2.0	11.0	63.0	27.0	<0.5	<2.0	<2.0	<1.0	<5.0	3.0	0.0
U202	35.0	<2.0	12.0	91.0	47.0	<0.5	<2.0	<2.0	<1.0	<5.0	3.0	-2.0
U249	32.0	20.0	11.0	40.0	26.0	<0.5	<2.0	<2.0	<1.0	<5.0	16.0	0.0
U251	155.0	46.0	10.0	48.0	36.0	<0.5	2.0	<2.0	<1.0	<5.0	22.0	2.0
U257	55.0	4.0	11.0	97.0	54.0	<0.5	<2.0	<2.0	<1.0	<5.0	0.0	1.0
U259	938.0	531.0	<0.9	20.0	44.0	1.4	0.8	<0.5	<0.1	1.6	1.0	1.0
U262	18.0	<2.0	13.0	123.0	19.0	<0.5	<2.0	<2.0	<1.0	<5.0	0.0	-1.0
U421	204.0	29.0	<0.9	51.0	54.0	1.5	3.3	6.2	<0.1	5.9	1.0	2.0
U472	135.0	18.0	<0.9	55.0	47.0	1.3	4.6	5.1	<0.1	3.1	4.0	1.0
STERKWATER SECTION (Sterkwater 472 IT)												
U385	90.0	10.0	<0.9	30.0	48.0	1.3	3.7	7.4	0.5	1.0	1.0	1.0
U391	175.0	20.0	<0.9	26.0	42.0	1.6	3.8	10.0	0.8	7.5	0.0	0.0
U393	43.0	61.0	<0.9	40.0	26.0	1.2	1.4	3.0	<0.1	3.4	1.0	3.0
MORGESTOND SECTION (Morgestond 418 IT)												
U542	93.0	56.0	<0.9	50.0	41.0	1.1	6.9	2.3	<0.1	<0.7	0.0	0.0
U552	77.0	29.0	<0.9	29.0	25.0	1.1	1.7	4.8	<0.1	2.6	0.0	1.0